GL-Lect Endocytosis in In-Vivo Model Systems

Alena Ivashenka

UNIVERSITÉ PARIS SUD
Comprendre le monde, construire l'avenir

GL-Lect endocytosis in *in-vivo* model systems

Thèse de doctorat de l'Université Paris-Saclay
préparée à l'université Paris Sud

École doctorale n°568 signalisations et réseaux intégratifs en biologie (Biosigne),aspect moléculaire et cellulaire de la biologie

Thèse présentée et soutenue à Paris, le 02 Décembre 2019, par

Alena Ivashenka

Composition du Jury :

Oliver Nüsse Professeur Laboratoire de Chimie Physique, Cnrs UMR8000	Président
Kai Simons Professeur, Max Planck institute	Rapporteur
Corinne Albiges-Rizo Directeur de recherche, institut pour l'avancée des biosciences	Rapporteur
Vignjevic Danijela Directeur de recherche, institut Curie	Examinateur
Ludger Johannes Directeur de recherche, institut Curie	Directeur de thèse

UNIVERSITE PARIS XI

FACULTE DE MEDECINE PARIS-SUD

2019 N° attribué par la bibliothèque

THESE

pour obtenir le grade de

DOCTEUR DE L'UNIVERSITE PARIS XI

Spécialité: Biologie cellulaire et moléculaire

Ecole doctorale de rattachement :

Signalisations, Neurosciences, Endocrinologie et Reproduction

présentée et soutenue publiquement

par

Alena Ivashenka

Le 02 Décembre 2019

GL-Lect endocytosis in *in-vivo* model systems

JURY

(y compris le directeur de thèse)

Professeur Oliver Nüsse	Président du jury
Professeur Kai Simons	Rapporteur
Docteur Corinne Albiges-Rizo	Rapporteur
Docteur Vignjevic Danijela	Examinateur
Docteur Ludger Johannes	Directeur de thèse
Docteur Massiullah Shafaq-Zadah	Co-directeur de thèse

GL-Lect endocytosis in *in-vivo* model systems

A thesis submitted for the degree of

DOCTOR OF PHILOSOPHY

in the faculty of Science by

Alena Ivashenka

Thesis supervisors: Ludger JOHANNES and Massiullah SHAFAQ-ZADAH

JURY
(Includes thesis supervisors)

Prof. Oliver Nüsse	President of the jury
Prof. Kai Simons	Reviewer
Dr. Corinne Albiges-Rizo	Reviewer
Dr. Vignjevic Danijela	Examiner
Dr. Ludger Johannes	PhD supervisor
Dr. Massiullah Shafaq-Zadah	PhD co-supervisor

Summary

A host of endocytic pathways exist at the surface of eukaryotic cells, which lead to the internalization of the bulk of membranes along with membrane proteins, signaling receptors, and other cargoes (Smith et al., 2017). For decades, the clathrin-mediated pathway has been the best characterized endocytic process, where clathrin polymerizes along with the associated adaptor proteins to corral ligand-bound receptors, leading to membrane bending, membrane scission, and endocytosis (Smith et al., 2017). Recently, multiple alternative mechanisms have been uncovered which facilitate the endocytic uptake of cargo molecules and membrane receptors even in the absence of clathrin machinery (Mayor et al., 2014). A model of endocytosis that doesn't require clathrin but rather sugar-binding galectins and glycolipids has been proposed by my host laboratory (Lakshminarayan et al., 2014). Galectins constitute a family of beta-galactoside–binding lectins, which to date consists of 15 members in mammals. Galectins are broadly distributed in a variety of cells and tissues (Leffler et al., 2004). They are translocated from the cytosol to the extracellular space by a process of non-classical secretion (Hughes, 1999). Glycosphingolipids (GSLs) are ubiquitous membrane constituents that are subdivided into neutral or acidic fractions. The term GSLs applies to compounds that contain at least one monosaccharide and a ceramide. Of note, the enzyme UDP-glucose ceramide glucosyltransferase (Ugcg) catalyzes the initial step for the biosynthesis of glycosylceramide-based GSLs.

Our current working model, which involves cooperation between glycolipids and lectins to generate endocytic pits, termed the GL-Lect hypothesis (Johannes et al., 2016), can be described as follows (Lakshminarayan et al., 2014):

i) Monomeric Galectin- 3 (Gal3) binds to glycoproteins

ii) Gal3 then starts to oligomerize

iii) Oligomerized Gal3 interacts with GSLs, which may induce their clustering

iv) Gal3-GSL-cargo clusters cause the invagination of the plasma membrane to generate tubular endocytic pits from which clathrin-independent carriers (CLICs, which are pre-early endosomes) are generated.

Oligomeric Gal3 is indeed able to bind to GSLs and to induce membrane deformation (Lakshminarayan et al., 2014) in a similar way the pathogenic lectin Shiga toxin B-subunit (STxB) does. Therefore, both processes could be summarized under the same hypothesis, the GL-Lect hypothesis, where GL stands for the glycolipid (Gb3 for STxB, and gangliosides for Gal3) and Lect stands for lectins (STxB, galectins, and possibly others as well).

Understanding in which physiological situations this clathrin-independent but Gal3-dependent internalization mechanism operates is one of the main challenges for the GL-Lect hypothesis. Here, we have characterized for the first time that in intestinal enterocytes, the GL-Lect mechanism facilitates endocytic uptake of cargo in a transcytosis-like proces . Indeed, we have found that lactotransferrin (LTF), a Gal3-binding protein that we have identified by pull-down and mass spectrometry, strongly requires Gal3 and GSLs for its efficient endocytosis and its transcytosis-like distribution pattern. Based on these findings in the mouse intestinal epithelium, we established a functional *in vivo* model system where GL-Lect mechanism is physiologically relevant.

Keywords: Glycosphingolipid, galectin, lactotransferrin, enterocytes, mouse intestinal model, endocytosis, CLIC, mucus, plasma membrane, endosomes, lectin, homeostasis, TLC, GSL, immunofluorescence microscopy, electron microscopy, tomography.

Resume (Francais)

Une multitude de voies endocytiques existent à la surface de la membrane plasmique, ce qui conduit à l'internalisation de la majeure partie des membranes ainsi que des protéines associées, des molécules de signalisation, des facteurs de croissance et autres cargos (Smith et al., 2017). Pendant des décennies, la voie dite clathrine-dépendante a été la plus étudiée, Cette voie d'endocytose se caractérise par la polymérisation de molécules de clathrine et de protéines adaptatrices au niveau de récepteurs liés à leurs ligands, entrainant la courbure de la membrane, avant sa scission et son endocytose (Smith et al., 2017). Récemment, plusieurs mécanismes alternatifs ont été découverts facilitant l'absorption endocytique des protéines cargo et des récepteurs membranaires, même en l'absence de la voie clathrine-dépendante (Mayor et al., 2014). Un modèle d'endocytose qui ne requiert pas de clathrine mais à la place des galectines et des glycolipides a été proposé par mon laboratoire hôte (Lakshminarayan et al., 2014). Les galectines sont des lectines qui se lient aux bêta-galactosides et qui, à ce jour, regroupent 15 membres (galectine-1 à galectine-15) chez les mammifères et sont retrouvées dans de nombreux types de cellules et tissus (Leffler et al., 2004). Les galectines sont probablement sécrétées extra-cellulairement par une voie encore mal caractérisée et non-classique (Hughes, 1999). Les glycosphingolipides (GSL) sont des constituants membranaires ubiquitaires, divisés en fractions neutres ou acides. Le terme GSL s'applique aux composés contenant au moins un monosaccharide et une céramide. Il est à noter que l'enzyme UDP-glucose céramide glucosyltransférase (Ugcg) catalyse l'étape initiale de la biosynthèse de GSLs à base de glycosylcéramides.

Notre modèle de travail actuel, impliquant les glycolipides et les lectines, a été qualifié d'hypothèse GL-Lect (Johannes et al., 2016), et préliminairement soutenu par des données expérimentales comme décrit par Lakshminarayan et al. en 2014. Il peut être décrit comme suit :

i) la galectine-3 (Gal3) se lie sous forme monomérique aux glycoprotéines

ii) Gal3 commence alors à oligomériser

iii) Gal3 oligomérisée a la capacité de se lier aux GSLs, ce qui conduit vraisemblablement à la formation de clusters de GSLs

iv) Ces clusters Gal3-GSL-protéines cargos induisent une invagination de la membrane plasmique, une endocytose des protéines cargo liées à Gal3 et la formation subséquente de CLIC (clathrin-independent carriers), endosomes pré-précoces.

Selon ce modèle, l'oligomère Gal3 est capable de se lier aux GSLs et d'induire une déformation de la membrane de la même manière qu'une autre lectine, la sous-unité B de la toxine de Shiga (STxB). Par conséquent, les deux processus pourraient être résumés sous la même hypothèse GL-Lect, où GL représente les glycolipides (Gb3 pour STxB et des gangliosides pour Gal3) et Lect corresponds aux lectines (STxB, Gal3 et éventuellement d'autres). Comprendre dans quels contextes physiologiques les processus d'internalisation indépendantes de la clathrine, mais dépendantes des galectines, sont opérés non est un défi majeur pour l'hypothèse GL-Lect.
Dans mon travail de thèse, j'ai obtenu des indications directes sur une implication du mécanisme GL-Lect dans l'endocytose et la transcytose au niveau de l'intestine grêle de la souris. Ce mécanisme implique la Gal3 et agit dans les entérocytes intestinaux dans un processus de transcytose qui s'avère d'être dépend des GSLs. En effet, nous avons découvert que la lactotransferrine (LTF), une protéine que nous avons identifié par pull-down et spectrométrie de masse comme étant un partenaire d'interaction de la Gal3, dépendait fortement de cette dernière et des GSLs pour son endocytose efficace et son mode de distribution analogue à la transcytose. Sur la base de ces découvertes dans l'épithélium intestinal de souris, nous avons établi un système modèle *in vivo* fonctionnel dans lequel le mécanisme endocytique récemment proposé, appelé dans notre laboratoire GL-Lect, semble se produire physiologiquement.

Mots clés: Glycosphingolipide, galectine, lactotransferrine, entérocytes, modèle souris d'intestin, endocytose, CLIC, mucus, membrane plasmique, endosomes, lectine, homéostasie, TLC, GSL, microscope à immunofluorescence, microscope électronique, tomographie.

Acknowledgements

Dedicated to my parents

Prof. Siarhei Ivashenka and Tatsiana Ivashenka

Acknowledgments

The undertaking of this Ph.D. was a real life-changing experience for me, and without the help and guidance I got from many individuals listed below, it would not have been possible to do it. Firstly, I would like to express my sincere appreciation to my advisor Dr. Ludger Johannes for the continuous support of my Ph.D. work, and for his patience, wisdom, motivation, and immense knowledge. His guidance helped me in all the time of research and writing of this manuscript. I could not have imagined having a better advisor and mentor for my Ph.D. study.

I am also especially grateful to my co-mentor Dr. Massiullah Shafaq Zadah for his suggestions and contributions to the project that he made during our scientific discussions. He has been a truly dedicated and thoughtful mentor. I am particularly beholden to Massiullah for his persistent faith in my lab work, and his support.

Besides my 2 advisors, I would like to thank the rest of my thesis committee: Prof. Nüsse, Prof. Simons, Dr. Albiges-Rizo and Dr. Vignjevic for their wise comments and encouragement, but also for their suggestions and questions which encouraged me to widen my research from various perspectives.

I am grateful to my collaborators on this project: Dr. Francoise Poirier for providing the mice and help in maintaining the mouse colony, and Dr. Hermann-Josef Gröne and his team for providing the Ugcg knock-out mice.

Also, I would like to thank Dr. Christian Wunder for his endless help, involvement in the project and suggestions to my work, and Valerie Chambon for her help with EM microscopy.

My deep appreciation goes out to Dr. Katrina Podsypanina, Dr. Anna Zagryazhskaya-Masson, Dr. Marina Glukhova, Dr. Estelle Dransart.

I am very grateful to all the past and present lab members of the "ENDOCYTIC TRAFFICKING AND INTRACELLULAR DELIVERY" team, and members of the UMR 3666 unit for creating a wonderful work environment and for making my stay in Paris pleasant.

I would like to thank the Nikon imaging center members at Institut Curie: François Waharte, Lucie Sengmanivong and Ludovic Leconte for their technical support.

I would like to thank the Association pour la Recherche sur le Cancer (ARC) for their financial support during the final year of my Ph.D.

I would also like to thank the administration at Institut Curie for all the administrative support which made my life easier in Paris.

I also want to thank everyone involved in this project.

Last but not least are my parents and friends. Your support is hard to estimate and appreciate. I am very happy that you always had my back during this time.

Table of Contents

Table of figures

Abbreviations

A4GALT	A1-4-galactosyltransferase
AlbCre	Albumin promoter
AP2	Adaptor protein-2
Arc	Arcuate nucleus
Arf6	ADP-ribosylation factor 6
ARH	Autosomal recessive hypercholesterolemia
B3GNT5	b-1,3-N-acetylglucosaminyltransferase
B4GALNT1	b1,4-N-acetylgalactosylaminyltransferase B4GALNT1
BAR	Bin/amphiphysin/Rvs domain
BB	Brush border
BFA	Brefeldin A
BG	Benzylguanine
CamK	Calcium/calmodulin-dependent kinase II α promoter
CB	Core bundle
CBC	Crypt base columnar cells
CCP	Clathrin-coated pit
CCVs	Clathrin-coated vesicles
Cer	Ceramide
CerS	Ceramide synthases
CERT	Ceramide transfer protein
CIE	Clathrin-independent endocytosis
CLIC	Clathrin-independent carrier
CME	Clathrin-dependent/mediated endocytosis
CnpCre	Cyclic nucleotide 3′ phosphodiesterase
CRDs	Carbohydrate-recognition domains
CTx	Cholera toxin
CTxB	Cholera toxin B-subunit
Dab2	Disabled homolog 2

DAD	Diaphanous Autoregulatory Domain
DAG	Diacylglycerol
EGF	Epidermal growth factor
EGFR	Epidermal growth factor receptor
EHD1	EH Domain-containing 1
EHD4	EH Domain-containing 4
ER	Endoplasmic reticulum
ERC	Endocytic recycling compartment
ESCRT	Endosomal sorting complex required for transport
F-BAR	Fes/CIP4 homology-BAR
Gal3	Galectin-3
GalCer	Galactosylceramide
GAPs	GTPase Activating Proteins
Gb3	Globotriaosylceramide
GDIs	Guanine nucleotide Dissociation Inhibitors
GEEC	GPI-AP enriched early endosomal compartment
GEFs	Guanine nucleotide Exchange Factors
GL	GlycoLipids
GlcCer	Glucosylceramide
GLUTs	Glucose transporters
GM	Monosialotetrahexosylganglioside
GPCRs	G protein–coupled receptors
GPI	Glycosylphosphatidylinositol
GPI-APs	Glycosyl phosphatidylinositol-anchored proteins
GRAF1	GTPase regulator associated with focal adhesion kinase-1
GSLs	Glycosphingolipids
HUS	Hemolytic uremic syndrome
I-BAR	Inverse-BAR
IL-2R-β	β-chain of the interleukin-2 receptor

KO	Knockout
LacCer	Lactosylceramide
LB	Lateral bridges
Ld	Liquid-disordered
LDL	Low-density lipoprotein
LDLR	LDL receptor
Lect	Lectin
Lo	Liquid-ordered
LTF	Lactotransferrin
MHCI	Major histocompatibility class I
MV	Microvilli
MVB	Multivesicular bodies
MVM	Microvillar membrane
N-WASP	Neural Wiskott–Aldrich syndrome protein
NesCre	Nestin promotor driven Cre recombinase
NPFs	Nucleation promoting factors
PA	Phosphatidic acid
PAK1	P21-activated kinase 1
PC	Paneth cells
PI3K	Phosphatidylinositol 3-kinase
PIP 5-kinase	Phosphatidylinositol 4-phosphate 5-kinase
PIP_2	Phosphatidylinositol 4,5-bisphosphate
PLD	Phospholipase D
PM	Plasma membrane
pN	Pico-Newton
PtdIns(4,5)P2	Phosphatidylinositol 4,5-bisphosphate
PtdIns3P	Phosphatidylinositol-3-phosphate
RhoA	Ras homolog gene family member A
SGLT1	Sodium-glucose co-transporter 1
SI	Small intestine
ST3GAL5	a-2,3-sialyltransferase
STxB	Shiga toxin B-subunit
SV40	Simian virus 40

TAM	Tamoxifen-inducible
TfR	Transferrin receptor
TGN	Trans-Golgi network
Ugcg	UDP-glucose ceramide glucosyltransferase
VTs	Verotoxins
WT	Wild-type

Preface

A host of endocytic pathways exist at the surface of eukaryotic cells, which lead to the internalization of bulk membranes and specific cargoes. Recently, multiple alternative mechanisms have been uncovered which facilitate the uptake of cargo molecules and membrane receptors even in the absence of the well-characterized clathrin machinery. A model of endocytosis that doesn't require clathrin but rather a lectin, namely galectin-3 (Gal3) and glycolipids such as glycosphingolipids (GSLs) has been proposed by my host team. According to this model, oligomeric Gal3 bound on carbohydrate-modified cargoes are subsequently able to bind GSLs to induce membrane deformation similarly to the pathogenic lectins, such as Shiga toxin B-subunit (STxB). Therefore, both processes could be summarized under the same endocytic mechanism: the GL-Lect hypothesis, where "GL" stands for GlycoLipids and "Lect" for lectin. My Ph.D. project was focused on Gal3, the Gal3-binding cargo protein lactotransferrin, and GSLs. .

In the first part of my Ph.D. manuscript, I will present the background and context on which my study was based. I will introduce the reader to various mechanisms of endocytosis, followed by a description of the galectin family and their physiological functions. I will then move on to GSLs highlighting their synthesis, function and physiological roles. The interacting partners of Gal3 are discussed further. At the end of the introductory section, the mouse intestine is presented as a model system for our study. I will then present the results that I have obtained in the course of my Ph.D. work. The results are discussed, and a perspective is provided at the end of my Ph.D. manuscript. Based on this work, a manuscript has been written for submission to an international journal.

Introduction

1 MECHANISMS OF ENDOCYTOSIS

Endocytosis allows cells to internalize extracellular material (Dmitrieff et al., 2017; Doherty and McMahon, 2009). During this process, the plasma membrane is bent into an invagination progressing inwards, which is severed and released in the cytoplasm as a vesiclar or tubular carrier. Endocytic mechanisms control composition of the plasma membrane, thereby regulating how cells interact with their environment (Doherty and McMahon, 2009). Endocytosis is crucial to maintain various cellular process, and its dysregulation is involved in various pathologies.

The term “endocytosis” was first proposed by Belgian biologist Christian de Duve in 1963 as a catch all term for a various similar events. However, amongst the endocytic processes, some such as phagocytosis operate only in specialized cells. These also differ on their ability to select cargo, leading rather to unspecific engulfment of extracellular volumes, such as for macropinocytosis (Figure 1). These will not be considered in further detail here. Rather, my Ph.D. manuscript is focused on so-called micropinocytic processes. These are classified either as clathrin-dependent or clathrin-independent (Thottacherry et al., 2019) (Figure 1).

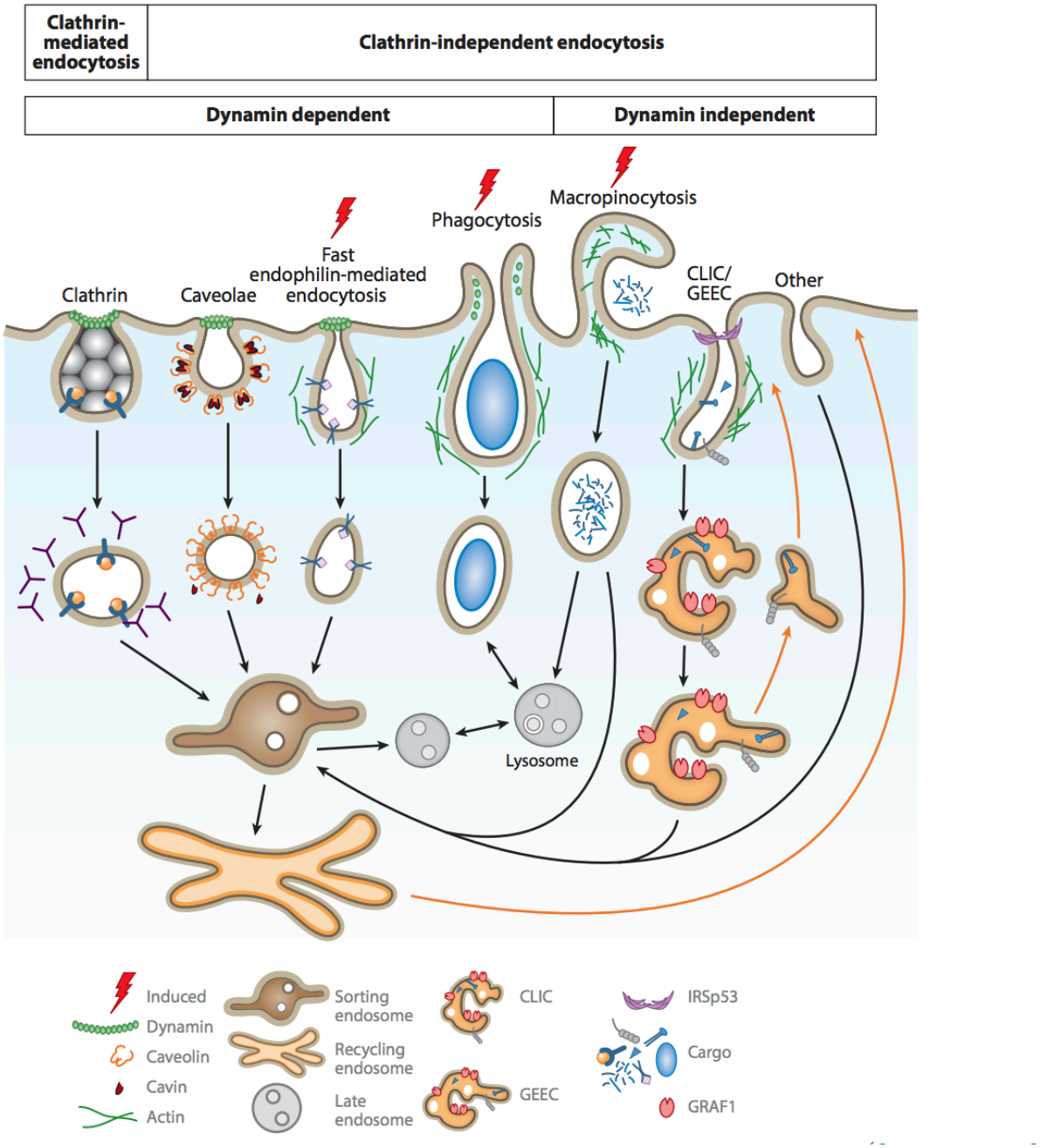

Figure 1: Pathways of internalization into cell. These are divided on the basis of their need for clathrin or dynamin. Large particles can be internalized by phagocytosis, whereas uptake of large volumes of fluid occurs by macropinocytosis. These processes strongly depend on actin. Specific uptake of cargoes occurs by micropinocytosis. This can either by clathrin-dependent/mediated endocytosis (CME), or calthrin-independent endocytosis (CIE) (Mayor and Pagano 2007). Figure from (Thottacherry et al., 2019).

Endocytic pathways vary in cargoes that they transport and in protein machinery that promotes the internalization process. Endocytosis can be classified based on mechanisms that are required to form an endocytic vesicle. Dynamin, a large GTPase, meditates many, but not all forms of endocytosis as well as vesicle formation from various intracellular organelles due to its ability to tubulate and disrupt membranes (Mayor and Pagano, 2007). Based on the involvement of dynamin, clathrin-mediated (CME) and clathrin-independent (CIE) endocytic mechanisms are divided into dynamin-dependent and dynamin-independent (Mousavi et al., 2004).
Another hallmark of the CIE pathway is the involvement of small GTPases. The internalization (or trafficking) of one particular set of CIE endocytic markers, but not another (Mousavi et al., 2004) can be affected based on the fact if they were interfering with CDC42-, RhoA- or ARF6 (ADP-ribosylation factor).

1.1 CLATHRIN-MEDIATED ENDOCYTOSIS (CME)

1.1.1 Clathrin structure and function

Advances in microscopy, particularly electron microscopy in 1931, allowed the discovery of a new endocytic pathway characterized by the presence of coated vesicles, termed CME. The main participants in CME include adaptor proteins and the large GTPase dynamin, which is directly involved in pinching off endocytic vesicles from the plasma membrane.
Clathrin consists of three heavy chains, with a supplementary light chain (Kirchhausen and Harrison, 1981). The clathrin heavy chains include an amino-terminal, β-propeller domain with seven WD40 repeats, followed by the polypeptide chain by 42 β-helical zig-zags of 30 amino acid residues each, a longer β-helix at the threefold contact, and a 45-residue carboxy-terminal segment with poorly defined structure. The carboxy-terminal segment has a short region with an sequence that is recognized by Hsc70, and is fundamental for Hsc70-driven uncoating (Kirchhausen et al., 1987b). The 42 zig-zags cover up the majority of the polypeptide chain and can create a “leg” for the clathrin triskelion, where the β-propeller “terminal domain” is located at its tip. The light chains connect with the threefold-proximal segment of the heavy-chain leg, through a long, central β-helix (Kirchhausen et al., 1987a).
Cargo adaptors and accessory proteins help to pack distinctive receptors and their ligands into clathrin-coated vesicles (CCVs) during CME.

Adaptor and accessory proteins coordinate clathrin nucleation at the level of plasma membrane (Mayor and Pagano, 2007). This process of nucleation stimulates the polymerization of clathrin into curved lattices (Mayor and Pagano, 2007). The process of nucleation stabilizes the deformation of the attached membrane (Mayor and Pagano, 2007).

Clathrin polymerization causes the formation of the vesicle neck. Dynamin forms a helical polymer around this neck and, after GTP hydrolysis, promotes cleavage of the vesicle from the plasma membrane. Auxilin and hsc70 are helping to remove the clathrin basket from the vesicle. This uncoated vesicle then undergoes further trafficking within the cell before delivery of its cargo through fusion with endosomes (Mayor and Pagano, 2007).

Adaptor protein-2 (AP2) complex recognizes dileucine- and tyrosine-based motifs on the cytoplasmic face of cargo molecules and links cargo to nucleating clathrin. Clathrin polymerization alone, however, is insufficient to explain the generation of the narrow membrane curvature according to theoretical analysis, implying the requirement of additional factors (Mayor and Pagano, 2007). One such factor could be the Bin/amphiphysin/Rvs (BAR) domain proteins, which are the best-studied regulators of membrane curvature (Simunovic et al., 2015).

1.1.2 Structure and function of BAR domain proteins

The BAR domain family of proteins consists of a diverse group of multi-functional effectors, that are characterized by their modular architecture (Carman and Dominguez, 2018).

Along with the membrane-curvature sensing (inducing BAR domain module), that mediates antiparallel dimerization (Carman and Dominguez, 2018), BAR domain proteins contain auxiliary domains that are involved in protein-protein and/or protein-membrane interactions, including SH3, PX, PH, RhoGEF, and RhoGAP domains (Carman and Dominguez, 2018).

According to the shape of the BAR domain, the family is divided into three major subfamilies: the classical crescent-shaped BAR (Peter et al., 2004), the more extended and less curved Fes/CIP4 homology-BAR (F-BAR) (Shimada et al., 2007), and the Inverse-BAR (I-BAR) subfamilies (Lee et al., 2007). Most members have been involved in cellular functions that require dynamic remodeling of the actin cytoskeleton during endocytosis, organelle trafficking, and T-tubule biogenesis in muscle cells (Carman and Dominguez, 2018).

BAR domain proteins were named after to the three first proteins from this family to discovered: mammalian Bin1 (Sakamuro et al., 1996) amphiphysin (Lichte et al., 1992), and yeast Rvs167 (Sivadon et al., 1995). Despite some similarities (Sakamuro et al., 1996), generally, BAR domain proteins are distinct at their sequence (Carman and Dominguez, 2018). Crystal

structures of the BAR domain sequence showed that it consists of a helical bundle of ~ 200–280 amino acids. This amino acid allies in an antiparallel fashion to form dimers of varying size and curvature (Habermann, 2004). During endocytosis, organelle trafficking, cell motility, and T-tubule biogenesis in muscle cells BAR proteins are involved in actin cytoskeleton remodeling (Antonny et al., 2016; Carman and Dominguez, 2018).

Most BAR proteins contain additional domains that participate together with the BAR domain in membrane binding and in protein-protein interactions. Among these so-called auxiliary domains, the most common is the Src homology 3 (SH3) domain that in many BAR domain proteins binds directly to cytoskeletal assembly factors and/or dynamin. Also abundant among these proteins are domains that either recruit or regulate Rho-family GTPases, which are the main regulators of the actin cytoskeleton (Hall, 2012; Ridley, 2015). Alternative common themes among BAR domain proteins is the presence of auto inhibitory intramolecular interactions, which are relieved by binding to other proteins and/or membranes (Carman and Dominguez, 2018).

The structural differences among BAR domain subfamilies can correlate with important differences in the way they interact with cellular membranes, since to a large degree the BAR domain is thought to impose its shape on the membrane substrate through a so-called scaffolding mechanism (Blood et al., 2008). Hence, the classical BAR domain is mostly more curved and shorter (~ 167 Å) than the F-BAR domain (~ 225 Å).

It is known that in addition to the structure of the BAR domain, other factors determine how these proteins are involved in the process of membranes remodeling. Most notable among these factors is the seemingly multiple ways in which BAR domains can interact with each other to form scaffolds on membranes (Shimada et al., 2007). Additionally, while the F-BAR domain of CIP4 and FBP17 forms helical scaffolds on membrane tubules via lateral and tip-to-tip interactions (Frost et al., 2008), the N-BAR domain of endophilin forms a lattice that is held together primarily through interactions between the extended N-terminal amphipathic helices of neighboring endophilin molecules (Mim et al., 2012). Consequently, the Endophilin lattice exposes larger areas of membrane surface than CIP4 and FBP17, which form more densely packed lattices.

An additional factor that influences membrane binding by BAR domain proteins is coincidence detection, whereby other domains participate along with the BAR domain in membrane binding (Moravcevic et al., 2012). Another way in which BAR domain proteins control actin cytoskeleton remodeling is through their ability to regulate Rho-family GTPases (Aspenstrom, 2014). Rho GTPases are master regulators of actin assembly dynamics (Hall, 2012). They act

as molecular switches due to their ability to cycle between active GTP bound state and inactive GDP-bound state (Ridley, 2015). This cycle is regulated by two types of proteins: guanine nucleotide exchange factors (GEFs), that catalyze the exchange of GDP for GTP, and GAPs, which catalyze the intrinsic GTPase activity of this class of molecules, leading them to adopt an inactive, GDP-bound confirmation.

Since these initial studies, most BAR domain proteins have now been linked to actin assembly pathways. An emerging view is that this large family of proteins provides probably the most diverse and well-known link between membranes and the actin cytoskeleton (Carman and Dominguez, 2018). Different studies have also shown that some BAR domains can bind actin filaments directly and influence actin polymerization *in vitro* (Drager et al., 2017).

The function of BAR domain proteins in CIE has been recently explored. A study from Boucrout (2015) found that the depletion of A1, A2 and A3 endophilin isoforms affected clathrin-independent, dynamin-dependent cellular uptake of G protein-coupled receptors like α2a- and β1-adrenergic receptors, dopaminergic D3 and D4 receptors, and muscarinic acetylcholine receptor 4; the receptor tyrosine kinases EGFR, hepatocyte growth factor receptor, vascular endothelial growth factor receptor, platelet-derived growth factor receptor, nerve growth factor receptor (also known as TNFRSF16) and insulin-like growth factor 1 receptor; as well as the CIE cargo IL-2 receptor (Boucrot et al., 2015). Endophilins A1–A3 can interact with some of these cargo proteins, as previously shown for β1-adrenergic receptor (Boucrot and Kirchhausen, 2007). Since endophilins can induce membrane curvature (Gallop et al., 2006), they may play key roles in the early construction of endocytic pits in these CIE events.

My host team has shown that endophilin A2 was required for the scission step but not for the formation of membrane invaginations in the CIE of bacterial Shiga or cholera toxins (Renard et al., 2015). Scaffolding membrane tubules with endophilin A2 make them prone to pulling force-induced scission (Johannes et al., 2015). As microtubule-associated motors were active on cellular Shiga toxin-induced membrane invaginations, a new scission mechanism emerges in which motors pull on membranes scaffolded by BAR domain proteins, which creates friction (Renard et al., 2015). The result of this membrane tension builds up, causes spontaneous squeezing of the tube until the scission threshold radius has been reached, which for a multicomponent membrane tube was calculated to be of the order of 3–5 nm (Allain et al., 2004). The detailed mechanism of this scission process has been further clarified in recent studies (Simunovic et al., 2017). In the case of Shiga toxin, this unique scission modality operates in an additive manner with dynamin and actin (Romer et al., 2010). This was shown

by measuring the length of toxin-induced tubules and the cellular intoxication reaction under single or combined interference conditions (Renard et al., 2015). We can see that in addition to their function in CME (Ferguson et al., 2009; Gad et al., 2000), endophilins have a predominant role in CIE, including functions in the synaptic vesicle cycle (Llobet et al., 2011; Kononenko et al. 2014).

Epsin family proteins were also shown to link cargo to clathrin. They bind directly to inositol lipids and drive membrane deformation in the process of assembling clathrin-coated pits (CCP), via the insertion of an amphipathic helix. Other accessory proteins can also participate in the process of membrane deformation. Apart from epsins, G protein–coupled receptors (GPCRs) might be similarly linked to clathrin due to the binding of β-arrestins. β-arrestins interact with inositol lipid PtdIns(4,5)P2, clathrin, and AP2 (Cestra et al., 1999).

Also, Disabled homolog 2 (Dab2) and autosomal recessive hypercholesterolemia (ARH) protein (ARH) can function as cargo-specific adaptor proteins during low-density lipoprotein (LDL) receptor internalization, and Numb appears to have a similar role during notch endocytosis (Cestra et al., 1999).

1.2 CLATHRIN-INDEPENDENT ENDOCYTOSIS (CIE)

The term "clathrin-independent endocytosis" is used to define entry pathways that operate in a complementary manner to the clathrin pathway. Profiles of lipids and cargo proteins, the mechanism of entry, and the presence of dynamin, actin, and small GTPase are different but not exclusive for different forms of CIE (Mayor and Pagano, 2007). BAR domain proteins in CIE were already briefly mentioned in the section above.

1.2.1 Dynamin-Dependent CIE processes

CIE endocytosis can be classified based on the presence of a dynamin.

1.2.1.1 Caveolae-mediated endocytosis

One of the examples of this endocytic pathway is caveolae-mediated endocytosis. Caveolae are flask-shaped plasma membrane invaginations (50-80 nm size) that are noticeable by the presence of cavin protein family members. Caveolae are widely present in many cell types. These membranes are enriched in sphingolipids and cholesterol, signaling proteins, and clustered glycosylphosphatidylinositol-anchored proteins (GPI-APs) (Mayor and Pagano, 2007). Whether caveolae are indeed bona fide endocytic carriers for the uptake of cargoes, or whether endocytosis of caveolae sets the number of the structures at the plasma membrane for

functions in mechanoprotection, mechanosignaling, and mechanotransduction is a current matter of debate (Lamaze et al., 2017).

1.2.1.2 RhoA-dependent endocytosis

Another type of dynamin-dependent CIE mechanism is a pathway dependent on the small GTPase Ras homolog gene family member A (RhoA). It was discovered while studying a pathway responsible for the internalization of the β-chain of the interleukin-2 receptor (IL-2R-β) (Lamaze et al., 2001). After ligand binding, IL-2R-β partitions into the detergent-resistant membrane fraction that is usually associated with CIE endocytic processes (Mayor and Pagano, 2007). If the RhoA-mediated process is required for the proper sorting of IL-2R-β into the endocytic pathway or during the endocytic events itself is currently unknown. As RhoA is a key player in the regulation of actin cytoskeleton dynamics, RhoA might be required for recruiting the actin machinery to regulate this endocytic pathway.

1.2.2 Dynamin-independent CIE processes

Dynamin-independent CIE endocytosis was first described in HeLa cells, where expression of mutant dynamin-1 blocked receptor-mediated endocytosis and increased fluid-phase uptake via a CIE pathway (Mayor et al., 2014). One typical feature of constitutive dynamin-independent CIE endocytosis is the involvement of small GTPases: the Rho family member CDC42 (Sabharanjak et al., 2002) and the Arf family member Arf1 (Kumari and Mayor, 2008). This dynamin-independent pathway is the main route for the non-clathrin, noncaveolar uptake of cholera toxin B-subunit (CTxB), *Helicobacter pylori* vacuolating toxin, and of a plant protein ricin (Mayor and Pagano, 2007). These carriers also serve as the main mechanism of fluid-phase internalization in many cell types, and are mainly devoid of cargo from the CME.

The primary carriers that are internalized from the cell surface by CDC42-regulated endocytosis have long and relatively wide surface invaginations, compared to the small spherical carriers (main characteristic of the clathrin and caveolar pathways). That's why a large volume of fluid phase can be co-endocytosed during one budding event in comparison with other mechanisms of internalization (Mayor and Pagano, 2007).

When endocytic processes function autonomously of clathrin and caveolae, electron-dense, clathrin-like coats could not be observed at sites of membrane invagination. Glycosylphosphatidylinositol (GPI)-anchored proteins are the first sets of specific cargo proteins that are associated as markers of clathrin- and caveolin independent endocytic

processes, termed as a clathrin-independent carrier (CLIC)–GPI anchored protein-enriched early endosomal compartment (GEEC) pathway.

Here, internalization occurs via tubular structures. CLIC-GEEC is unaffected by the inhibition of clathrin or dynamin, but it is reactive to the inhibition of the small GTP-binding protein CDC42 (Sabharanjak et al., 2002). Additional studies have identified the cell-surface glycoprotein CD44 as a specific cargo, nd the small GTP-binding protein ADP-ribosylation factor 1 (ARF1), GTPase regulator correlated with focal adhesion kinase 1 (GRAF1; also known as ARHGAP26), cholesterol and actin as main factors in this pathway (Howes et al., 2010; Johannes et al., 2014; Kumari and Mayor, 2008; Lundmark et al., 2008). GRAF1 is a membrane-sculpting BAR domain protein with GTPase-activating activity that colocalizes with and regulates CDC42. Depletion of GRAF1 moderates the uptake of markers of CLIC–GEEC endocytosis without affecting internalization via clathrin-coated pits (Lundmark et al., 2008). The early carriers in the CLIC–GEEC pathway were described at the ultrastructural level. They have uncoated tubular and ring-shaped structures (Kirkham et al., 2005). The pathway is highly active in migrating cells and polarizes to the leading edge of the cells. CLIC–GEEC carriers fuse with early endosomes in a process that is influenced by phosphatidylinositol 3-kinase activity (Kalia et al., 2006).

1.2.3 Other types of CIE

Another process, which can overlap with the CLIC–GEEC pathway, was described by the internalization of major histocompatibility class I (MHCI) molecules and regulation by ARF6 (Naslavsky et al., 2003; Radhakrishna and Donaldson, 1997). These early studies demonstrated that MHCI was internalized into tubular endosomes that were distinguishable from those that contain clathrin-dependent cargo, and initial entry was assumed to be CIE (Naslavsky et al., 2003).

Rab22, HOOK1 and membrane-associated RING-CH (MARCH) ubiquitin ligases are crucial proteins for this ARF6-dependent endocytic process (Eyster et al., 2011; Maldonado-Baez et al., 2013). Other proteins and processes have been associated with CIE. The trafficking pathways in which they participate have been less characterized. These proteins include the epidermal growth factor receptor (EGFR), which is endocytosed via CIE and degraded in response to high EGF concentrations involving reticulon-3 and membrane contact sites (Sigismund et al., 2008; Caldieri et al., 2017). Furthermore, the regeneration of synaptic vesicles at synapses was shown to involve an ultrafast CIE uptake step of large endocytic vesicles of >100nm in diameter (Watanabe et al., 2014).

1.2.4 Actin and CIE

The overall composition of the plasma membrane (PM) is set via an amalgamation of many processes that include lipid synthesis and transport, vesicular secretion and endocytic retrieval. PM local organization arises from its interaction with a dynamic cortical actin and myosin layer juxtaposed to the cell surface. A detailed examination of the cortical layer of the cell surface showed that the membrane is created as a multilayered structure (Rao and Mayor, 2014). It consists of actin filaments of different lengths: longer actin filaments form the static actin mesh, and shorter actin filaments (Rao and Mayor, 2014). They are dynamic structures and ephemerally attached to the cell membrane via linker proteins (Rao and Mayor, 2014).

The actin mesh and fluid-like actin interrelate with the membrane components in order to build an active actin membrane composite. Localized and dynamic remodeling platforms created from short actin filaments are driven by myosin motors into aster-like structures (Gowrishankar et al., 2012). Experimental work suggests that a dynamic actin architecture at the cell cortex engages with lipid-tethered proteins, that are localized at the outer leaflet of the plasma membrane, for creation of regions, where specific lipids are concentrated (Gowrishankar et al., 2012). Although the detailed chemistry underlying the transbilayer coupling of lipids or lipid-anchored proteins and cortical actin filaments demands further elucidation, it involves long acyl chain-containing lipids, which couple across the bilayer in the presence of cholesterol. Cholesterol extends the acyl chains to favor the indentation of these lipids at the interface between monolayers (Johannes et al., 2015). That's why the dynamic actin filament-driven clustering of lipid-anchored proteins could create specialized lipid domains that could serve as sites for endocytosis in the CLIC–GEEC pathway. Besides, a lot of proteins in the membrane are associated with actin. It can be either directly through actin-binding motifs, or indirectly through the presence of sequences that bind to actin linkers (Chen et al., 2014). These motifs allow the dynamic actin machinery to recruit specific proteins and/or drive their dynamics (Johannes et al., 2015).

Actin dynamics can influence CIE. In the RHOA-dependent pathway of CIE, elaborate actin-recruiting machinery that consists of cortactin, p21-activated kinase 1 (PAK1) and neural Wiskott–Aldrich syndrome protein (N-WASP) is necessary for endocytosis (Grassart et al., 2010).

In the CLIC–GEEC pathway, the process of CDC42 cycling between an active or GTP-bound state and it's inactive (GDP-bound form) is required to drive actin polymerization and thus endocytosis (Kumari et al., 2010). Actin polymerization is an important component of membrane scission. Experimental results with model membranes suggest that the recruitment

of actin to an endocytic membrane contributes to local phase segregation of lipids (Liu et al., 2006). This process might act as a driving force for scission via a line-tension-driven mechanism (Liu et al., 2009). Line tension contributes to scission by privileging the spontaneous reduction of tubule diameter in an attempt to reduce the energy penalty associated with domain interfaces (Johannes et al., 2014).

Internalization of Shiga toxin requires actin polymerization on toxin-induced endocytic invaginations to drive the scission of the vesicle via a mechanism that involves membrane reorganization (Romer et al., 2010). That's why actin dynamics coupled to membrane composition and organization can serve as a mechanism to affect CIE from the inside of the cell.

1.2.5 GL-Lect hypothesis

CIE may also be driven by cargoes that bind to the outside of the cell, such as protein toxins (Johannes et al., 2015). The first cargoes that were described to be endocytosed through a non-CME pathway were cholera toxin (from bacteria) (Montesano et al., 1982) and ricin (a plant toxin) (Moya et al., 1985). Further studies revealed that 50% of the early uptake structures for cholera toxin are negative for markers of the clathrin pathway (Kirkham et al., 2005), strongly suggesting that primarily CIE processes facilitate the entry of cholera toxin into cells, even if other endocytic mechanisms might also contribute (Torgersen et al., 2001).

The cellular receptor of Shiga toxin on the apical part of plasma membrane is the GSL globotriaosylceramide (Gb3). It is important for the CIE construction of endocytic pits. According to the current model (Figure 2a), Shiga toxin reorganizes Gb3 molecules (Solovyeva et al., 2015; Pezeshkian et al., 2017a) in order to generate a mechanical membrane potential that creates membrane bending without clathrin (Johannes et al., 2015). Toxin-induced invaginations are then disconnected from the plasma membrane by scission that involves dynamin (Romer et al., 2007), actin (Romer et al., 2010) and the BAR domain protein endophilin A2 (Renard et al., 2015).

Glycosphingolipids (GSLs) participate in the cellular entry of a large number of pathogens and pathogenic factors, like viruses (polyomaviruses, rotavirus, influenza virus and HIV), and toxins such as Shiga, cholera, botulinum and tetanus toxins (Ravindran et al., 2013).

For Shiga toxin, cholera toxin and simian virus 40 (SV40, a polyomavirus), the crystal structures of their carbohydrate-binding (lectin) subunits in interaction with analogs of their cellular GSL receptors have been solved (Ling et al., 1998; Neu et al., 2008; Zhang et al., 1995). These lectins do not have sequence similarity, and yet the 3D structures overlay so that the

carbohydrate moieties of the GSL receptors are similarly oriented: these lectins are pentamers (or have a pentameric fold), and the positioning of their carbohydrate recognition sites with respect to the membrane are conserved (Johannes et al., 2015). These lectins all induce membrane invaginations on interacting with GSLs, and for SV40 the structure of the lipid tail of its cellular receptor, the GSL monosialotetrahexosylganglioside (GM1), was necessary for membrane invagination, CIE and infection (Ewers et al., 2010). Correspondingly, the GSL-based membrane-bending mechanism operates across a broad range of pathogens and pathogenic factors, and a specific molecular architecture that may have evolved to satisfy the geometric requirements of clathrin-independent membrane deformation.

A groundbreaking study extended the concept of lectin-driven, GSL-dependent, clathrin and caveolae-independent endocytosis to endogenous cargo proteins. It was shown that a cellular lectin, galectin-3 (Gal3), drives the biogenesis of CLICs and the cellular uptake of the CLIC cargoes CD44 and β1 integrin (Lakshminarayan et al., 2014). Gal3 functions as an endocytic adaptor that recruits cargoes (glycosylated proteins) and curvature-inducing components (GSLs) into molecular nanoenvironments, the intrinsic properties of which force the plasma membrane to bend. During this process of internalization, tubular endocytic pits are formed without the cytosolic clathrin machinery (Figure 2c).

Gal3 was previously reported to have a stimulatory or an inhibitory effect on endocytosis (Gao et al., 2012). The finding that CIE of the CLIC cargo CD44 was stimulated at concentrations of Gal3 between 0.01 μg ml−1 and 1 μg ml−1 and inhibited at 10 μg ml−1 (Lakshminarayan et al., 2014) provides a possible explanation for this apparent contradiction. It seems likely that endocytic nanocluster formation is favored at low concentrations of Gal3, whereas an extended lattice of Gal3 that prevents cargo internalization can be formed at high concentrations (Johannes et al., 2015). Biological levels of serum localized Gal3 are in the range of 10–60 ng ml−1(Christenson et al., 2010; Iurisci et al., 2000). Such concentrations are consistent with a role for Gal3 in endocytosis. However, higher local concentrations of Gal3 could be reached by the stimulation of Gal3 secretion and its subsequent retention in the glycocalyx (Johannes et al., 2015).

The interaction of Gal3 with the GSL monosialodihexosylganglioside (GM3) has been postulated (Hirabayashi et al., 2002), but it seems to be weak because Gal3 did not visibly bind to pure lipid vesicles or to cells.

1.2.6 Model for pit construction in CIE

Model for pit construction in CIE can be based on 4 elements:

Element 1: intracellular clustering.

The first part of endocytic uptake is that the actin cytoskeleton is a key clustering force in processes of CIE (Rao and Mayor, 2014). However, it is certain that several challenges will be present and should be solved. One of these difficulties is having a more detailed comprehension of the mechanisms of transbilayer coupling for cargoes, like as GPI-anchored proteins, that are associated with the exoplasmic leaflet of the membrane even though actin is on the cytoplasmic leaflet (Johannes et al., 2015). Another challenge is knowing the mechanisms by which the actin-driven long-range (>100nm) focusing on cargoes in certain areas of the plasma membrane leads to their short-range (nanometre distances) condensation within endocytic pits. Evidence is likely to come from unbiased screens (Gupta et al., 2014) or screens dedicated to specific protein classes.

Possible candidates for bridging these gaps are BAR domain proteins like endophilins (Boucrot et al., 2015) if their capacity to interact with endocytic cargo was combined with their scaffolding function (Mim et al., 2012). Extracellular clustering forces can have a role too.

Element 2: Extracellular clustering.

The second part of the endocytosis is that lectins drive CLIC biogenesis (Lakshminarayan et al., 2014). As an oligomeric protein, Gal3 clusters glycosylated cargoes (Partridge et al., 2004). Since Gal3 may also bind directly to protein sequences, it is possible that non-glycosylated cargoes could also be clustered (Shalom-Feuerstein et al., 2008). This has not yet been shown directly, though.

Element 3: Intracellular membrane-bending forces.

A cargo-specific recruitment of BAR domain proteins (Boucrot et al., 2015) could drive clustering and bend membranes by scaffolding (Mim et al., 2012) and/or by helix insertion (Gallop et al., 2006). However, some BAR domain proteins show their membrane-shaping potential only at non-negligible local surface density (Sorre et al., 2012), and specific classes of BAR domain proteins are recruited at later stages of the endocytic membrane invagination process, at least for clathrin-dependent uptake (Daumke et al., 2014). Also, because BAR domain proteins produce very stable domains of phosphoinositide lipids (Zhao et al., 2013), these could be platforms for binding other bending proteins (like epsins), or these domains could drive bending directly by generating line tension (Johannes et al., 2015).

Element 4: Extracellular membrane-bending forces.

The lectin-driven reorganization of membranes containing the raft fabric GSLs represents another driving force for endocytic membrane bending and is the fourth component of the endocytic model (Lakshminarayan et al., 2014). The idea here is that an initial, highly bent

membrane invagination is induced by lectins when they are bound to glycosylated cargoes and GSLs (Johannes et al., 2015). Such narrow plasma membrane curvature radii would then be recognized by cellular machinery, like a BAR domain proteins, that can favor further invagination and regulate the invagination diameter and length, as well as subsequent processing events like scission.

Key tasks are to identify the full list of lectins and cargoes that operate according to this mechanism and their classification within endocytic groups in relation to specific physiological events in living organisms (Johannes et al., 2015).

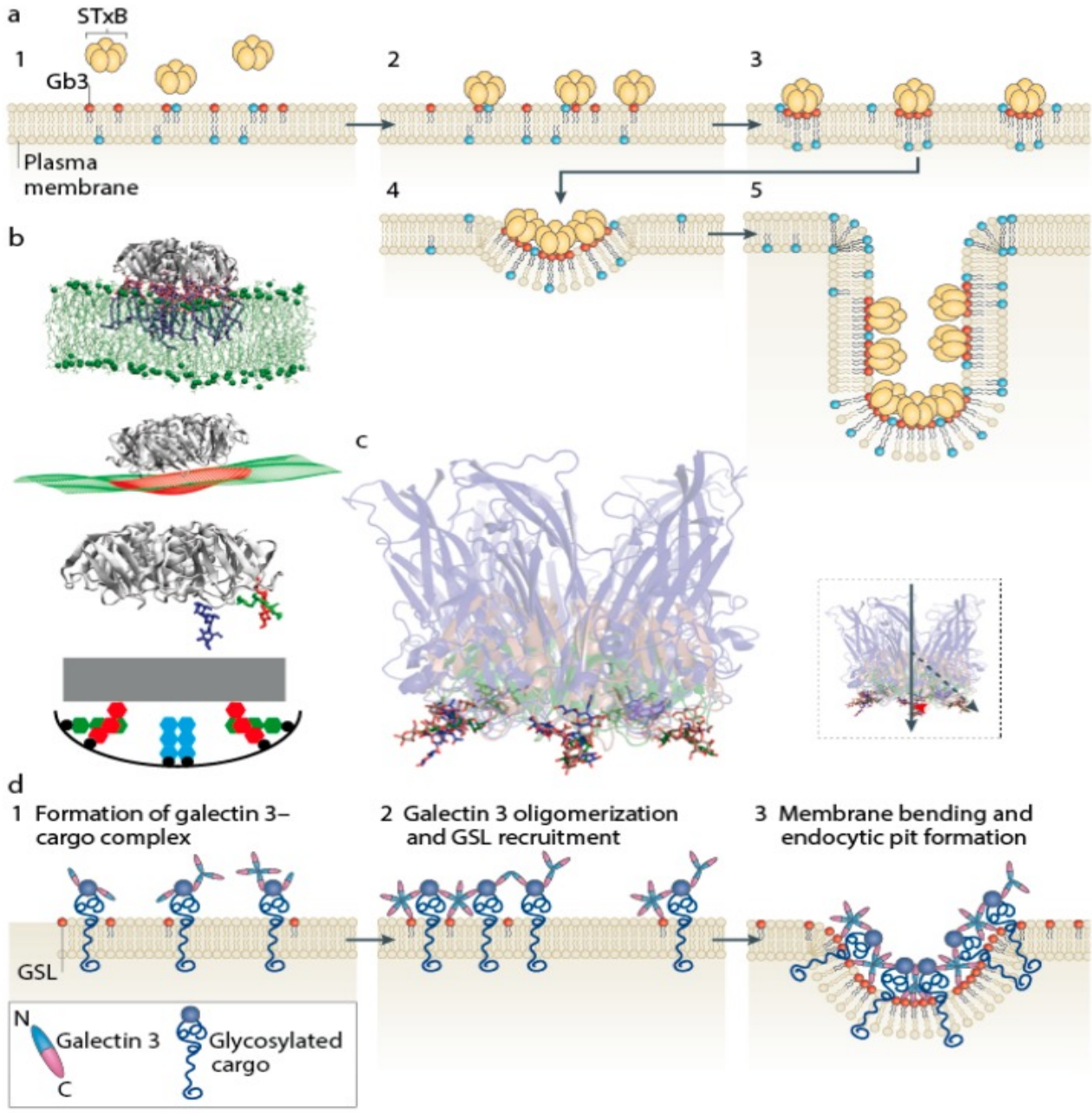

Figure 2: Lectin-driven assembly of tubular endocytic pits. (a) Model for Shiga toxin B-subunit (STxB)-driven endocytosis. Gb3 molecules are represented as a red dots. (b) Height differences between different STxB binding sites imprint an increment of local curvature onto the bilayer. Gb3 head groups in binding sites are represented as red, green and blue. Figure on the bottom: Schematic outlook of Gb3 carbohydrate moieties. STxB represented as gray, Gb3 sugar moieties in the binding sites is represented as red, green, and blue hexagons. (c) Overlays of crystal structures of STxB (represented as green color), cholera toxin B-subunit (represented as red color), and VP1 capsid protein (represented as blue), from SV40. (d) GL-Lect hypothesis on the Gal3-induced, glycolipid-dependent formation of endocytic pits. Glycolipids are represented as red dots. Figure from (Johannes et al., 2016).

2 RECYCLING

Endosomal recycling allows to return internalized proteins and lipids back to the plasma membrane. The balance between endocytosis and recycling process helps to control the composition of the plasma membrane. Recycling plays a role in diverse cellular processes: nutrient uptake, cytokinesis, cell adhesion and others (Grant and Donaldson, 2009).

Internalized are delivered to early endosomes where sorting occurs (Naslavsky et al., 2004), and then from early to late endosomes/lysosomes for degradation, to the trans-Golgi network (TGN) by retrograde trafficking, or to the plasma membrane for recycling.

Early endosomes receive incoming material from primary vesicles that were produced by endocytosis. The small GTPase Rab5, phosphatidylinositol 3-kinase (PI3K) and its product phosphatidylinositol-3-phosphate (PtdIns3P) mark the early endosome and are required for its function. The mildly acidic environment in the lumen of early endosomes facilitates conformational changes on proteins and leads to the release of ligands from receptors (Boucrot and Kirchhausen, 2007).

In the endocytic recycling pathway, proteins can either undergo fast recycling or be transferred to a later, juxtanuclear, endocytic recycling compartment (ERC) (Grant and Donaldson, 2009). Membrane proteins that have been tagged with monoubiquitin or poly-ubiquitin are corralled by the endosomal sorting complex required for transport (ESCRT) and enter multivesicular bodies (MVB).

For the ‘classic’ CME cargo proteins, the transferrin receptor (TfR) and the LDL receptor (LDLR), recycling back to the plasma membrane appears to happen by default and does not require any specific cytoplasmic sequences for recognition and sorting. By contrast, recycling of CIE cargo and signaling receptors may involve a positive selection process (Grant and Donaldson, 2009).

Rab and Arf GTPases and their effectors, the RME-1 family, or Eps15 homology domain proteins (EHD1–4) are regulators of recycling (Grant and Donaldson, 2009).

TfR and GSLs can undergo recycling via a fast route back to the plasma membrane. Rab4 and Rab35 proteins are important for the recycling of the TfR and GSLs from early endosomes (Grant and Donaldson, 2009).

In contrast to fast recycling, the ‘slow’ recycling route involves the transport of cargo proteins from early endosomes to the ERC, and from the ERC to the plasma membrane. One of the hallmarks of ERC is the presence of Rab11 and/or EHD1. Morphologically, the ERC has the shape of a tubular compartment (Grant and Donaldson, 2009).

For the juxtanuclear positioning of the ERC and proper transport of delivered cargo to the ERC some proteins are critical. One of the examples is EH Domain Containing 4 (EHD4). EHD4 is important for export from early endosomes (Sharma et al., 2008). EHD3, also binds to the NPF (Asn-Pro-Phe) motifs of two Rab effectors, rabenosyn5 and Rab11-FIP2 (Naslavsky et al., 2006). The Rab11 effector FIP5 is critical for the transport of TfR from early endosomes to the ERC (Schonteich et al., 2008). The Rab11 effector FIP3 interacts with Rab11 and Arf6 and is important for the juxtanuclear positioning of the ERC (Horgan et al., 2007). Additionally, ASAP, an Arf GAP, can bind to FIP3 and influences ERC positioning (Inoue et al., 2008). Rab22a is also important for the movement of cargo from the early endosome to the ERC (Magadan et al., 2006).

Different recycling pathways from the ERC back to the plasma membrane exist. In HeLa cells the bifurcation from the ERC is distinctive. TfR is recycled back to the plasma membrane in recycling endosomes that are separate from the tubular recycling endosomes that carry CIE cargo back to the plasma membrane (Powelka et al., 2004). Analysis in *C. elegans* also indicates genetically separable recycling for a model CME cargo and a model CIE cargo, suggesting the conservation of bifurcated export from the ERC (Shi et al., 2007).

The CIE recycling pathway was originally described to include Arf6-associated tubular endosomes that emanate from the juxtanuclear ERC carrying recycling cargoes, such as MHCI, back to the plasma membrane (Weigert et al., 2004).

The membrane tubules align with microtubules and undergo recycling back to the plasma membrane. This depends on both, microtubules and actin (Radhakrishna and Donaldson, 1997). Arf6 is essential for the activation of phospholipase D (PLD) (Jovanovic et al., 2006). On tubular recycling endosomes PLD is present. The lipid products of PLD, phosphatidic acid (PA) and diacylglycerol (DAG), are also essential for the recycling function (Jovanovic et al., 2006). PA promotes the release of recycling carriers as it is involved in membrane fission. DAG promotes the fusion of these carriers with the plasma membrane.

Arf6 activates phosphatidylinositol 4-phosphate 5-kinase (PIP 5-kinase), an enzyme that generates phosphatidylinositol 4,5-bisphosphate (PIP_2) (Donaldson et al., 1995). At the cell surface, and at distal portions of tubular endosomes PtdIns (4,5) P2 is present. It is important for the recruitment of membranes of proteins that are involved in vesicle formation, fusion and actin polymerization (Donaldson et al., 1995).

One of the hallmarks of ERC is the presence of Rab11 and of other proteins that can interact with it. As the ERC is the site where slow recycling of TfR occurs, interfering with Rab11 or its interactors can inhibit recycling and alter positioning of the ERC within the cell. The

recycling of CIE cargo MHCI and β-integrin is dependent on Rab11 function (Powelka et al., 2004). Other Rabs are also associated with the ERC or involved in differentiation of the ERC, to form the recycling tubules that carry CIE cargoes back to the plasma membrane (Grant and Donaldson, 2009).

Specific sorting of cargo for endosomal recycling is especially evident in polarized epithelial cells. Schematic representation of recycling is represented on (Figure 3).

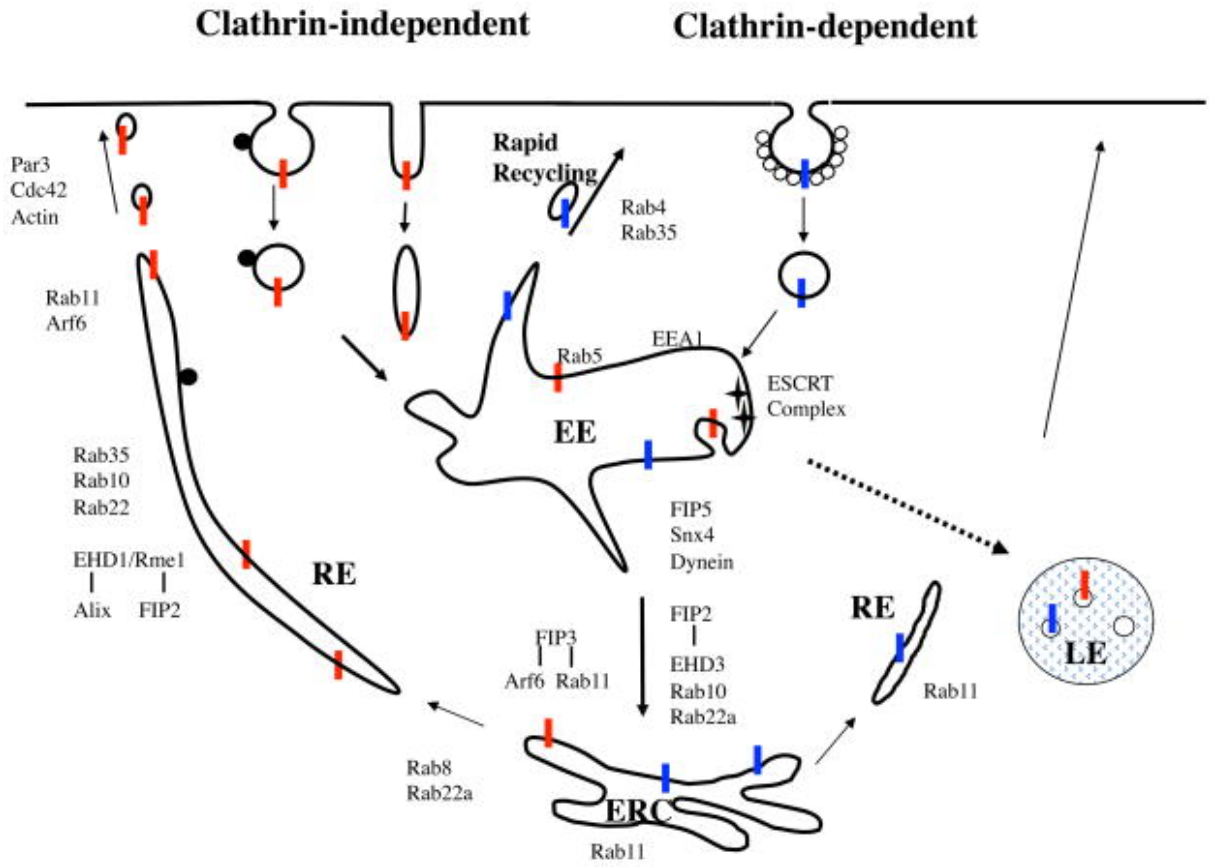

Figure 3: Schematic representation of recycling. Cargo proteins can be endocytosed by CME (represented as blue cargo) or by CIE (represented as red cargo). All cargos are delivered to an early endosome where sorting occurs. Later on cargoes are transported either to late endosomes/lysosoms for degradation, to the TGN, or to the recycling endosomal carriers. Recycling endosomal carriers brings cargo back to the plasma membrane. Rab5 and early endosome antigen 1 (EEA1) are required for the proper function of early endosomes. Certain cargoes (usually those that are tagged with monoubiquitin) are picked in the early endosome by the ESCRT machinery. They then enter the multivesicular body pathway, from where they are transported to the late endosomes (pathway represented as a dashed arrow). CME cargoes can in addition be recycle back to the PM via a rapid recycling route. This pathway involves Rab4 and Rab35. Cargoes from CME and CIE can be transported from the early endosome to the ERC by a route that involves sorting nexin 4 (SNX4), dynein, Rab22A, Rab10, Rab11 family-interacting protein 2 and Rab11FIP5. From the ERC cargo recycling involves Rab11. In addition, distinctive Rab8- and Rab22A-dependent tubules are needed to recycle CME cargo. This is a combined scheme and it can vary between cell types. Figure from (Grant and Donaldson, 2009).

2.1 Transcytosis

Macromolecules can be transferred from one extracellular space to the opposing one via transcytosis (Wang et al., 2018). During transcytosis, receptors and cargoes are internalized and then transported from endosomes to diverse plasma membrane domains. One of the well-known model of transcytosis is the intestinal system of rodents (Wang et al., 2018). Transcytosis in the intestine is a mix of different endocytic pathways.

Rat pups obtain antibodies from their mother's milk by transporting them across the epithelium of their gut via transcytosis. Milk helps to protect the pups against infection. Antibodies in the milk can bind to appropriate receptors on the apical surface of the enterocytes in acidic pH conditions. The receptor-antibody complexes are internalized via clathrin-coated pits and carried to early endosomes. The complexes remain intact. Then they are rescued in transport vesicles. These transport vesicles detach from the early endosome and merge with the basal part of the plasma membrane. Antibodies start to dissociate from receptors after being transported to the neutral pH of the extracellular fluid. Like that they arrive to the offspring bloodstream (Wang et al., 2018). A schematic representation of IgA transcytosis is shown in Figure 4.

Recycling endosomes play a role of an intracellular reservoir of appropriate plasma membrane proteins. This allows them to be mobilized when needed. How transcytosis regulation is occurring is not well known. Transcytosis allows recycling endosomes to adjust the concentration of specific plasma membrane proteins. In polarized epithelial cells, endocytosis occurs from both apical and basal parts of the plasma membrane. Substance that got endocytosed are first delivered into an early endosomal compartment that is specific to the corresponding plasma membrane domain. It allows to endocytosed receptors to be recycled back to the plasma membrane domain from which they came if they don’t hold signals that would permit them to be moved to an alternative part of the cell. Molecules endocytosed from any part of the plasma membrane that are not retrieved from early endosomes get degraded in lysosomes (Wang et al., 2018).

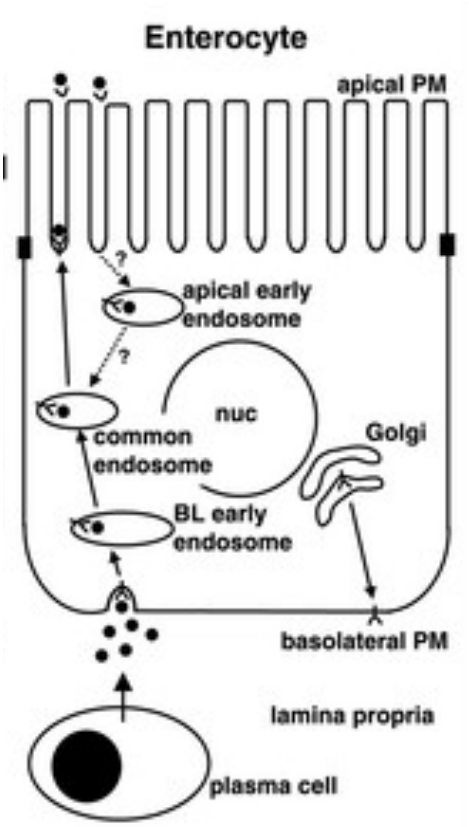

Figure 4: Schematic representation of IgA transcytosis. One of the first described molecules that can undergo trafficking via transcytosis is IgA. IgA receptor (pIgA-R) is synthetized in ER and gets translocated to trans-Golgi network. In *trans*-Golgi network it undergoes sorting. After sorting it is transported to the basal side of the enterocyte. There receptor binds to its ligand. Complex got transcytosed via numerous intracellular intermediates to the apical part of the cell. Figure from (Tuma and Hubbard, 2003).

3 MAIN PLAYERS OF GL-Lect ENDOCYTOSIS

Multiple alternative mechanisms have been uncovered which facilitate the endocytic uptake of cargo molecules and membrane receptors even in the absence of clathrin machinery. One such pathway that has been proposed is the one induced by lectins called galectins. One of these, Gal3, binds to the glycosylated cargoes (like CD44, CD98, integrins) on the plasma membrane, which can further recruit GSLs. In my PhD work, we explored this GL-Lect endocytic pathway in *vivo* in the context of mouse intestinal epithelium. In the next chapters, we will describe the main players of this GL-Lect endocytosis, and then the mouse intestine in which we have studied the physiological role of GL-Lect endocytosis in nutrient uptake.

3.1 GSL

Glycosphingolipids (GSLs) were discovered by Johann Thudichum in 1874. GSLs are ubiquitous membrane constituents. The term GSLs applies to compounds that contain at least one monosaccharide and a sphingoid (Zhang and Kiechle, 2004). GSLs can be subdivided into neutral and acidic GSLs. Acidic GSLs comprise of following sets: the sialosylglycosylsphingolipids or gangliosides, and the sulfoglycosylsphingolipids or sulfatides. GSLs may be categorized as ganglio-series, globo-series, lacto-series type 1, and lacto-series type 2 based on the oligosaccharides core structure.

3.1.1 GSL metabolism

GSL synthesis initiates in the endoplasmic reticulum (ER) by ceramide synthases (CerS) (D'Angelo et al., 2013). This reaction leads to condensation of a sphingoid base with an acyl-CoA. Two products are formed in this reaction: ceramide (Cer) and dihydroceramide. This depends on the substrate that was used (sphingosine or sphinganine) for the reaction (Mullen et al., 2012). Various CerS can catalyze an identical reaction but differ in their substrate preference concerning to the acyl-CoA that is involved (Mullen et al., 2012). This is why Cer and dihydroceramide with diverse acyl chain lengths are produced by different CerS.

Cer is taken up from ER membranes by CERT (ceramide-transfer protein) and transported to the trans-Golgi network (TGN). At the TGN it is used for the synthesis of sphingomyelin (after translocation across the bilayer) (Hanada et al., 2003). Alternatively, Cer can reach the cis-Golgi through vesicular transport, where it undergoes glucosylation in order to produce glucosylceramide (GlcCer) or galactosylceramide (GalCer) (Hanada et al., 2003).

GlcCer and GalCer the main progenitors of all of the GSLs that get synthesized by glycosyltransferases of the Golgi (Merrill, 2011). These enzymes transfer a specific carbohydrate from the proper sugar nucleotide (e.g. UDP-Glc, UDPGal, CMP-sialic acid) to an

appropriate position on a specific type of acceptor (Cer, or the nonreducing end of a growing carbohydrate chain attached to Cer) (D'Angelo et al., 2013).

GlcCer is formed on the cytosolic leaflet of early Golgi membranes. It gets transferred to the lumenal membrane leaflet of the Golgi by an undefined transporter, and gets glycosylated by Golgi-resident glycosylating enzymes, to produce complex GSLs (Holthuis et al., 2001). Alternatively, GlcCer might be picked up from the cis-Golgi membranes by FAPP2-lipid-transfer protein (D'Angelo et al., 2007). With the help of FAPP2, GlcCer is delivered to the TGN, where it is translocated to the lumenal membrane leaflet. This is most probably mediated by the multidrug transporter P-glycoprotein (D'Angelo et al., 2007). GlcCer is later on used for the production of complex GSLs via the action of TGN-specific glycosyltransferases.

After translocation of GlcCer to the luminal leaflet of the Golgi and TGN membranes, it gets galactosylated to produce lactosylceramide (LacCer; Galb1-4Glcb1Cer) by β4-galactosyltransferases V and VI (Nishie et al., 2010). When LacCer is produced, it cannot be transported back to the cytosolic leaflet (Holthuis et al., 2001). LacCer then plays a role as a metabolic branch point for the formation of different classes of complex GSLs:

(a) the β1,4-N-acetylgalactosylaminyltransferase B4GALNT1 for production of GA2 (GalNAc β 1-4Gal β 1-4Glc β 1Cer) (Ishii et al., 1998);

(b) the α-2,3-sialyltransferase ST3GAL5 to produce GM3 (NeuAc α 2-3Gal β 1-4Glc β 1Cer) (Ishii et al., 1998);

(c) the α 1-4-galactosyltransferase A4GALT to produce Gb3 (Gal α 1-4Gal β 1-4Glc β 1-Cer) (Kojima et al., 2000);

(d) the β -1,3-N-acetylglucosaminyltransferase B3GNT5 to produce Lc3(GlcNAc β 1-3Gal β 1-4Glc β 1Cer) (Biellmann et al., 2008).

GA2, GM3, Gb3 and Lc3 are the progenitors for the synthesis of GSLs belonging to the asialo, ganglio, globo/iso-globo and lacto/neo-lacto series. GalCer is transported to the Golgi complex where it undergoes sialylation in order to generate GM4 ganglioside, or sulfated to generate sulfogalactolipids (Merrill, 2011). From the TGN, GSLs and sphingomyelin get translocated to the plasma membrane through membrane-bound transport carriers (D'Angelo et al., 2013). At the plasma membrane, GSLs undergo partial remodeling by appropriate glycosidases (Aureli et al., 2011). Also, GSLs can be translocated along the endocytic routes from the PM to lysosomes, where they undergo degradation. Degradation in lysosomes happens by a number of glycohydrolases and accessory proteins. They assist in step-by-step disassembling of the glycan moieties, up to Cer base (Schulze and Sandhoff, 2011). The Cer in lysosomes then gets catabolized by acid ceramidase for generation of a fatty acid and sphingosine. They can be

translocated to the ER and utilized again for the generation of GSLs (salvage pathway) (Figure 5) (D'Angelo et al., 2013).

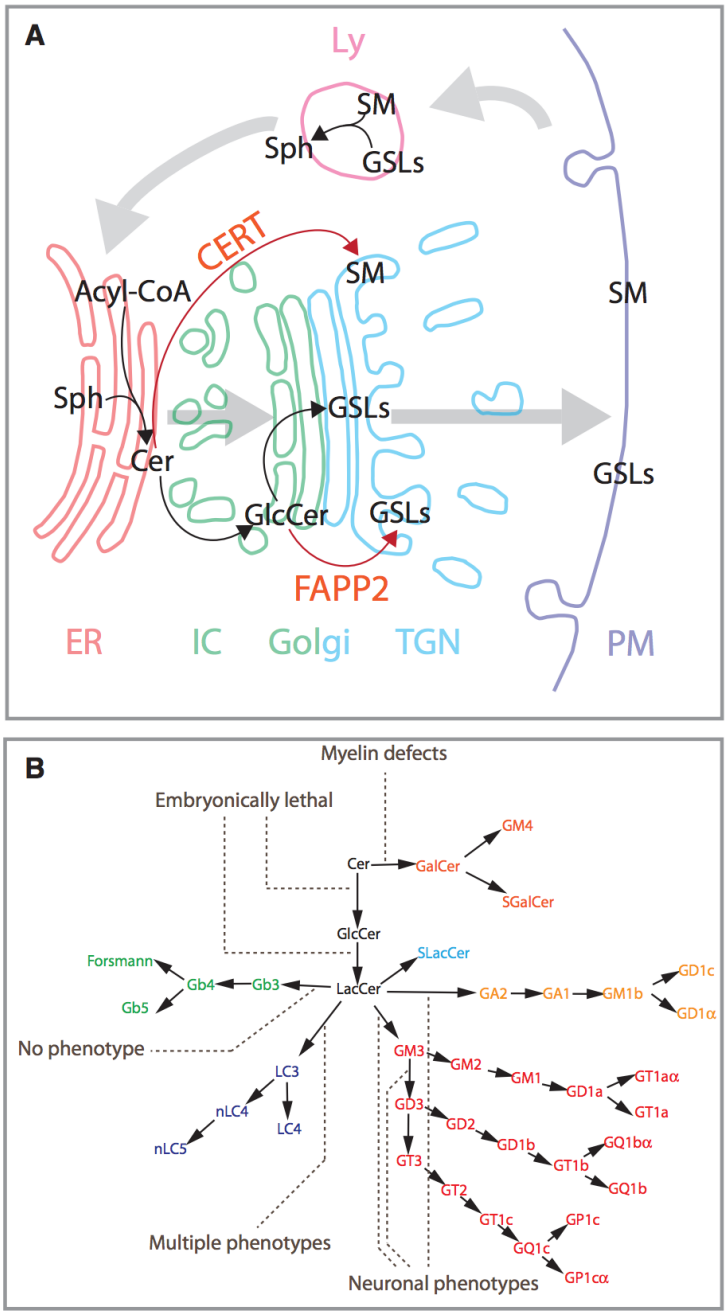

Figure 5: GSL metabolism at glance. (A) Localization of metabolites in the GSL metabolic pathways. IC, abbreviation for intermediate compartment; Ly, abbreviation for lysosomes. (B) Schematic representation of GSL metabolism. Green color indicates globo series GSLs; blue color indicates lacto/neolacto series GSLs; red color indicates ganglio series GSLs; light orange color indicates asialo series GSLs; dark orange color indicates gala series GSLs. Figure from (D'Angelo et al., 2013).

3.1.2 GSL function

3.1.2.1 GSL as a plasma membrane component

GSLs comprise less than 5% (in erythrocytes) to more than 20% (in myelin) of the total plasma membrane lipids in "higher" animals (Schnaar and Kinoshita, 2015). GSLs are not uniformly distributed in the plane of the membrane but cluster in "lipid rafts".

The raft hypothesis had a great influence on the field of cell biology (Simons and Ikonen, 1997). The hypothesis suggested that mixtures of particular types of amphiphilic molecules will phase-separate into nanodomains, that will be enriched in sphingolipids and cholesterol (the raft lipids) that coexist in thermodynamic equilibrium, with the bulk membrane enriched in phospholipids. This phase separation is controlled by the difference of the molecular packing of the raft lipids and the bulk membrane lipids.

According to a more recent version of the raft hypothesis, proteins (or other inducers) directly influence on raft lipid distributions (Niemela et al., 2010). Protein-induced proximity between raft lipids enables 'raft connectivity', which then contributes to the stabilization of larger protein–lipid raft assemblies that can carry out biological functions (Simons and Gerl, 2010).

When several small raft domains exist in a membrane, it will be energetically more convenient to bring them along into one bigger domain. This reduces the total domain perimeter length. (Johannes et al., 2018b).

Multicomponent lipid membranes have the capacity to form domains associated with equilibrium phase coexistence, like the liquid-ordered (lo) – liquid-disordered (ld) coexistence known from domains in multicomponent vesicles *in vitro*. The lo phase has been identified with the previous-mentioned raft phase (Johannes et al., 2018). Even at conditions of phase coexistence, such nanodomains can be stabilized by the presence of membrane proteins (Gil et al., 1997). Membrane proteins insert themselves in the bulk of the domain (Johannes et al., 2018). The term 'lipid shell' has been coined in order to describe this situation (Anderson and Jacobson, 2002). At close distances, bridging between such nanodomains gives rise to strong attraction between proteins with a free energy gain of lD, where l is the line tension and D is the lateral extent of the protein (Johannes et al., 2018). This mechanism gives rise to aggregation of specific proteins into clusters in a lipid-sorted environment, such as in the lipid rafts described above (Johannes et al., 2018).

It should be mentioned that this clustering mechanism is different from the partitioning of proteins into the lipid domains (Johannes et al., 2018).

Another interesting capillary type of protein aggregation mechanism occurs if the proteins are

interfacially active (i.e., different parts of the protein solubilize in distinct lipid environments, e.g., lo and ld) (Gil et al., 1998). These proteins sit at the boundary between domains and experience an attractive force that results from their mutual lowering of the interfacial energy (Johannes et al., 2018). Such proteins can be stabilized in clusters within a microphase separated lipid environment (Johannes et al., 2018).

Analysis of different biological membrane preparations have demonstrated many cell membranes have lipid compositions that are close to lo–ld coexistence in equilibrium driven by lipid chain melting and cholesterol (Heimburg and Jackson, 2005).

3.1.2.2 GSL function *in vivo*

Despite the progress that was achieved on the understanding the function of GSL *in vitro*, their molecular mechanisms of function *in vivo* are not yet well known. Studies involving genetic elimination of the GSL synthesis pathways in mice have been used in order to uncover in their function *in vivo* (Allende and Proia, 2014).

Some of the mechanisms by which GSLs apply their functions at a cellular and molecular level are beginning to be understood (Merrill, 2011). Their primary function is to serve as building blocks of the plasma membrane. In this case, GSLs, because of their ability to phase separate, can stabilize the formation of functionally and structurally discrete plasma membrane domains (Cantu et al., 2011). GSLs, through their glycan head groups, act as binding sites for pathogens and toxins (D'Angelo et al., 2007): Shiga toxin (Gb3), cholera toxin (GM1), and the heat-labile *E.coli* toxins LT-1 (GM1), LT-IIa (GD1b>GD1a>GM1), LT-IIb (GD1a). Via lateral interactions with membrane proteins, such as the insulin and epidermal growth factor receptors, GSLs can control the force of receptor-mediated signaling pathways (Coskun et al., 2011). EGFR activity can be regulated by its lipid environment and is inhibited by interaction with the ganglioside GM3 (Coskun et al., 2011). GSLs can function during endocytosis by participating in the internalization of diverse cargoes (Lakshminarayan et al., 2014).

UDP-glucose:ceramide glycosyltranferase (GlcCer synthase) is the vital enzyme for GlcCer-based GSL biosynthesis. In the mouse it is expressed by the Ugcg gene (Miljan et al., 2002). GlcCer synthase catalyzes the creation of GlcCer by the transfer of a glucose from UDP-glucose to ceramide.

Ttal genetical elimination of the Ugcg gene in mice is early embryonic lethal (Yamashita et al., 2002). Ugcg knockout (KO) embryos grew until gastrulation at E6.5, where they still form ectodermal, endodermal, and mesodermal layers (Allende and Proia, 2014). The following day, mutant embryos show signs of apoptosis, demonstrating that GlcCer-based GSL synthesis is

essential for mammalian embryonic development (Yamashita et al., 1999). GSLs (in the form of gangliosides) play a critical role during the formation of these tissues (Lopez and Schnaar, 2009). To identify the function of these lipids during the formation of a fully-functional nervous system, two independently derived lines of mice missing Ugcg in neuronal and glial cells were established. This was done through combination of a floxed Ugcg allele and Cre recombinase under the nestin promoter and enhancer (NesCre) (Jennemann et al., 2005; Yamashita et al., 2005). NesCre-Ugcg KO mice were normal at birth. The animals established neurologic abnormalities later on. In animals done by Jennemann et al. (Jennemann et al., 2005), levels of Ugcg mRNA and gangliosides in brain were nearly eliminated. These mice died by 3 weeks of age. These animals exhibited very stark neurological symptoms. The line bred in the Proia laboratory (Yamashita et al., 2005) demonstrated vestigial Ugcg expression, and partial elimination of ganglioside levels in the brain, as well as a longer life span. These mice also displayed atypical gait, with a loss of Purkinje cells (Jennemann et al., 2005).

These studies show that GlcCer-based GSL synthesis is not required for embryonic development of the nervous system, but is needed for its appropriate development, stability, and function after birth (Allende and Proia, 2014).

The genetical elimination of Ugcg restricted to neuronal cells was achieved by generating floxed Ugcg mice expressing the Cre under the L7 control. These mice showed loss of Purkinje cells at about 3–4 months of age (Allende and Proia, 2014).

During other experiments, Ugcg was deleted after birth in neurons with an inducible Cre recombinase (Cre-ERT2) and calcium/calmodulin-dependent kinase II α promoter (CamK). These mice showed radical body-weight gain. This phenotype was rescued by virus-induced expression of Ugcg in the arcuate nucleus (Arc) of the hypothalamus (Nordstrom et al., 2013).

Ugcg was deleted specifically in oligodendrocytes due to mating floxed Ugcg mice with Cre mice carrying the myelin-associated enzyme 2′, 3′ cyclic nucleotide 3′ phosphodiesterase (CnpCre) promoter (Saadat et al., 2010). The newborn CnpCre-Ugcg KO mice did not show any myelin abnormalities, indicating that oligodendrocyte GlcCer-derived GSLs, unlike those produced by neuronal cells, are not essential for myelin structure and stabilization.

Keratinocytes create significant amounts of GSLs, primarily GlcCer. It covers 4 % of the total lipid content in the epidermis. It is packed into lamellar bodies and transported to the stratum corneum for further modifications in order to generate ceramide (Rabionet et al., 2014). Floxed Ugcg mice were mated with a line, having a keratin specific promoter (Jennemann et al., 2007). New-born mice showed epidermal dehydration and died at 4 days of age. These experiments revealed that Ugcg expression is vital for the construction of an efficient epidermal permeability

barrier via the generation of GlcCer, a precursor for the development of ceramide in the skin.
The liver is a main organ monitoring sphingolipid metabolism (Li et al., 2009). A liver-specific elimination of Ugcg was achieved by mating floxed Ugcg mice with mice carrying Cre with albumin promoter (AlbCre-Ugcg mice) (Jennemann et al., 2010). These mice had greatly reduced GSL levels in liver and plasma, pinpointing the liver as the major source of plasma GSLs. No other additional phenotype was detected in the AlbCre-Ugcg mice, even after shifting animals to a high-fat diet, arguing against a vital role of hepatic GlcCer synthesis in glucose control, liver steatosis, or cholesterol metabolism.
GSLs are highly condensed in the enterocytes. Enterocyte-specific Ugcg-deficient mice were generated by mating floxed Ugcg mice with mice expressing Cre recombinase under the control of the villin promoter. This promoter was induced either in the embryo (using VilCre-expressing mice) or during adult life (using VilCre-ERT2-expressing mice) (Jennemann et al., 2012). Glycerol-derived GSLs were absent in the intestines of the VilCre-Ugcg offsprings. Although indistinguishable from control litter at birth, VilCre-Ugcg offsprings did not gain weight and died by postnatal day 8. These animals showed normal polarization of the enterocytes, but had atypical mucosal villi, decreased fat deposits, and a decrease in the capacity of enterocytes to take up lipids. Inducible VilCre-ERT2-Ugcg mice showed a complete absence of intestinal GSLs 4 days after tamoxifen induction, which was associated with significant structural modifications in the villous epithelia (Jennemann et al., 2012). These mice had decreased body weight and reduced lipid absorption by enterocytes. These studies showed that GlcCer-derived GSLs are needed for proper intestinal function (Jennemann et al., 2012).
Since the establishment of the first GSL knockout mice (Takamiya et al., 1996), researchers have seen a remarkable increase in understanding of the roles of GSLs in physiology. Researchers have understood that they are not only required for embryonic development, but also have many tissue-specific functions (Allende and Proia, 2014).

3.1.3 GSL as receptors for exogenous microbial virulence factors

3.1.3.1 Cholera toxin

Cholera toxin (CTx) is the cause of cholera and it consists of a homopentameric B-subunit (5x11 kDa) and a single A-subunit with two domains termed the A1- and A2-peptides. The homopentameric B-subunit (55 kDa) binds with high apparent affinity at the apical cell surface to its ligand GM1. In 1974 Heyningen described a function of GSLs as receptors of CTx. In order to find the GM1 binding sites of the B-subunit, co-crystallization was performed (Merrill,

2011).

Binding of B-subunit to GM1 drives the toxin's endocytosis and its retrograde transport through endosomes, trans-Golgi network, and Golgi to the ER. In the ER, the A-subunit fragments separates and are translocated through the Sec61 channel into the cytosol (Figure 6) (Schmitz et al., 2000; Wernick et al., 2010). CTx can also bypass the Golgi to access the ER (Spooner et al., 2008).

Retrograde ER transport is an intrinsic property of GM1 (Wernick et al., 2010; Wolf et al., 1998). Acyl saturation promotes GM1 association with lipid rafts in the cell (Panasiewicz et al., 2003).

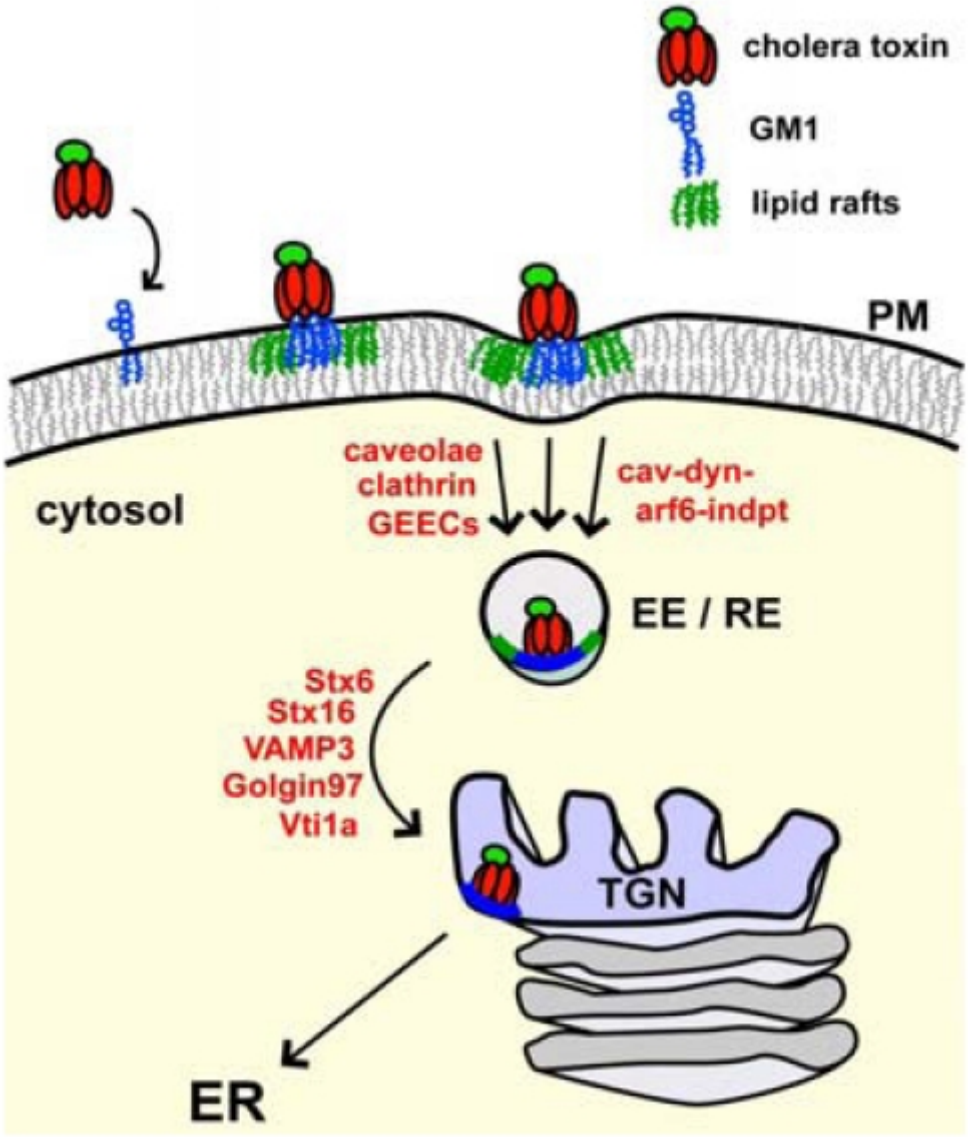

Figure 6: Schematic representation of CTxB retrograde trafficking from the plasma membrane to the ER. CTx binds to the ganglioside GM1 (blue) that can be found in membrane microdomains (lipid rafts-green) at the plasma membrane of host cells. The toxin enters the cell by different endocytic mechanisms. Retrograde trafficking to the TGN involves different proteins like V- and T-SNAREs. From the TGN, the toxin traffics to the ER. In the ER, the A1-chain is unfolded and retro-transported to the cytosol. Figure from (Wernick et al., 2010).

3.1.3.2 Verotoxins (VTs, Shiga toxins)

Verotoxins (VT) are a family of *E. coli* produced AB5 subunit toxins that are responsible for the pathology of hemolytic uremic syndrome (HUS) (Wolf et al., 1998). This disease is primarily renal glomerular nephropathy that causes anemia and thrombocytopenia (Ray and Liu, 2001). The toxins' target are endothelial cells of the microvasculature. Shiga toxin is a VT homolog and it is a pathogenic protein that is produced by *Shigella dysenteriae.*

In the cytosol of target cells, the A-subunits of Shiga/verotoxins promote the deadenylation of position 4324 of 28S ribosomal RNA, which leads to protein biosynthesis inhibition and causes cell death. The A-subunits by itself cannot enter the cells. For cellular entry, they need the non-covalent interaction with receptor-binding homopentameric B-subunits. All of these toxins have a unique cellular receptor: the neutral GSL globotriaosylceramide (Gb3 or CD77) (Johannes and Romer, 2010).

The receptor-binding B-subunit of Shiga toxin (STxB) is a homopentameric protein of 35 kDa. Each STxB pentamer displays a total of 15 Gb3 binding sites (Ling et al., 1998), and each of these binding sites has only millimolar affinity for the globotriose sugar moiety of Gb3 (Pina and Johannes, 2005). One STxB pentamer can be in contact with several Gb3 molecules at a time. In order to remove STxB from the membrane, all of these interactions have to be dissociated at the same time, which is statistically unlikely (Johannes and Romer, 2010). This avidity effect is a general hallmark of lectins and will be favored if the GSLs that function as toxin receptors, are clustered themselves, such that several receptor binding sites on toxin pentamers would be occupied right at the initial contact with the plasma membrane of target cells. Using an electron microscopy technique, nanoclusters have indeed been found for the gangliosides GM1 and GM3 (Fujita et al., 2007). This corresponds to the situation that is known for another class of glycosylated lipids, glycosylphosphatidylinositol (GPI)-anchored proteins, which were equally described to exist in membranes as nanoclusters of a few molecules (Goswami et al., 2008).

No direct interaction between Shiga toxins has been found. Yet, on model membranes (Romer et al., 2007) and cells (Pezeshkian et al., 2017b), Shiga toxin clusters. This fact suggests that a membrane-mediated mechanism drives toxin molecules together. Based on theoretical considerations, computer simulations, and experiments in model membrane systems and on cells, an novel hypothesis has been proposed according to which Shiga toxin molecules would suppress thermally excited membrane fluctuations not only at sites at which they bind but also on the membrane patch between 2 adjacent toxin molecules, as long as these are not further apart then roughly the size of toxin itself (Pezeshkian et al., 2017b). Unperturbed fluctuation of

the membrane outside this toxin-delineated patch would push the toxin molecules together, even if there is no direct attractive force. On theoretical considerations, such thermally induced membrane fluctuation forces (also termed thermal Casimir-like forces) (Nguyen et al., 2016) are expected to be as strong as electrostatic or van der Waals interactions, as long as the membrane inclusions that generate them are several nanometers in size (Pezeshkian et al., 2017b). As opposed to electrostatic or van der Waals interactions that operate at subnanometric distances, membrane fluctuation forces would have an effective radius of several nanometers, which corresponds to a gap in the interaction landscape of biological membranes between cytoskeleton-driven clustering that operates at tens to hundreds of nanometers (Rao and Mayor, 2014), and the conventional subnanometric interaction forces. Thus, initial contacts that could be favored by the fluctuation forces would need to be further stabilized by other interactions for the generation of biologically meaningful outputs and to avoid that all proteins (or nanoparticles) that are submitted to fluctuation forces coalesce into one big aggregate.

Next, Shiga toxin does not directly reach through the plasma membrane in order to interact with the clathrin machinery. Despite this, Shiga toxin has been found in CCP (Sandvig et al., 1989), even if blockage of clathrin function causes at most a 35% reduction of Shiga toxin uptake (Lauvrak et al., 2004). How this localization into the clathrin pathway is operated is not yet well understood.

A sizable fraction of Shiga toxin is internalizedin cells that have been treated with inhibitors of clathrin pathway inhibition (Johannes, 2017). How membrane bending and endocytic pit formation are operated in these cases had remained unknown. Based on the fact that the formation of a Shiga toxin-Gb3 complex is necessary and sufficient to drive the formation of narrow tubular membrane invaginations (Romer et al., 2007), a molecular hypothesis has recently been suggested for how this might be achieved (Figure 7a). According to the model, the Shiga toxin-Gb3 complex have curvature-active properties, i.e., the capacity to deform the membrane without the need of the cytosolic clathrin machinery.

The binding site geometry is preserved for the receptor-binding parts of cholera toxin and simian virus 40 (SV40), for which it was shown previously that they also have curvature-active properties, endowing them with the capacity to drive tubular membrane invaginations through interaction with their GSL receptor molecules (Ewers et al., 2010), as known for Shiga toxin (Romer et al., 2007). Strikingly, these GSL-binding pathogenic lectins do not have sequence similarities, and the capacity to induce narrow membrane bending may originate from convergent evolution towards a common function: membrane mechanical work for inward-oriented curvature generation for the construction of endocytic pits.

Shiga toxin-induced membrane invaginations can be scissioned from the plasma membrane via the fusion of the opposing walls of invaginated tubular endocytic pits. Dynamin affects Shiga toxin uptake, but is not strictly required (Romer et al., 2007). The difficulty with coming to a conclusion for the involvement of dynamin is that feedback loops exist to actin (Taylor et al., 2012), which also contributes to the scission of Shiga toxin-induced membrane invaginations (Romer et al., 2010). It was shown that these invaginations are prone to undergo domain formation, thus generating domain boundary forces that drive the spontaneous line tension-driven squeezing of the tubule membrane. This process leads to scission (Johannes et al., 2014). Actin was found as one of the domain formation triggers (Romer et al., 2010).

Recent studies showed that an additional scission mechanism might operate on Shiga toxin-induced membrane invaginations. Endophilin-A2 (EndoA2) was shown to be localized onto Shiga toxin-induced membrane invaginations (Renard et al., 2015). Furthermore, it was shown for Shiga (Renard et al., 2015) and cholera toxin (Day et al., 2015) that these invaginations are pulled upon by microtubule-based dynein motor activity. Several scission modalities operate on Shiga toxin-induced membrane invaginations: dynamin (Romer et al., 2007), actin (Romer et al., 2007), and EndoA2/dynein (Renard et al., 2015). It could be shown that when interfering with each of these individually or in combination, the effects on scission appear to be roughly additive (Renard et al., 2015), proposing that the overall probability of scission is the result of individual contributions (Figure 7) (Johannes and Romer, 2010).

When Shiga toxin-containing carriers are formed, they are trafficking to endosomes. This is happening in association with microtubules (Hehnly et al., 2006). vSNARE proteins (VAMP2, VAMP3, and VAMP8) can be recruited to endocytic carriers with Shiga toxin (Johannes, 2017). From endosomes, Shiga toxin is transported through the retrograde route to the TGN, the Golgi apparatus, and to the ER. From ER the Shiga toxin catalytic A-subunit is translocated to the cytosol (Spooner and Lord, 2012). The research on Shiga toxin proposed the existence of a trafficking interface between early endosomes and the TGN (Mallard et al., 1998), which has since become a hotspot of membrane biology research. Shiga toxin trafficking at this interface has been described to depend on Rab6 (Mallard et al., 2002), SNARE complexes involving syntaxin-16 (Mallard et al., 2002) and syntaxin-5 (Tai et al., 2004), epsinR (Saint-Pol et al., 2004), Arl1 (Tai et al., 2005), OCRL (Choudhury et al., 2005), retromer (Popoff et al., 2007), the tethering complex GARP (Perez-Victoria et al., 2008) and the GARP interactor TSSC1 (Gershlick et al., 2016), the ARF1 GAP protein AGAP2 (Shiba et al., 2010), GPP130 (Mukhopadhyay and Linstedt, 2012), the ERM proteins ezrin and moesin (Kvalvaag et al., 2013) annexins A1 and A2 (Tcatchoff et al., 2012), and UNC50 (Selyunin et al., 2017).

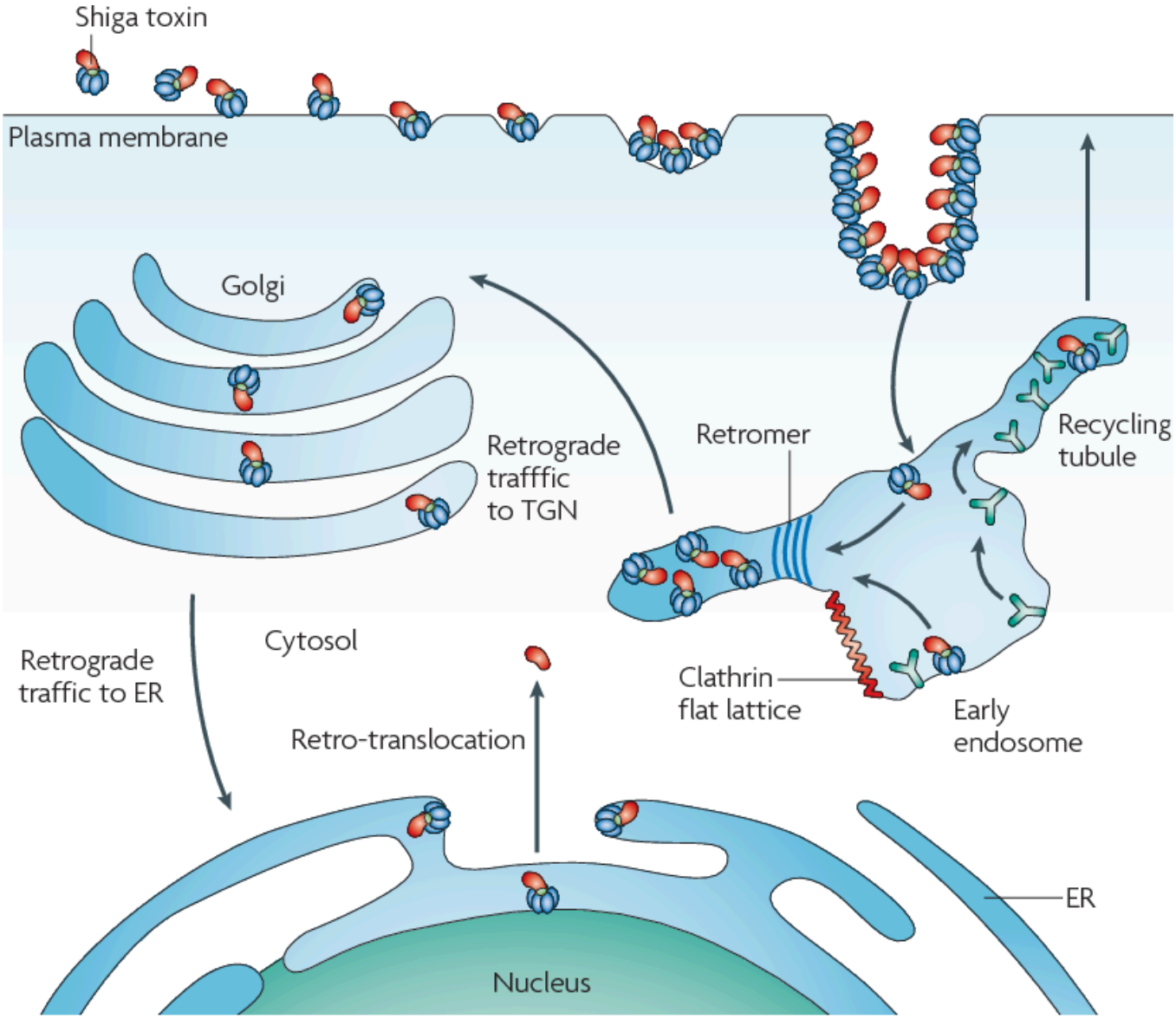

Figure 7: Trafficking of Shiga toxins. A schematic representation of intracellular trafficking of Shiga toxins. Toxin binding to the plasma membrane induces local spontaneous membrane curvature followed by clustering and endocytosis. Then toxin follows retrograde sorting in early endosomes, where retrograde tubules are formed. These retrograde tubules then undergo scission in a retromer-dependent manner. Then, Shiga toxins bypass the late endocytic pathway and are transferred directly from early endosomes to the trans-Golgi network and from there on to the endoplasmic reticulum (ER). Shiga toxins use ER-associated degradation machinery for retrotranslocation into the host cell cytosol. Figure from (Johannes and Romer, 2010).

3.1.4 Glycosphingolipid-related diseases

GSLs are involved in the pathogenesis of different diseases. Congenital metabolic disorders involving GSL pathway enzymes cause glycosphingolipidoses. The main hallmark of these disorders is a blockage of GSL degradation in lysosomes due to enzyme deficiency. Glycosphingolipidoses are the most predominant subgroup of the lysosomal storage disorders and are categorized by the accumulation of one or multiple GSLs (Jeyakumar et al., 2002). Glycosphingolipidose disease is frequently present with progressive neurodegenerative disease course (Jeyakumar et al., 2002). Tay–Sachs and Sandhoff diseases form a subcategory, termed GM2 gangliosidoses, which are due to GM2 ganglioside accumulation in cells, secondary to hexosaminidase deficiency (Schnaar and Kinoshita, 2015).The primary enzyme deficiencies are ß-hexosaminidase A in Tay–Sachs disease and ß-hexosaminidases A and B in Sandhoff disease. As only ß-hexosaminidase A degrades GM2 ganglioside, the substrate accumulates in both diseases. Both diseases lead to early death in childhood.

GSLs function as allogeneic antigens in humans (eg, blood group ABH, Lewis, I/I and PP1Pk), or as heterogenetic antigens (eg, Forssman antigen and Gal) (Hakomori, 2003). Anti-ganglioside antibodies can be detected in different autoimmune diseases, such as Guillain-Barré syndrome, chronic idiopathic ataxic neuropathy, multifocal motor neuropathy, Miller-Fisher syndrome, and neuropathy with IgM paraproteinemia (Fredman, 1998). GSLs are involved in numerous biological processes and they form a unique group of molecules because they consist of chemically joined carbohydrate and lipid parts.

3.2 GALECTINS

Galectins were discovered based on their galactoside binding activity. Members of this protein family share primary structural homology in their carbohydrate-recognition domains (CRDs). The canonical CRD of galectins has approximately 130 amino acids, although only eight residues are involved in carbohydrate binding (Cummings and Liu, 2009).

Also, another dozen residues appear to be highly conserved. Galectins have been identified in animals based on the conserved CRD. Although most of them recognize simple β-galactosides, the binding affinity for such structures is relatively weak. 15 galectins are expressed in mammals, but only 12 galectin genes are found in humans, including two for galectin-9 (Cummings and Liu, 2009). They have various physiological and pathological functions (Johannes et al., 2018).

Galectins have been classified into three major groups (Figure 8) (Sciacchitano et al., 2018):

1) The prototypical galectins. These have one CRD and may associate to form homodimers.

2) The chimeric Gal3, which is structurally unique as it contains a C-terminal CRD linked to an N-terminal protein-binding domain.
3) The tandem-repeat galectins (galectin-4, -6, -8, -9 and -12) with two CRDs that are linked via a small peptide domain.
Galectin transcripts can be differentially spliced in order to generate different isoforms.
Most members of galactin family bind simple β-galactosides, such as disaccharides or trisaccharides, but the affinity is relatively weak (i.e. in the high micromolar to low millimolar range). On the contrary, galectin binding to natural glycoconjugate ligands expressed on the cell surfaces or in the extracellular matrix is usually of much higher affinity (i.e., in the micromolar or submicromolar range) (Leffler et al., 2002). Different factors contribute to increasing affinity, such as the natural multivalency through the oligomeric state of the galectins, the multivalency of their natural glycoconjugate ligands, and the mode of presentation of the glycans (Leffler et al., 2002).
Each galectin CRD recognizes different types of glycan ligands and shows the highest affinity binding to different structures (Leffler et al., 2002). The binding sites of galectins can be viewed as containing several subsites: one for galactose, another for N-acetylglucosamine, and still other subsites that may be filled by other sugars and the aglycone moiety, such as a peptide or lipid (Rabinovich and Thijssen, 2014).
Galectins can bind selectively to the cell-surface and extracellular matrix ligands. The exact physiological roles of these interactions with each galectin are not well understood. However, it is known that galectins are synthesized as cytosolic proteins, reside in the cytosol or nucleus for most of their lifetime and reach their galactoside ligands only after non-classical secretion that bypasses the Golgi complex (Cummings and Liu, 2009). Galectins and their binding ligands can contribute to cell-cell and cell-matrix interactions (Leffler et al., 2002). Galectin-dependent signaling at the cell surface can modulate cellular functions. Also, intracellular galectins can interact with their intracellular ligands in order to regulate cellular activities and can contribute to the fundamental processes such as pre-mRNA splicing (Rabinovich and Thijssen, 2014).

3.2.1 Roles of galectins in immune responses, inflammation, and animal development

One of the major functions of galectins is to regulate immune and inflammatory responses (Cummings and Liu, 2009). Gal1 function is associated with attenuating inflammatory responses. In contrast, Gal3 has a proinflammatory role. Different galectins (including Gal1, 2, 3, 7, 8, 9, and 12) are able to induce apoptosis in different types of blood cells (Leffler et al.,

2002). Galectins play important, but rather subtle roles in animal development. Lack of Gal3 in knockout mice is associated with phenotypic changes, such as fatty liver disease, reduced mast cell function, reduced liver fibrosis upon induced liver damage, and age-dependent glomerular lesions (Sciacchitano et al., 2018). Lack of galectin-1 in mice is associated with a decreased sensitivity to noxious thermal stimuli, altered primary afferent neural anatomy, aberrant topography of olfactory axons, and reduced muscle regeneration ability after injury (Sciacchitano et al., 2018). It might be possible that the redundancy between galectin family members contributes to the survival of null mutants, or that these particular galectins are involved only in post-developmental processes, such as immune regulation. Consistent with this possibility, the inflammatory response in Gal3-null mice is dampened, and there is a decline in infiltrating neutrophils (Leffler et al., 2002).

3.2.2 Roles of Galectins in Cancer

Melanomas, astrocytomas, bladder and ovarian tumors overexpress different types of galectins, and their overexpression usually correlates with the clinical progression of the tumor. Gal1, 3, and 9 are involved in cancer progression and metastasis (Rabinovich and Thijssen, 2014). The apoptotic and immunosuppressive effects of Gal1 might contribute to tumor pathology, as revealed by knockdown studies, where decreased Gal1 expression is associated with decreased tumor survival, due to increased survival of IFN-γ-producing Th1 cells and heightened T-cell-mediated tumor rejection (Rabinovich and Thijssen, 2014). Thus, galectins might play important roles in tumor progression and metastasis due to indirect effects in regulating tumor immune responses and direct effects in tumor angiogenesis (Rabinovich and Thijssen, 2014).

3.2.3 Roles of Galectins in Innate Immunity

Even though the expression of galectins in animal tissues is tightly regulated, their expression can be induced, and this is very crucial in innate immune responses (Rabinovich and Thijssen, 2014). Also, Gal3 directly induces the death of *Candida albicans* via binding to β1-2 oligomannosyl residues (Liu et al., 2002).

Despite the incredible increase in understanding the functions of galectins, there are still questions that should be answered such as the molecular mechanisms of their actions in the intra- and extracellular space, and the relationship between these behaviors, as well as any associated regulatory loops.

The many physiological and pathological functions of galectins in cells and in organism are presented on Figure 9 and 10. One of the major challenges in the field of glycobiology is to

elucidate the quantitative aspects of galectin localization in cells and tissues, and the redundancies and role of galectins in health and disease. Uncovering these issues will help to clarify the cellular and organismal functions of galectins and their potential therapeutic applications (Johannes et al., 2018).

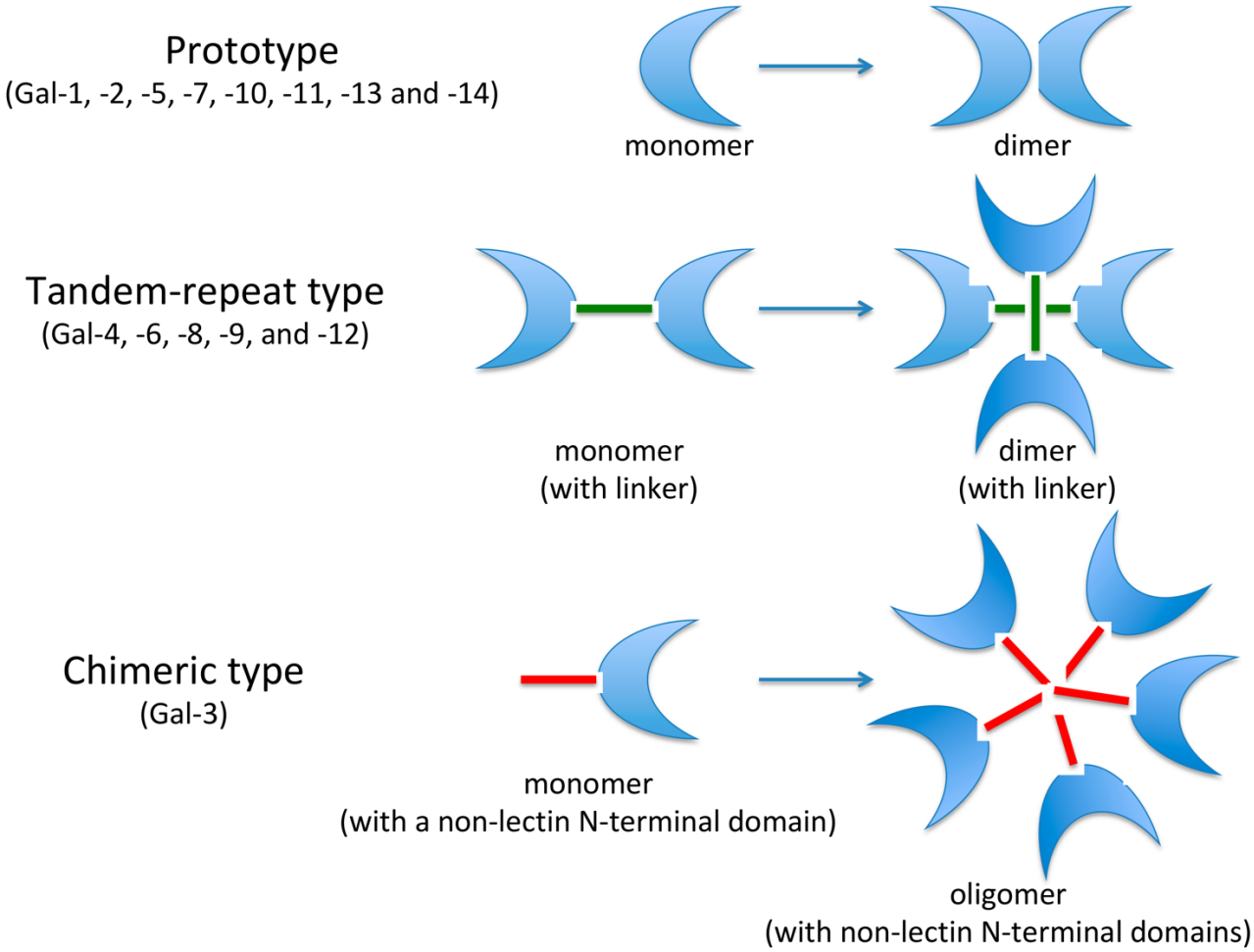

Figure 8: Schematic representation of the structure of the galectin family members. The galectin family members are divided into three types: The prototype with only one carbohydrate recognition domain (CRD), the tandem-repeat type with two CRDs connected by a non-conserved linker, and the chimeric type with one CRD and a non-lectin N-terminal domain (ND). Figure from (Sciacchitano et al., 2018).

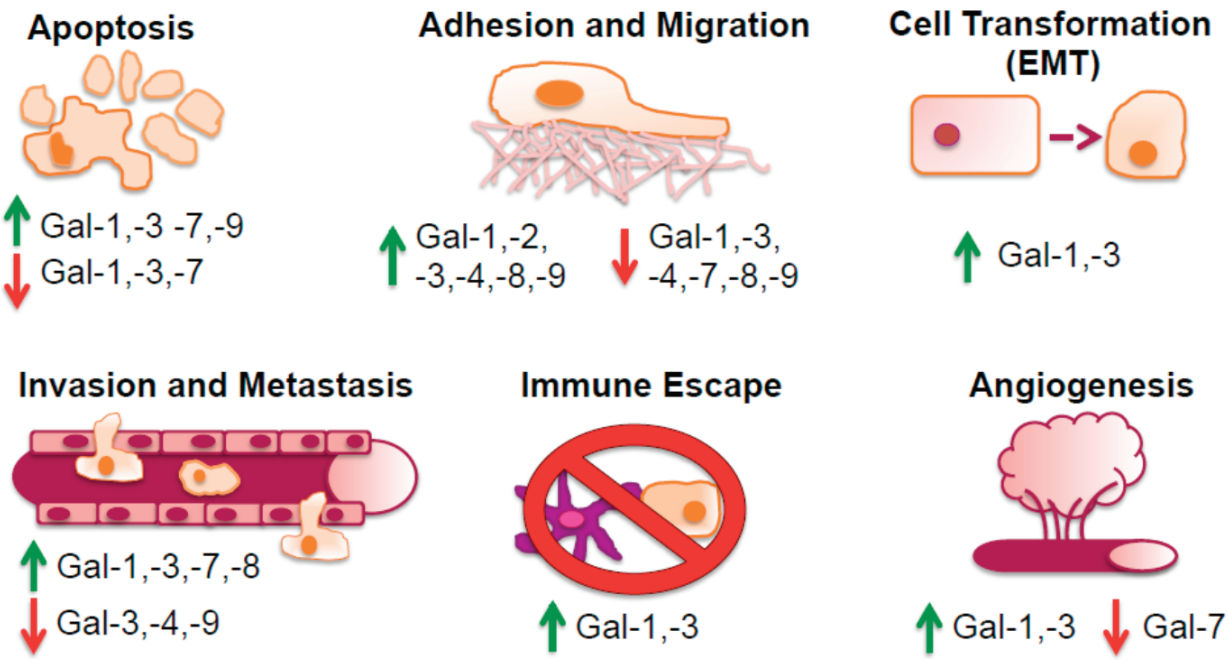

Figure 9: Physiological and pathological processes where galectins are involved. Galectins are expressed in a variety cells and tissues. They are participating in many physiological and pathological processes. They are notably involved with key aspects of carcinogenesis, like apoptosis, adhesion and migration, cell transformation (EMT), invasion and metastasis, immune escape, and angiogenesis. Galectins have protumorogenic (represented as green arrow) or antitumorigenic (represented as red arrows) effects. Figure from (Dings et al., 2018).

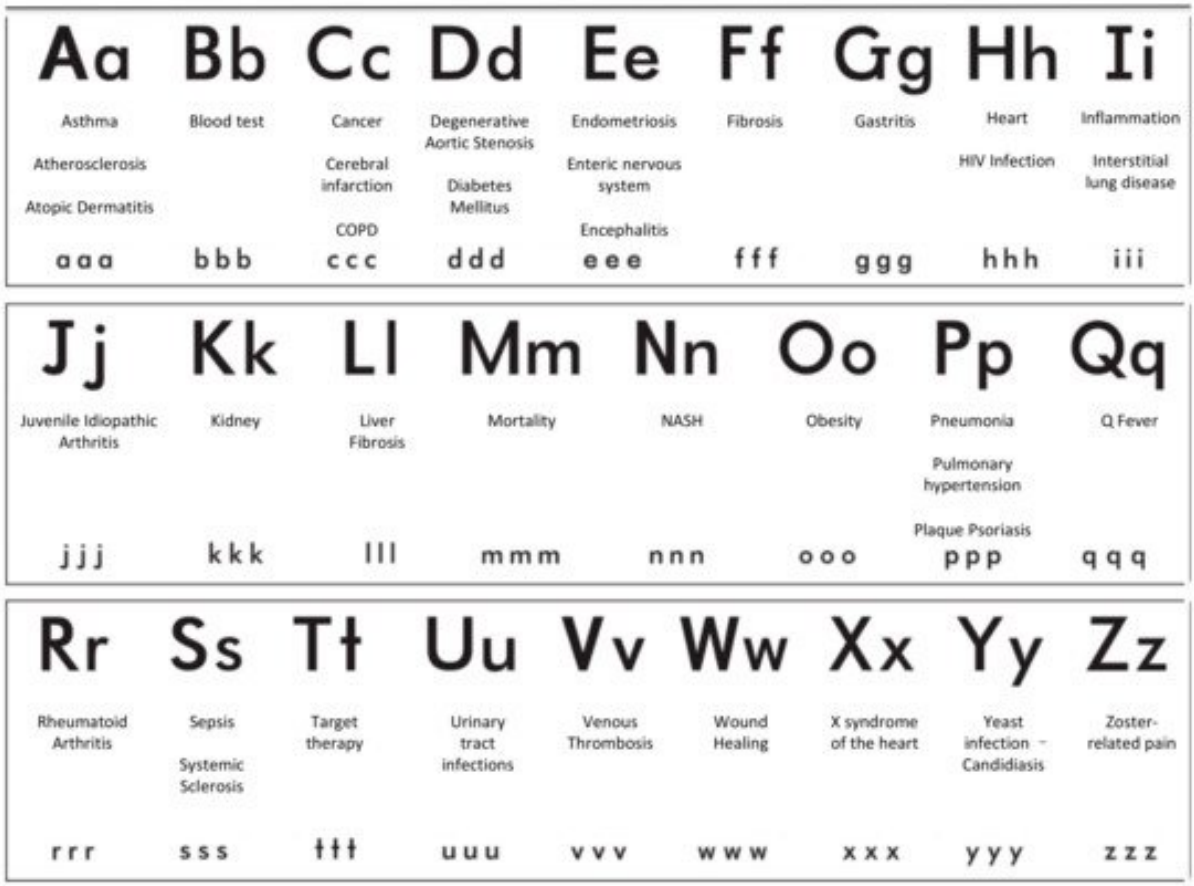

Figure 10: Conditions and diseases in which Gal3 might be involved. During our studies we particularly focused on Gal3. Gal3 can be involved in various diseases. These are represented in alphabetic. Figure from (Sciacchitano et al., 2018).

3.3 LACTOTRANSFERRIN

One of the interacting partners of Gal3 in the mouse intestine is lactotransferrin (LTF) (see Results chapter, below).

LTF is a 80 kDa glycoprotein and a member of transferrin family of proteins that bind Fe^{3+} ions (Metz-Boutigue et al., 1984). LTF was isolated by Sorensen and Sorensen from bovine milk in 1939. Due to an increase in its concentration during most inflammatory reactions and some viral infections, some authors classify LTF as an acute-phase protein (Kanyshkova et al., 2001). During inflammation, its concentration increases in all biological fluids, and the highest levels can be detected at the start of inflammatory process. Thus, LTF has a wide variety of biological and physiological functions, which are not always connected with its capacity to bind iron (Hendrixson et al., 2003). LTF has 60% sequence identity with serum transferrin (Metz-Boutigue et al., 1984). Predominant cell types involved in LTF synthesis are of the myeloid series and secretory epithelia (Rak et al., 2018). In adults, LTF is highly expressed in milk and colostrum. It can also be detected in mucosal secretions such as uterine fluid, vaginal secretion, seminal fluid, saliva, bile, pancreatic juice, small intestine secretions, nasal secretion, and tears (Bartoskova et al., 2009). Most of plasma LTF originates from neutrophils. LTF is predominantly stored in specific (secondary) granules (Levay and Viljoen, 1995). LTF is present in blood, plasma or serum in low concentrations. LTF synthesis and production in the mammary gland is controlled by prolactin, in reproductive tissues by estrogens, and in endometrium by estrogens with epidermal growth factor (Levay and Viljoen, 1995). Exocrine glands produce and continuously secrete LTF. In neutrophils, LTF is synthesized during their differentiation and then is stored in specific granules. Mature neutrophils cease to produce LTF (Kanyshkova et al., 2001). The biological properties of LTF are controlled by specific receptors on the target cell surfaces. Some cells have also “main receptors”, that enable them to bind not only LTF but also transferrin (Kanyshkova et al., 2001).

LTF can be eliminated from the organism either through receptor-mediated endocytosis by phagocytic cells (macrophages, monocytes, and other cells belonging to the reticuloendothelial system) with subsequent iron transfer to ferritin, or through direct uptake by the liver. Endocytosis performed by Kupffer cells, liver endothelial cells, and hepatocytes contributes to LTF removal (Levay and Viljoen, 1995).

LTF is an important part of the innate immune system. At the same time, LTF indirectly takes part in specific immune reactions (Levay and Viljoen, 1995). Due to its localization on the mucosal surface, LTF represents one of the first defense systems against microbial agents invading the organism mostly via mucosal tissues. LTF affects the growth and proliferation of

a variety of infectious agents including both Gram-positive and negative bacteria, viruses, protozoa, or fungi. Its ability to bind free iron which is one of the essential elements for the growth of bacteria is responsible for the bacteriostatic effect of LTF (Rak et al., 2018). A lack of iron inhibits the growth of iron-dependent bacteria like *E. coli*. LTF also can serve as a donor of iron, and by doing that it supports the growth of some bacteria with lower iron uptake like *Lactobacillus sp*. or *Bifidobacterium sp*. (Levay and Viljoen, 1995). LTF can bind to certain DNA and RNA viruses (Kanyshkova et al., 2001). It's main contribution to antiviral defense consists in its binding to the glycosaminoglycans on the host cell membrane. Like that LTF prevents viruses from entering cells and infection is stopped at an early stage.

LTF can also act as a growth factor activator. The effect of LTF alone on small intestine epithelial cells is more potent than that of the epidermal growth factor. LTF by itself (in the absence of any other cytokines and factors) is able to stimulate the proliferation of endometrium stroma cells. LTF has also been identified as a transcription factor due to its ability to penetrate the cell and activate the transcription of specific DNA sequences (Bartoskova et al., 2009). LTF has unique antimicrobial, immunomodulatory, and even antineoplastic properties and seems to have great therapeutic potential.

4 SMALL INTESTINE

As a model system and the tool for our studies we used mouse intestine. The main function of intestinal enterocytes is to absorb nutrients, vitamins and water. Mice in which the UDP-glucose ceramide glucosyltransferase (Ugcg) gene is knocked out in an enterocyte-specific manner (Cre recombinase expression under the villin promoter) died very fast. The team of Prof. Hermann-Josef Gröne showed that death is due to the failure to absorb lipids from milk and other nutrients from the intestinal lumen. Since GSLs are key players in the GL-Lect hypothesis, we reasoned that one of the physiological functions of this mechanism might be in nutrient absorption in the small intestine.

The small intestine (SI) serves as interface between the external environment and the body. That's why it has dual function: absorptive and protective. It faces a fluctuating diet and bacterial composition, and at the same time has to maintain a dynamic but balanced microflora within its lumen while being intermittently exposed to pathogens. All of its functions—mixing and propulsion, secretion, digestion, absorption, regulation of blood, immunologic reaction and tolerance, and elimination—are fully integrated through both local and remote neuroendocrine and immunologic mechanisms. The SI thus has a complex task and requires specialized anatomic mechanisms to perform them (Zentek et al., 2002).

4.1 Anatomic Regions

The SI is an elongated tube, which begins at the pylorus of the stomach and ends at the ileocolic valve. It is divided arbitrarily into three anatomic segments: the duodenum (proximally), then the jejunum, and the ileum (distally) (Zentek et al., 2002) (Figure 11).

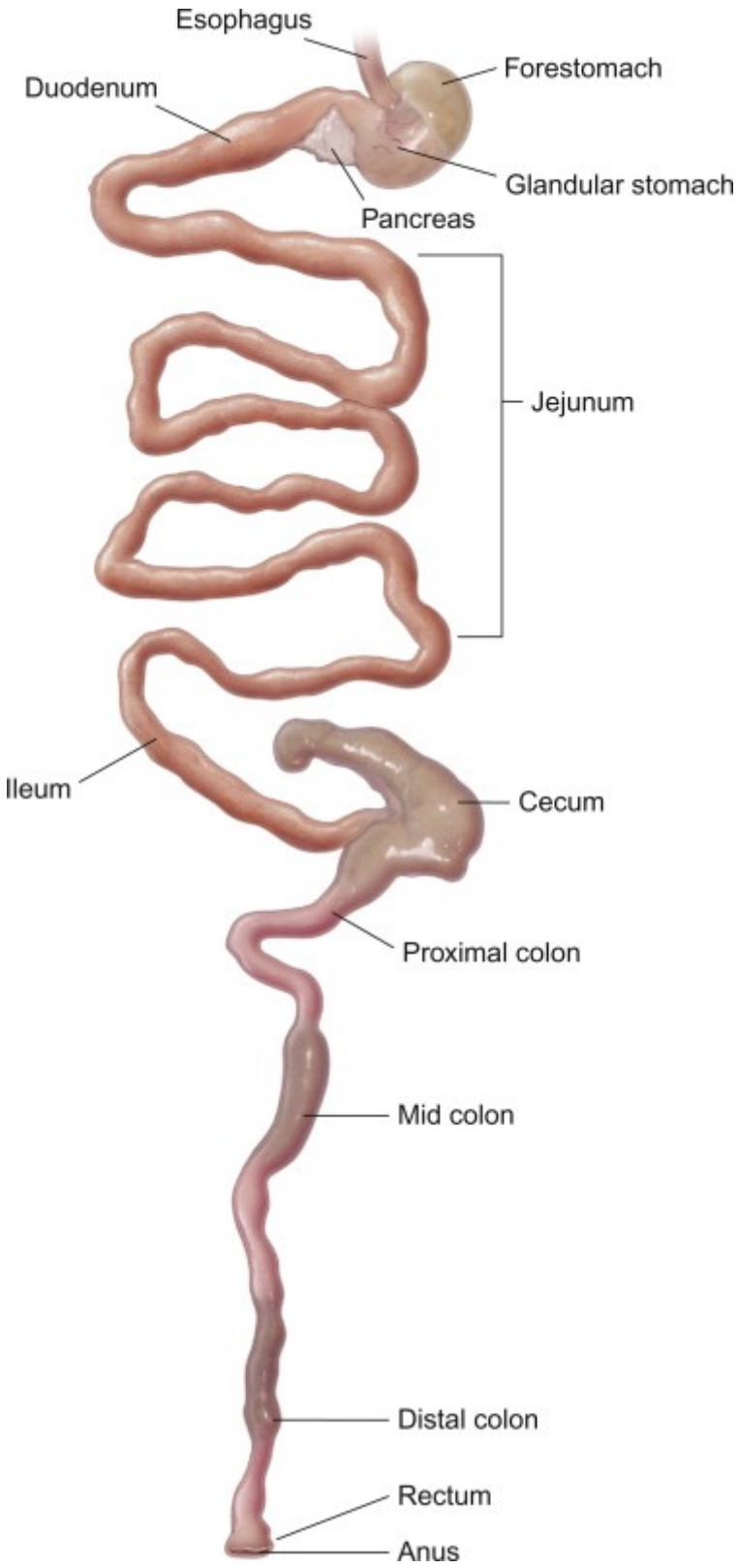

Figure 11: Anatomic regions of small intestine mouse. The SI is divided arbitrarily into three anatomic segments: the duodenum proximally, then the jejunum, and the ileum distally. Figure from (Treuting et al., 2012).

4.1.1 Duodenum

Duodenum is a first part of the SI. Duodenum, includes approximately 10% of SI length. It goes from the pylorus dorsally and to the right at the level of the ninth intercostal space. Duodenum is immobilized by the hepatoduodenal ligament. Hepatoduodenal ligament turns caudally into the descending duodenum. It is in contact with the right flank, turning again at the caudal flexure near the pelvic brim. It is associated with the common bile duct and the head and right limb of the pancreas, which lie in its mesentery (Zentek et al., 2002).

4.1.2 Jejunum

Jejunum is located in the middle part of the SI. It starts as an indistinct structural and functional transition from the duodenum and it forms the majority of the SI (Zentek et al., 2002).

4.1.3 Ileum

The basic structure of the ileum is not significantly different from the rest parts of the SI, and it is not defined microscopically from the jejunum. However, it does have some unique functional features, like the absorption of bile salts and cobalamin, and it is also a site of dense lymphoid follicle expression (Zentek et al., 2002).

4.2 Blood supply, lymphatic drainage, and innervation

The blood supply to the proximal duodenum is from the celiac artery. The venous drainage of the SI is ultimately due to the liver via the hepatic portal vein. Multiple embryonic vessels linking portal venous drainage and the systemic venous system do exist, but only become functional shunting vessels if there is chronic portal hypertension as a consequence of liver disease. Lacteals in the villi drain via intestinal lymphatics in the mesentery to the mesenteric lymph nodes and then the cisterna chyli and on to the thoracic duct. Vagal and sympathetic innervation coordinate with the intrinsic enteric nervous system and enteric hormones to regulate SI motility and function (Malo, 1988).

4.3 Intestinal Compartments

4.3.1 Microfora

The microflora of the SI is a fundamental part of its structure and function and immunity. There is a gradual increase in bacterial amount along the SI. It can change from aerobic to anaerobic organisms advancing distally down the SI (Buddington et al., 2003).

4.3.2 Mucosa

The SI mucosa plays the role as intestinal barrier and has absorptive functions. Mucosa consists of intestinal epithelium that covers the lamina propria and that hosts the local mucosal immune system and is delimited by the submucosa and the outer muscle layers (Farrugia, 2008).

The mucosal layer is responsible for secretion and absorption, and it is a barrier to the luminal environment. The submucosa, between the muscularis mucosa and muscularis, provides connective tissue support and delivers blood vessels, nerves, and lymphatics (Lammers and Stephen, 2008).

Mucosa is clinically the most important layer of the intestine. It consists of the epithelium and lamina propria overlying the muscularis mucosa and is modified by gross folds and the villi (Lin and Chen, 2003).

4.3.3 Crypt-villus unit

An assembly of crypts and their associated villus is the main functional unit of the SI. Crypts are constantly restored by cell division, generating undifferentiated epithelial cells. It is considered that there are between 4 and 40 stem cells per crypt in the adult intestine, with further division of daughter cells happening as the cells pass up the crypt. As the crypt cells pass through a maturation zone, they undergo a final division and then differentiate into immature epithelial cells of different types (Ohshiro et al., 2008) (Figure 12).

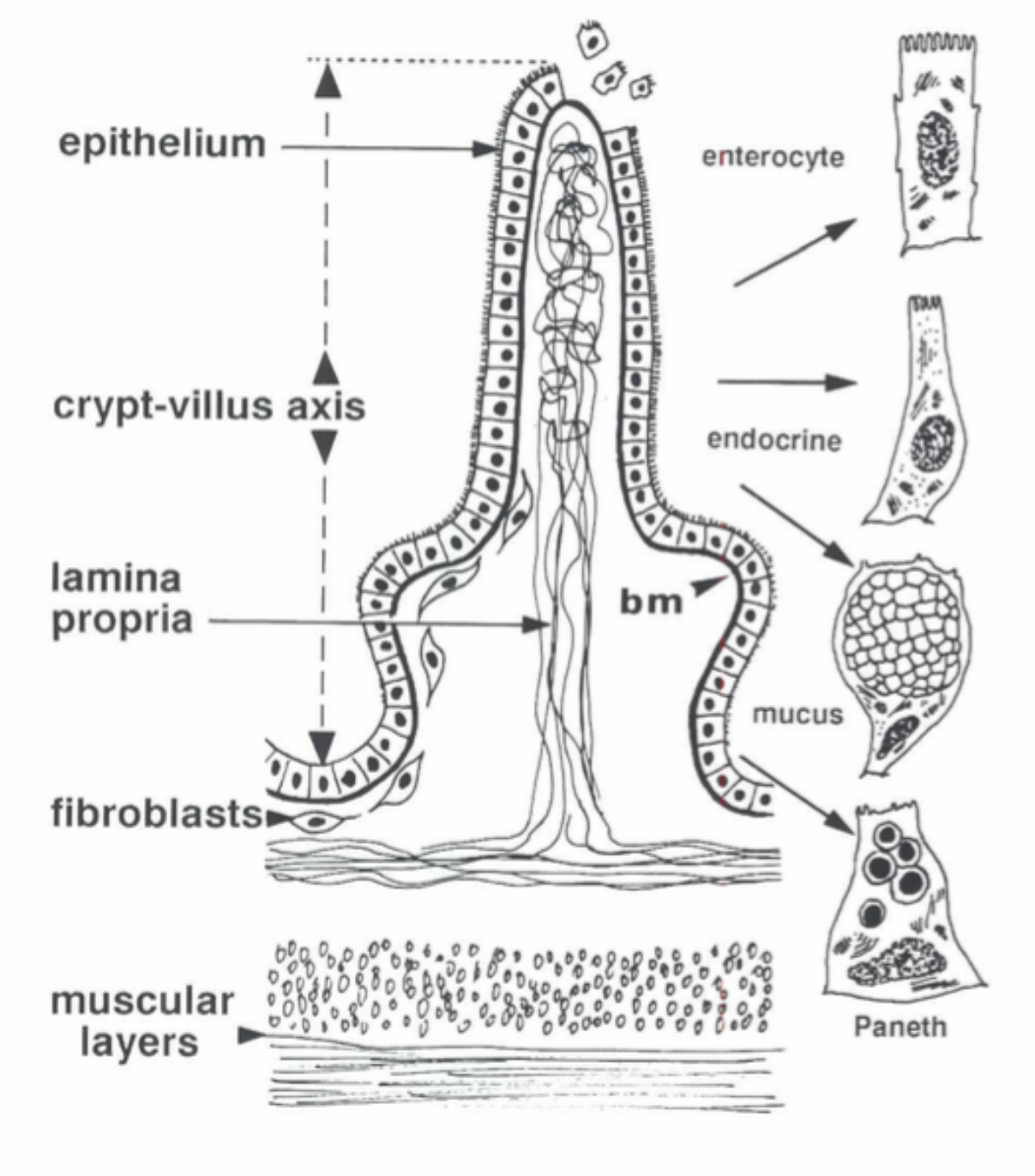

Figure 12: Scheme of a cross section through the small intestinal wall that shows different intestinal cell layers and epithelial cell types (Dauca et al., 1990). Figure from (Dauca et al., 1990).

4.3.4 Mucosal Epithelium

The intestinal surface is covered by a monolayer of polarized epithelial cells. The luminal surface of these cells are structurally and functionally distinct from their basolateral membrane. The epithelial basement membrane is readily permeable to nutrients and has an important role as the structural matrix on which the epithelium grows (Olsson and Holmgren, 2001). It expresses glycoproteins, called laminins, that interact with transmembrane recognition molecules expressed by epithelial cells – the integrins (Olsson and Holmgren, 2001). It endorse cell adhesion and differentiation. Enterocyte differentiation during migration up the villus can be programmed but is also likely to be modulated by the expression of different integrins at different sites on the crypt-villus axis (Olsson and Holmgren, 2001). Communication between epithelial cells is mediated by E-cadherin, a transmembrane molecule, linked to intracellular catenins, proteins that transmit signals to the actin cytoskeleton and intracellular growth control pathways (Sarna, 2008).

A mucosal barrier is formed by the intestinal epithelium. This barrier depends on intercellular tight junctions between enterocytes. Old enterocytes are shed from the villus tip by a mechanism that maintains the mucosal barrier (Zentek et al., 2002).

Crypt cells have a potent secretory capacity. They represent the site of most mucosal fluid secretion. As enterocytes migrate to the villus tip, maturation involves loss of secretory activity and the expression of digestive and absorptive molecules in the apical cell membrane (Olsson and Holmgren, 2001). Some enterocytes undergo random cell death, but the majority undergoes apoptosis via a caspase-mediated process and are removed at the tips of the villi. The duration of migration from crypt to villus tip is believed to be around 3 days (Zentek et al., 2002).

Enterocytes predominate in the epithelium, representing approximately 80% of all cells, with interspersed mucus-secreting cells – the goblet cells (Figure 13). Goblet cell density in the SI mucosa can vary, being highest in the ileum. The main function of Goblet cells is mucus secretion. Paneth cells, a population of cells found in some species below the proliferation zone in crypts and that secrete antibacterial peptides; endocrine- and paracrine- secreting cells are also present in the mucosal surface layer and have important trophic and functional activities (Wen et al., 1998).

In addition to locally formed growth factors, different luminal factors act as physiologically active growth regulators. Receptors for epidermal growth factor (EGF) can be found on the luminal and basolateral sides of enterocytes. That suggests that they may respond to bloodborne EGF and to EGF secreted into the lumen by salivary and pancreatic tissue or transported in milk (Rehfeld, 1998).

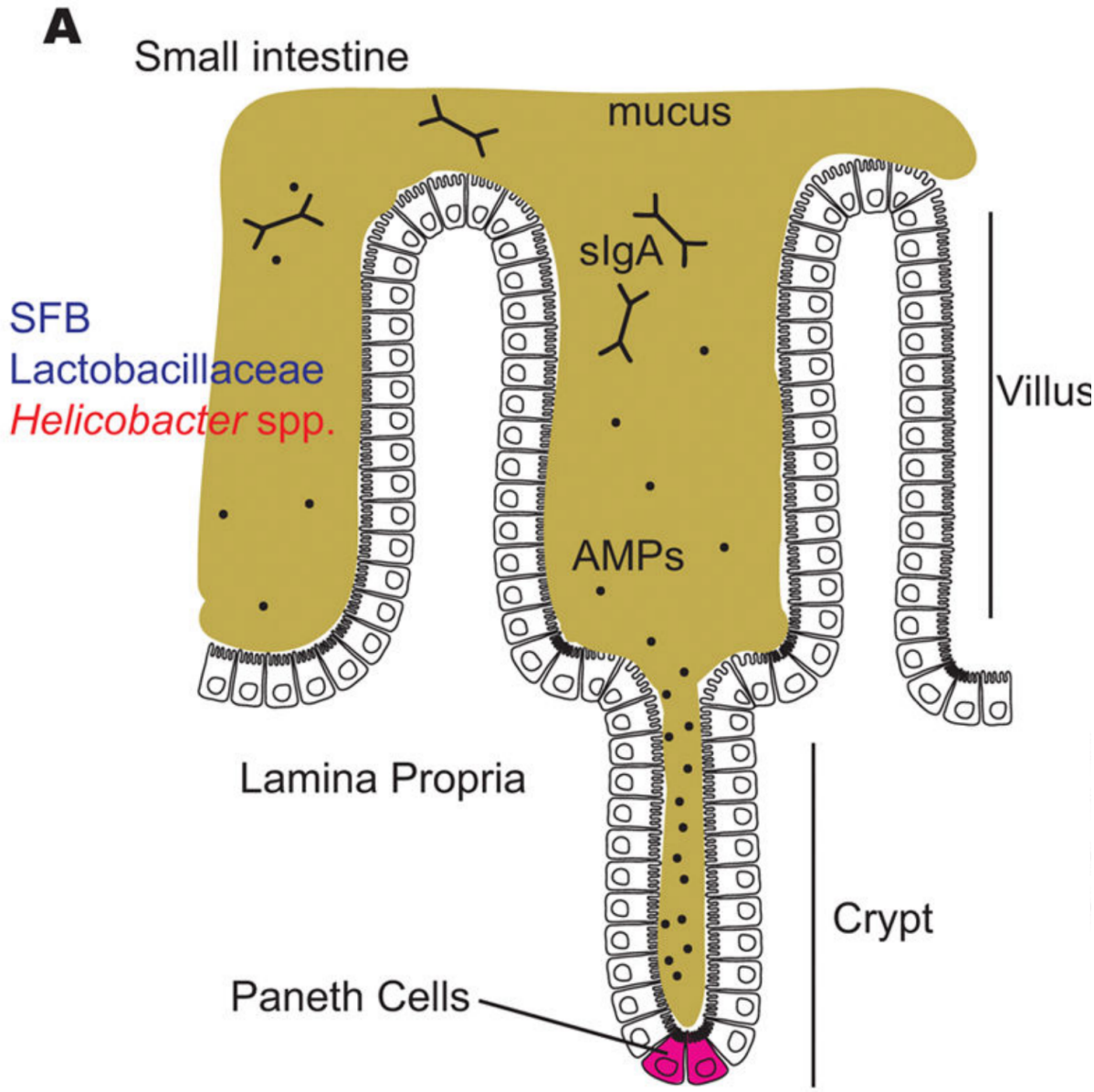

Figure 13: The mucus layers of the small intestine. Several factors can limit the ability of gut bacteria to have an access to the host cells, including the mucus layers in the small intestine; antimicrobial peptides in the small intestine, including those produced by Paneth cells at the base of the crypts; secreted immunoglobulin A in both the small intestine and colon; and a steep oxygen gradient that impacts which bacteria are capable of surviving close to the epithelial surface. The surface of the small intestine is molded into villi and crypts and is colonized by certain species, like segmented filamentous bacteria (SFB), *Lactobacillaceae* and *Helicobacter spp.* Figure from (Donaldson et al., 2016).

4.3.5 Enterocytes

Enterocytes comprise intracellular organelles, like mitochondria, endosomes, lysosomes, endoplasmic reticulum and Golgi apparatus, that are common to all cells. These organelles support normal cellular functions and also play a role in definite digestive and absorptive functions (Olsson and Holmgren, 2001). Enzymes that are expressed on the surface of enterocytes perform terminal digestion of polysaccharides and peptides in combination with luminal hydrolysis of food polymers and with additional help of pancreatic enzymes. The enterocytes can absorb the simple nutrients (Olsson and Holmgren, 2001). These functions depend on the polarity of the enterocyte, and involve a microvillar membrane (MVM). MVM is a specialized quantity of the cell membrane on the luminal surface. It consists of thousands of microvilli, having the digestive enzymes and specific carrier proteins, which gave them an alternative name – the "brush-border" (Hore and Messer, 1968).

The MVM is a phospholipid bilayer that has specific proteins inserted into it (Hore and Messer, 1968). Enzymes responsible for the terminal stages of carbohydrate and protein digestion are anchored in the MVM by a small hydrophobic terminal sequence (Hore and Messer, 1968). Their active site is uncovered to the intestinal lumen. Specific carrier proteins in MVM or basolateral membranes shuttle nutrients in and out of the enterocyte, by undergoing conformational changes (Hore and Messer, 1968). The maximal brush-border enzyme and transport activities are expressed in the mid-villus region (Hore and Messer, 1968). As enterocytes drift to the villus tip, enzymes are slashed from the brush-border via bacterial and pancreatic proteases. Then they are discharged into the lumen where they comprise solubilized enzyme activities, that is entitled digestive juice (Hore and Messer, 1968) (Figure 13).

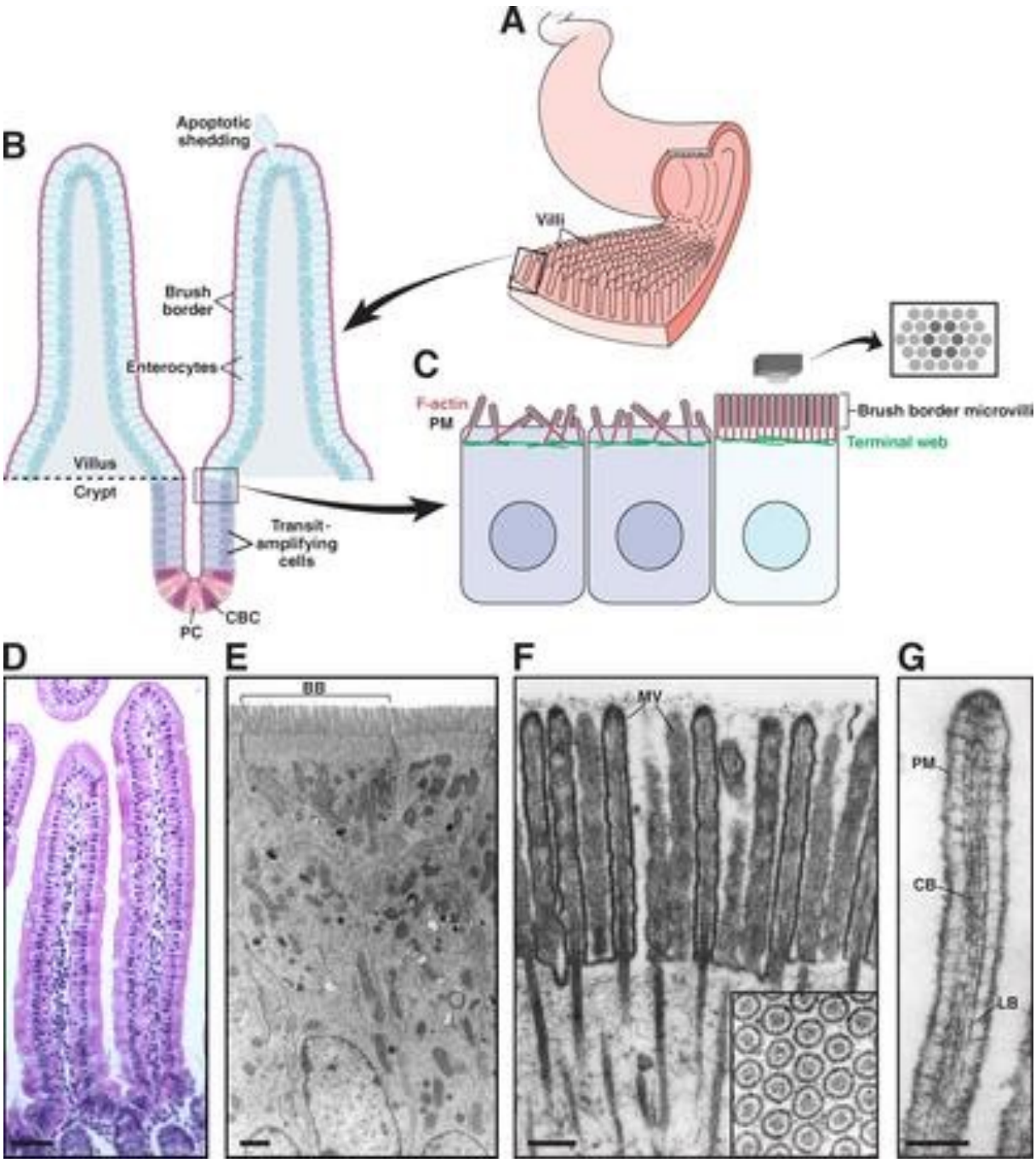

Figure 14: Functional structure of the intestinal epithelium. (A) The small intestinal epithelium is defined by ubiquitous small folds of tissue - villi. (B) Enterocytes, are the most abundant cell type lining the villus. They are generated in a stem cell niche composed of crypt base columnar (CBC) cells and flanking Paneth cells (PC), that are located in crypts near the base of each villus. CBC cells endure division, resulting in a new stem cell plus a committed daughter cell. Daughter cells endure further separation in the transit-amplifying region before differentiating into enterocytes and exiting the crypt. Enterocytes migrate to the tip of the crypt-villus axis over

a period of 2–3 days. At the tip, cells endure apoptosis and are extruded from the epithelium. (C) Apical surface association of enterocytes before and after differentiation; brush border microvilli on the surface of differentiated cells are crammed in tight, hexagonal arrays. (D) Villi in mouse small intestine. (E) Enterocytes structure; brush border (BB) from a single cell is showed. (F) Brush border microvilli (MV) from small intestine. (G) A single microvillus. Plasma membrane (PM) is linked to the core bundle (CB) by lateral bridges (LB) that are formed at least in part by myo1a. Figure from (Crawley et al., 2014).

4.4 Small intestinal function

The basic functions of the SI are digestion, absorption, and elimination. These processes can occur as a result of complex intracellular interactions between epithelial cells, immune cells, mesenchymal and neuronal cells and with luminal nutrients and microbes. The SI is also the largest immunologic organ in the body. Intestine interacts with the intestinal microbial flora and food antigens (Kruhoffer and Muntz, 1954).

4.4.1 Digestion

To be transferred crosswise the MVM, key dietary constituents must be hydrolyzed from their initial polymeric structure into monomers. This process is achieved within the SI lumen by mechanical disruption (in conjunction with bile salt emulsification of fats) that allows enzymatic hydrolysis of polysaccharides, proteins, and triglycerides (Kruhoffer and Muntz, 1954).

The SI provides the optimum environment in terms of temperature, pH, and mixing for the actions of bile salts and digestive enzymes, but most enzymes are secreted by the pancreas. The brush-border peptidase enterokinase is vital in the initial activation of pancreatic trypsin from trypsinogen by cleaving a terminal octapeptide, trypsinogen activation peptide, from the native protein (Kruhoffer and Muntz, 1954).

4.4.2 Absorption of digested Nutrients

Simple sugars, amino acids and oligopeptides, fatty acids and other lipids are delivered to the body across the mucosal barrier and later on via the lymphatics or bloodstream. Uptake happens either by passive/active diffusion or by facilitated carrier-mediated transport mechanisms. Endocytosis of small, antigenic peptides is of no nutritional significance, but is involved in the neonatal absorption of colostral antibodies, and is important to the mucosal immune response (Knedlik et al., 2017).

The products of fat digestion can be absorbed by passive diffusion from mixed micelles across the MVM and eventually lipoproteins are passed into lacteals. The reducing factors, supposing normal function of pancreatic system, are the intestinal surface area and lymphatic functionality. That’s why villus atrophy and lymphangiectasia are likely to cause malabsorption of fat (Knedlik et al., 2017).

4.4.2.1 Mechanisms of Absorption

4.4.2.2 Passive diffusion

Lipid-soluble products of digestion don't require a specific carrier mechanism in order to be absorbed across the mucosal barrier and can bypass passive diffusion by "dissolving" in the brush-border membrane. This absorptive process complies with the Graham Law of Diffusion, being proportional to the concentration gradient across the membrane, non-saturable, and limited only by the surface area of the membrane. Diffusion back across the brush-border is prevented by re-esterification of free fatty acids within the enterocyte (Noon et al., 1977).

4.4.2.3 Carrier-mediated transport

Some small, nonpolar, water-soluble molecules can be absorbed by passive diffusion through "pores" in the mucosal membrane. The structure of these hypothetical pores is likened to that of ion channels in other membranes. Molecules with a molecular radius bigger than 0.4 nm appear to be excluded, but larger, although numerically fewer pores, may cross the tight junctions (Young et al., 2016).

4.4.2.4 Endocytosis

Small antigenic peptides can be engulfed nonspecifically within endocytotic vesicles of epithelial cells. The amounts absorbed by this route are insignificant from a nutritional standpoint, but this sampling of luminal contents is crucial to the mucosal immune response. Receptor-mediated endocytosis allows the uptake of small amounts of specific intact nutrients and is the mechanism of cobalamin absorption (Noon et al., 1977).

4.5 Nutrient Absorption

4.5.1 Carbohydrate

Glucose is the main product of carbohydrate digestion. It is absorbed by active transport on a stereospecific carrier that recognizes a D-pyranose structure with a C-2 hydroxyl group. A family of facilitated glucose transporters (GLUTs) with different isoforms perform and facilitate/mediate transport of glucose across mammalian cell membranes. One member of this family, GLUT2, can be found on the basolateral membrane of enterocytes, where it shuttles glucose, galactose, and fructose out of the enterocyte by diffusion. GLUT2 is absent from the brush-border, and so a mechanism exists for active transport of glucose across the MVM into the enterocyte by sodium-glucose co-transporter 1 (SGLT1) and facilitated transport into the body by GLUT2 (Noon et al., 1977). Another member of this facilitated glucose transporter

family is GLUT5. It is found at the brush-border of the cell. It shares homology with other family members but also allows facilitated diffusion of fructose; it is not even competitively inhibited by glucose. Although dietary carbohydrates must be hydrolyzed to monosaccharides to be absorbed and be nutritionally useful, a small amount of disaccharide can cross the brush-border, likely through leaky tight junctions. This is of no nutritional significance, but increased uptake and subsequent urinary excretion of disaccharides can be a marker of increased intestinal permeability when damaged (Zentek et al., 2002).

4.5.2 Protein

The products of protein digestion are absorbed via carriers that are stereospecific for L-amino acids. Sodium-linked active transport is responsible for free amino acid uptake through one of four different carriers that have a variable degree of selectivity for neutral (Gly, Ala), acidic (Asp, Glu), basic (Arg, Lys), and imino (Pro, HO-Pro) amino acids. Peptide uptake has been considered to be a facilitated diffusion, with the concentration gradient being maintained by intracellular peptide hydrolysis, and only free amino acids being exported from enterocytes into the portal blood (Zentek et al., 2002).

4.5.3 Lipid

The products of fat digestion are absorbed by passive diffusion from mixed micelles into lacteals. The fat digestion products are re-assembled within enterocytes to prevent re-diffusion back out of the enterocyte. They can be combined with synthesized lipoproteins for passage into the lymphatics as chylomicrons. Anyway, medium-chain triglycerides (length 8-12 carbon atoms) can be absorbed directly into the portal blood and provide an alternative route for fat uptake when lymphatic flow is impaired, as in lymphangiectasia (Batt and McLean, 1987).

4.5.4 Fat-Soluble Vitamins

Dietary fat-soluble vitamins A, D, E, and K are solubilized in mixed micelles before the passive diffusion across the brush-border. Fat malabsorption associated with inadequate amounts of bile salts, lymphangiectasia, or severe villus atrophy also results in vitamin deficiency (Noon et al., 1977).

4.5.5 Water-Soluble Vitamins

Water-soluble vitamins B and C are absorbed by a mixture of passive diffusion (e.g., pyridoxine [B_6] and C), saturable facilitated transport (e.g., riboflavin [B_2]), or active and facilitated transport (e.g., thiamine [B_1]) (Lin and Chen, 2003).

4.6 Motility

Slow-wave, segmental, and peristaltic contractions of the SI are generated by the coordinated contraction of smooth muscle in response to spontaneous electrical activity. Interstitial cells of Cajal are considered as coordinating/pacemaker cells and smooth muscle contraction is modulated by coordinated neurohumoral and neurochemical molecule release. Many of these molecules have elaborate regulation of intestinal secretion and absorption and in mucosal immune responses, creating a complex synchronized process for food digestion (Olsson and Holmgren, 2001).

4.7 Secretion and absorption of water and electrolytes

One of the main functions of the villus is intestinal secretion. This process resulted by passive osmotic flux of water following active transcellular chloride secretion into the intestinal lumen. The capacity of the intestine to absorb liquid and electrolytes differs according to the place. The quantity of fluid and electrolytes in the GI tract replicates a balance between absorption and secretion, with the net absorption in healthy tissue (Buddington et al., 2003).

The absorption of water is passive. This process follows the transport of solutes through the GI epithelium by one of following processes: passive absorption, active absorption, or solvent drag. The jejunum absorbs 50%, the ileum 75%, and the colon approximately 90% of the fluid. It secrets around 2% in feces. This grade in absorptive capability is a function of enterocyte pore size, membrane potential difference, and the type of transport routes allied with each intestinal fragment. The site of the enterocyte in the villus is also essential. It is known that enterocytes located in villus mainly absorb, while crypt cells secrete (Wang et al., 2018).

4.8 Mucosal Immunity

The mucosal immune system is a large and complex organ. It is essential for the health of not only the intestine, but the whole animal (Wang et al., 2018).

Results

5 STUDY OF GL-LECT ENDOCYTOSIS *IN VIVO* MODEL SYSTEMS

5.1 Objectives and summary

Previous work in the team has proposed a novel model for endocytosis that doesn't require clathrin but rather a lectin, namely Gal3 in cooperation with glycolipids. According to this model oligomeric Gal3 can bind to GSL and induce membrane deformation in a similar way as the pathogenic lectins do, such as STxB. Therefore, both processes could be summarized under the same hypothesis, the GL-Lect hypothesis (see introduction).

The aim of my PhD work was to investigate in which physiological context(s) the GL-Lect model operates, and the choice was made to explore the GL-Lect mechanism *in vivo* at the level of the mouse intestine.

The main objective of my PhD was to characterize the Gal3 and GSL-dependency of endocytosis in mouse enterocytes. To do so, different axis of investigation have been followed, such as:

- The expression of Gal3 in the intestinal epithelium and the ability of purified human recombinant Gal3 to bind the apical membrane of enterocytes for subsequent internalization experiments.

- The contribution of GSLs in this process, using a mouse model in which the Ugcg gene was inducibly removed.

- The role of other Galectins in this process, using Gal3 knockout mice or lactose as a competitive inhibitor.

- The identification of Gal3 binding proteins and the analysis of their endocytosis in function of GSL and Gal3 expression/function.

My experiments led me to:

- Observe the expression of endogenous Gal3 in intestinal epithelium cells (enterocytes), and the internalization of exogenous Gal3.

To test the expression of Gal3 in mouse enterocytes, we performed immunofluoresce staining with an anti-Gal3 antibody on the intestine of wild-type C57 black 6 mice. We observed subapical and basolateral localization of endogenous Gal3. To test the internalization of

recombinant exogenous Gal3 in intestine, the protein was added into the lumen of the jejunum. In initial experiments, we failed to see internalization of exogenous Gal3, as the protein accumulated in the mucus part of the jejunum. To overcome this problem, we decided to perform mucus permeabilization. Indeed, Gal3 was able to be internalized in the mouse intestine after mucus removal, and showed us a basolateral accumulation. This pattern of accumulation reminded us of a transcytosis-like phenotype.

- Identify lactotransferrin as a Gal3 interacting partner in mouse intestine.

To identify the binding partners of Gal3 in the jejunum of the mouse, we performed Gal3–His pull-down for mass spectrometry analysis. One of the interacting partners of Gal3 was LTF. LTF is a major iron-binding and multifunctional protein found in breast milk and mucosal secretions with antimicrobial activity. Some authors proposed that LTF increases iron absorption. Two main LTF receptors are known: Intelectin-1, also known as Omentin or intestinal LTF receptor, and the moonlighting glycolytic enzyme glyceraldehyde-3-phosphate dehydrogenase (GAPDH).

- Establish the functional contribution of GSLs in Gal3 and LTF endocytosis.

Gal3 and LTF were incubated with mouse jejunum lacking GSL. Inducible GSL knockout mice were obtained from Prof. Hermann-Josef Gröne. In these mice, the UDP-glucose ceramide glucosyltransferase (Ugcg) gene can be removed in a tissue-specific manner (villin promoter). We observed a dramatic decrease in endocytosis events (Gal3 and LTF internalization) in GSL knockout mice, compared with wild-type mice. These results indicated that the endocytosis of Gal3 and its binding partner LTF is GSL dependent.

- Establish the functional contribution of Gal3 in LTF endocytosis.

Our results showed that in the presence of sucrose and PBS, LTF exhibited a transcytosis phenotype, similar to Gal3. In contrast, lactose which competitively inhibits Gal3 binding to carbohydrates strongly inhibited LTF transcytosis.

To have additional evidence for the dependency of LTF internalization on Gal3, we used intestine from Gal3 knockout mice. The pattern of LTF internalization was the following: In presence of Gal3, LTF was found in a basolateral localization. In absence of Gal3, targeting to the basolateral domain was strongly reduced. Instead, Gal3 accumulated in the nuclear area. When LTF was co-incubated with exogenous Gal3 on the jejunum of Gal3 knockout mice, basolateral accumulation of LTF could be rescued.

- Observe CLICs in mouse enterocyte.

After incubation of HRP-coupled Gal3 with jejunum of wild-type mice, we observed crescent-shaped tubular elements that exhibiting the characteristic hallmarks of CLIC morphology.

Altogether, my data showed for the first time the role of GSLs and Gal3 in cargo uptake (here: LTF) in an intact organ. Our work functionally dissected the functional contribution of the GL-Lect mechanism to endocytic uptake not only on cells in culture, but also *in vivo*.

The detailed description of results and methods for all experiments are presented in section 5.2 in the form of an article that will be submitted to an international journal.

5.2 Results

Article 1

Glycolipid-dependent and lectin-driven transcytosis in mouse enterocytes

To be submitted to an international journal

GLYCOLIPID-DEPENDENT AND LECTIN-DRIVEN TRANSCYTOSIS IN MOUSE ENTEROCYTES

Alena Ivashenka [1], Christian Wunder [1], Valerie Chambon [1], Roger Sandoff [2], Richard Jennemann [2], Katrina Podsypanina [3], Bérangère Lombard [4], Damarys Loew [4], Christophe Lamaze [5], Francoise Poirier [6], Hermann-Josef Gröne [7], Ludger Johannes [1]*, Massiullah Shafaq-Zadah [1]*

[1] Institut Curie, PSL Research University, Cellular and Chemical Biology unit, Endocytic Trafficking and Intracellular Delivery team, U1143 INSERM, UMR3666 CNRS, 26 rue d'Ulm, 75248 Paris Cedex 05, France

[2] Lipid Pathobiochemistry Group, German Cancer Research Center, 69120 Heidelberg, Germany

[3] Institut Curie, PSL Research University, Cell biology and cancer, UMR144, CNRS, 26 rue d'Ulm, 75248 Paris Cedex 05, France

[4] Institut Curie, Centre de Recherche, PSL Research University, Mass Spectrometry and Proteomics facility, Paris, France

[5] Institut Curie, PSL Research University, Cellular and Chemical Biology unit, Membrane Dynamics and Mechanics of Intracellular Signaling team, U1143 INSERM, UMR3666 CNRS, 26 rue d'Ulm, 75248 Paris Cedex 05, France

[6] Institut Jacques Monod, UMR 7592 CNRS - Université Paris Diderot, 15 rue Hélène Brion, 75205 Paris Cedex 13, France

[7] Institute of Pharmacology, University of Marburg, 35043Marburg, Germany

**** Correspondence to***: massiullah.shafaq-zadah@curie.fr and ludger.johannes@curie.fr

Running title: GL-Lect in enterocytes

Abbreviations: CLIC — Clathrin-independent carrier; STxB — Shiga toxin B-subunit; Gal3 — Galectin-3; GSL — Glycosphingolipid; HRP — Horseradish peroxidase; LTF — Lactotransferrin; KO — Knockout; DTT — Dithiothreitol; *Ugcg* — UDP-glucose ceramide glucosyltransferase; TAM — Tamoxifen; TLC — Thin-layer chromatography; MS — Mass spectrometry; GAPDH — glycolytic enzyme glyceraldehyde-3-phosphate dehydrogenase.

ABSTRACT

The glycosylation of proteins and lipids is critical for life. At the cell surface, glycoproteins and glycolipids have a number of functions ranging from molecular homeostasis and growth factor signaling to cell adhesion and migration. Glycoconjugates undergo endocytic trafficking. According to the recently proposed glycolipid-lectin (GL-Lect) hypothesis, the construction of tubular endocytic pits is driven in some cases by a glycosphingolipid (GSL)-dependent mechanism through sugar-binding proteins of the galectin family. Here, we provide evidence for a function of the GL-Lect mechanism controlling transcytosis in enterocytes of the mouse small intestine. We found that galectin-3 (Gal3) and its newly identified binding partner lactotransferrin (LTF) are transported from the apical membrane to the basolateral side, in a process that is fully dependent on the expression of GSLs. The transcytotic trafficking of LTF is also dependent on the expression of Gal3, and can be rescued in Gal3 knockout mice by the addition of exogenous Gal3. By electron microscopy, Gal3 is found in intracellular structures with typical morphologies of clathrin-independent carriers (CLICs), which in cultured cells are a hallmark of the GL-Lect mechanism. These data pioneer the existence of GL-Lect endocytosis in enterocytes of the murine small intestine, and strongly suggest that aspects of polarized trafficking across the intestinal barrier rely on this mechanism.

KEYWORDS

Glycosphingolipid, galectin, lactotransferrin, enterocyte, mouse small intestine, jejunum, endocytosis, clathrin-independent carrier, raft domain, mucus, plasma membrane, endosomes, lectin, homeostasis, immunofluorescence microscopy, electron microscopy.

INTRODUCTION

Endocytic uptake of adhesion molecules, growth factor receptors, and other cargoes is controlled by numerous mechanisms, of which the clathrin pathway is the best characterized[1-3]. How cargoes are recruited, and the plasma membrane bent to form endocytic pits in the case of clathrin-independent endocytosis is currently a dynamic field of exploration[4, 5].

Evidence has been provided that in some cases, tubular endocytic pits for clathrin-independent uptake into cells are generated by the interaction of pathogenic or cellular lectins of the galectin family with glycolipids[6-8]. The mechanism by which these oligomeric lectins induce narrow membrane bending has been termed the glycolipid-lectin (GL-Lect) hypothesis[4, 9-12]. For the cellular uptake of glycosylated cargo proteins such as the cell adhesion molecules CD44 and α5β1 integrin, the current model is as follows at the example of the well-explored galectin-3 (Gal3): Once non-conventionally secreted in an autocrine or paracrine manner into the extracellular milieu[13], Gal3 binds as a monomer to the carbohydrate groups of cargo proteins at the cell surface, and then oligomerizes[7, 14]. Oligomerized Gal3 gains the capacity to interact with glycosphingolipids (GSLs) in a way such as to drive the formation of deep and narrow membrane invaginations, both on model membranes and on cells[7]. Thereby, tubular endocytic pits are formed that are then transformed into clathrin-independent carriers (CLICs). CLIC structures have been well described for the bacterial cholera toxin, GPI-anchored proteins, and CD44 (Ref.[15, 16]). Of note, convergent evidence indeed strongly suggests that the GL-Lect mechanism is also used by GSL-binding Shiga toxin[6], cholera toxin, simian virus 40 (Ref.[17]), and norovirus[18], and by the GPI-anchored protein CD59 (Ref.[8]). However, the physiological contexts in which it operates have remained unexplored.

UDP-glucose ceramide glucosyltransferase (GCS), encoded by the gene (*Ugcg*) is an essential enzyme that catalyzes the first step of GSL biosynthesis[19]. In the inducible *Ugcg*flox/Cre-villin mouse model the GCS enzyme is genetically removed in a spatio-temporally controlled manner, to acutely deplete GSLs from mouse enterocytes[20]. Using this model, it was clearly shown that GSL content in intestinal tissue is crucial for viability, since animals were dying within a few days after *Ugcg* elimination, mainly because of malnutrition caused by a failure of nutrients uptake[20]. Since GSLs are key players in the GL-Lect hypothesis, we reasoned that one of the physiological functions of this mechanism might be in lipid and nutrient absorption.

Enterocytes are the most abundant cell type lining the intestine. Their contribution to nutrient uptake is well established, notably in the small intestine[21]. Examples are fat-soluble vitamins[22], the iron transporter transferrin[23, 24], and the glucose clearance hormone insulin[25]. All these are

internalized by endocytosis from the apical membrane that faces the intestinal lumen, and then released after intracellular trafficking on the opposing basolateral side to reach the bloodstream. This process is known as transcytosis, for which the macromolecular neonatal Fc receptor is amongst the best-studied examples (reviewed in Ref.[26]).

Lactotransferrin (LTF; also termed lactoferrin) from breast milk and mucosal secretions has been involved in iron transport across the intestinal lining, notably during early stages of life[27, 28]. LTF binds iron with high affinity and at a broad pH range, which is favorable for its function under the acidic conditions of the small intestine[29]. Two LTF receptors have been identified: Intelectin-1, also known as Omentin or intestinal lactoferrin receptor[30], and moonlighting glycolytic enzyme glyceraldehyde-3-phosphate dehydrogenase (GAPDH)[31, 32]. Of note, other iron transport mechanisms appear to be able to substitute for LTF, as iron absorption in infants was found to be even increased after depletion of LTF from mother milk[33], and LTF knockout mice have a normal iron status[34]. Furthermore, LTF has been described to have immune-modulatory functions and anti-microbial, anti-viral, antioxidant, anti-cancer, and anti-inflammatory activities[29]. Interestingly, studies on Caco-2 cells indicated that LTF is taken up from the apical membrane and undergoes transcytotic trafficking[35, 36].

In the current study, we have analyzed the involvement of key molecules of the GL-Lect mechanism in endocytic trafficking at the level of the enterocytes of the small intestine of mice. We have found that Gal3 and its newly identified interacting partner LTF are both transcytosed from the apical to the basolateral surface of enterocytes in the intact jejunum. Endocytosis of Gal3 and LTF were both strongly inhibited upon inducible depletion of GSLs, and LTF was itself dependent on Gal3 expression to be efficiently transcytosed across enterocytes. In ultrastructural experiments Gal3 was found in morphologically defined CLICs. These data collectively demonstrate that the GL-Lect mechanism is operating in enterocytes for polarized transcytotic trafficking from the apical to the basolateral membrane.

RESULTS

Gal3 is expressed within the intestinal epithelium of the jejunum

The endocytic phenotype of GSL-depleted enterocytes[20] incited us to test whether the GL-Lect mechanism was operating in these cells. We focused our attention on the jejunum of the small intestine of C57BL/6 mice, which has developed a morphological organization into villi and crypts (**Fig. 1a**). To identify galectins that are expressed in this tissue, cells of the intestinal mucosa were collected, lysed, and galectins were pulled down using a lactose affinity column (see **Methods** for details). The following galectins were detected using mass spectrometry: Gal1, Gal2, Gal3, Gal4, Gal8, and Gal9 (**Fig. 1b**), consistent with published findings[37].

We focused our attention on Gal3, which in the context of the GL-Lect hypothesis is the galectin that is the best studied[7]. To analyze and validate the expression profile and localization of endogenous Gal3 in enterocytes of the jejunum, we performed immunofluorescent staining using anti-Gal3 antibodies. In wild-type C57BL/6 mice, Gal3 expression in enterocytes was detected in the cytosol with sub-apical and basolateral localization patterns (**Fig. 1c**, left panels). The same experiment was performed on C57BL/6 Gal3 knockout mice[38], where no labeling was observed, confirming the specificity of the Gal3 signal (**Fig. 1c**, right panels).

Previous studies had shown that Gal3 is expressed at the surface of epithelial cells in the gastric mucosa, and that the protein is abundantly secreted into the mucus layer[39]. However, in our previous immunostaining assay, no Gal3 signal was detected at the more apical region of enterocytes where the mucosa is located (**Fig. 1c**), likely because PFA-fixation did not preserve the mucus layer during sample preparation. To address this point, we used Carnoy's fixative instead. Immunofluorescent analysis demonstrated abundant Gal3 labeling at the apical surface, overlapping with the mucus marker UEA-1 (**Fig. 1d,** left column), confirming that Gal3 was indeed largely localized within the mucus. Tissue from Gal3 knockout mice again served as specificity control (**Fig. 1d**, right column).

Endocytosis of exogenous Gal3 in enterocytes of the jejunum

To study the endocytic uptake of Gal3 into enterocytes of the jejunum, the intestine was removed from mice, and recombinant purified fluorophore-labeled Gal3 was injected at 20 µg/ml into the lumen. For these experiments, the intestinal mucus layer needed to be fragilized to allow exogenous Gal3 to have access to the apical epithelium membrane. Mucus indeed prevents inflammation in the digestive tract by forming a barrier that seals the paracellular space and connects individual epithelial cell membranes[40]. Mucus permeabilization was achieved by

incubation of the intestinal tissue with dithiothreitol (DTT). Under DTT conditions and using Carnoy's fixative, endogenous Gal3 signal was still observed at the levels of the mucus (**Fig. 1d**, DTT condition, middle column). This showed that the mucus was permeabilized, but not removed, and that endogenous Gal3 was retained, likely in interaction with highly O-glycosylated proteins of the mucus. A number of controls were performed with or without DTT to ascertain that DTT treatment did not damage epithelial integrity: Immunolabeling for the tight junction marker Z0-1 was indistinguishable (**Fig. 2a**, left); the ultrastructure of apically localized electron-dense tight junctions was preserved (**Fig. 2a**, middle) and the brush border marker villin was evenly distributed (**Fig. 2a**, right). We also examined the tissue permeability under DTT treatment and found that upon incubation at 4°C, the fluid-phase marker 10 kDa dextran (**Fig. 2b**, left) or exogenously added Gal3 (**Fig. 2b**, right) did not leak into the intestinal tissue, documenting that the tight junctions were still intact.

Note that in the intestine without DTT treatment of Fig. 2b (right), Gal3 likely bound to the mucus, and not to microvilli of the apical membrane. The localization of horseradish peroxidase (HRP)-labeled Gal3 to microvilli of the enterocytes could indeed directly be detected by electron microscopy only after DTT incubation (**Fig. 2c**, right panel; see arrowheads to indicate HRP-catalyzed precipitates). In contrast, no precipitate was observed in the absence of Gal3-HRP (**Fig. 2c**, left panel). In the absence of DTT treatment, dark granular precipitates from Gal3-HRP were detected above the apical microvillar membrane (**Fig. 2d**, right panel), likely because the proteins remained trapped in the mucus layer. In the absence of Gal3-HRP, the mucus could be seen but remained devoid of dark granular precipitates (**Fig. 2d**, insets). The ultrastuctural studies thus clearly establish that exogenous Gal3 reaches the apical membrane of small intestinal enterocytes only after DTT treatment.

To assess the Gal3 internalization profile, exogenous fluorophore-labeled Gal3 (Gal3-488) was bound at 4°C to the apical surface of enterocytes in DTT-permeabilized intestinal tissue, after which the tissue was shifted to 37°C to allow internalization. After the indicated periods of time, the intestinal tissue was placed on ice again, and Gal3 that had not yet been internalized (i.e. that was still cell surface accessible) was removed by incubation with a 200 mM lactose wash solution. Therefore, Gal3 labeling that is visible in **Fig. 3a** represents internalized molecules. Already after 5 min of incubation at 37°C, such internalized Gal3 labeling could be detected in sub-apical localizations (**Fig. 3a**, arrowheads). After 10 min of incubation at 37°C, we observed Gal3-containing dotted structures mainly at the lateral side of the cell, which then started to be located more basally after 15 minutes of internalization. After 20-30 min, the Gal3

signal became most prominent at the basolateral domain (**Fig. 3a**). These results clearly document a gradual transcytotic trafficking pattern of Gal3 from the initial site of binding at the apical membrane of enterocytes to the basolateral membrane.

Electron microscopy was used to analyze the morphology of Gal3-containing trafficking carriers at the ultrastructure scale. For these experiments, we again worked with HRP-coupled Gal3, which maintains the intracellular trafficking characteristics of non-modified Gal3 (Ref.[7]). After 30 min of incubation of 40 µg/ml of Gal3-HRP at 37°C with DTT-permeabilized intestinal tissue, electron-dense precipitates were found in vacuolar structures of 200-400 nm in diameter, mostly located at the basal side (**Fig. 3b**, upper panel, left). These structures were devoid of electron-dense precipitates in the absence of Gal3-HRP (**Fig. 3b**, lower panel, left), which documented the specificity of the signal. Interestingly, we also observed Gal3-HRP positive tubular and crescent-shaped structures of 300-600 nm in diameter close to the basal surface, which had the typical morphology of CLICs (**Fig. 3b**, right panels).

Gal3 undergoes GSL-dependent transcytosis

According to the GL-Lect hypothesis, oligomeric Gal3 interacts with GSLs to induce narrow membrane bending for the construction of tubular endocytic pits[9]. To test the functional implication of GSLs in Gal3 endocytosis and transcytosis in mouse enterocytes, we took advantages of the inducible *Ugcg* knockout mouse model to deplete major GSLs specifically in these cells. To analyze GSL expression levels on the first three days after tamoxifen injection, enterocytes were scraped off the lamina propria of the jejunum, GSLs were extracted, and analyzed by thin-layer chromatography (TLC) (**Fig. 4a**), or mass spectrometry (**Fig. 4b**). We focused our analysis on glucosylceramide (GlcCer), the initial product of GCS, and asialo GM1 (GA1), both of which are major GSLs of adult adult enterocytes[20]. Using both analytical methods we found that these 2 GSLs were efficiently depleted already at day 1 post tamoxifen injection in *Ugcg*flox/Cre^{+} genetic background (75% decrease of GA1), which further dropped by day 2 (80%) and 3 (90%) (**Fig. 4a,b**).

GSLs are major lipids of the membranes of the intestinal epithelium, and key players for the maintenance of apico-basal polarity[20, 41]. It was therefore of outstanding importance to characterize the integrity of epithelial features at different days of GSLs depletion. The apical localization pattern of villin remained unchanged at days 1 and 2 post-tamoxifen induction (**Fig. 4c,** -GSLs), which is quantified in **Fig. 4d**. Note that GA1 was already dramatically decreased at these time points (**Fig. 4b**). At day 3 post-tamoxifen induction, the villin signal was hardly

detectable any more (**Fig. 4c,** -GSLs). Fluorescence measurement indeed showed a dramatic drop, close to the background signal when compared to the control (**Fig. 4d**). Similarly, the tight junction protein ZO-1 was correctly localized at days 1 and 2 post-tamoxifen induction, and strongly mislocalized at day 3 (**Fig. 4e**). Taken together, these experiments demonstrate that the overall integrity of the enterocyte tissue remained unperturbed up to 2 days post-tamoxifen induction.

Tamoxifen treated, GSL-depleted intestinal tissue was DTT treated, and incubated at 4°C with 20 µg/ml of Gal3-488, followed by washing and, when indicated, shifted to 37°C for 30 min. Gal3 binding to cells was similar at days 1 and 2 after tamoxifen injection, but dramatically dropped to background levels at day 3 (**Fig. 5a**). Unperturbed binding at days 1 and 2 is consistent with previous findings on cells in culture in which it was also shown that GSLs were not required for Gal3 binding[7]. Interestingly, the endocytic uptake of Gal3 was already reduced by half on day 1 after tamoxifen injection, and was further decreased by 65% or 80% on days 2 or 3, respectively (**Fig. 5b**). This increasing inhibition of Gal3 endocytosis was closely correlated to the gradually decreasing levels of GSLs (**Fig. 4a,b**), strongly suggesting that both are causally linked.

To further confirm the specific implication of GSLs in Gal3 endocytosis, we analyzed the overall endocytic activity of the intestinal tissue under GSL depletion conditions. For this, we measured bulk fluid-phase uptake, using 40 kDa dextran that enters into the cells via all available endocytic processes[42] to accumulate into typical supranuclear vacuolar-shaped lysosomes. We have observed that dextran uptake was unperturbed for up to 2 days after tamoxifen injection (**Fig. 5c**), and expectedly dropped at day 3 (**Fig. 5c**) when the mice start dying[20]. Collectively, these data validate the biological relevance of our phenotypes on GSL-dependent Gal3 internalization, when measured short times after the onset of tamoxifen-induced GSLs depletion.

Transcytosis of the Gal3 interactor LTF depends on GSLs

Up to now, we have seen that the GL-Lect driver Gal3 undergoes GSL-dependent endocytosis and transcytosis in mouse enterocytes of the jejunum. To identify cargo proteins whose trafficking in enterocytes would be regulated by Gal3, we have performed co-immunoprecipitation experiments. DTT-treated jejunum was incubated for 30 min at 4°C with 20 µg/ml of His-tagged Gal3. Enterocytes were scraped off the lamina propria, lysed, and Gal3 binding proteins were identified by mass spectroscopy after Gal3-His immobilization onto

cobalt-agarose beads. In addition to other proteins, LTF showed up as one of the potential Gal3 binding partners with a systematic occurrence (**Fig. 6a**, top panel). To confirm this interaction, purified human Gal3-Cy3 and mouse LTF-His were incubated together. His-tagged LTF was immunoprecipitated via cobalt-agarose beads, and elution was done either with denaturing sample buffer to remove all proteins from beads, or with lactose to specifically break the interaction between bead-immobilized Gal3 and the sugar groups of its binding partners. Eluates were analyzed by SDS-PAGE. Gal3 was clearly co-immunoprecipitated with LTF (**Fig. 6a**, bottom; 1st lane). When elution was done with lactose, only Gal3 was found on the gels (**Fig. 6a**, bottom; 3rd lane), which confirmed the specificity of the interaction between both proteins. Furthermore, when incubation was performed in the presence of the specific Gal3 inhibitor I3 that acts as specific inhibitor of Gal3 binding to the carbohydrates of natural glycoproteins[43], the co-immunoprecipitated amount of Gal3 was significantly reduced (**Fig. 6a**, bottom; 2nd lane), which again confirmed the specificity of this interaction.

Fluorophore-labeled human Gal3 (Gal3-488, green) and mouse LTF (LTF-Cy3, red) were then incubated together for 30 min at 37°C with small intestinal tissue preparations on which the mucus had been permeabilized by DTT treatment. A strong overlap was observed between both markers within endocytic structures (**Fig. 6b**, see line profiles), located mainly laterally within cells (**Fig. 6b-1**, RGB profile), or basally (**Fig. 6b-2**, RGB profile). The overlap was quantified using Manders' coefficient (**Fig. 6b**, right). It is important to note a similar transcytotic pattern for both Gal3 and LTF.

The GSL dependency of LTF transcytotic trafficking within DTT-permeabilized enterocytes was determined in experiments that were similar to the ones described above for Gal3. Upon incubation at 4°C, fluorophore-labeled LTF bound efficiently to the apical membrane of enterocytes from control mice (+GSLs) at all time points after tamoxifen injection (**Fig. 6c**, top panel). Up to 2 days after tamoxifen injection, an unperturbed LTF binding level was observed in GSL-depleted (-GSLs) mice, while at day 3, LTF binding was hardly detectable any more (**Fig. 6c**, bottom panels and quantification to the right). These findings closely mirror those observed for Gal3 binding under corresponding experimental conditions (**Fig. 5a**).

Upon incubation for 30 min at 37°C, LTF could be detected at the basolateral domain of enterocytes of control mice (+GSLs) at days 1, 2, and 3 after tamoxifen injection (**Fig. 6d**, upper panel). In contrast, endocytic uptake and transcytosis of LTF were already strongly decreased 1 day after tamoxifen injection, and totally inhibited after 2 or 3 days (**Fig. 6d**, bottom panel), again mirroring the results that were observed for Gal3 under the same experimental conditions

(**Fig. 5b**).

Transcytosis of LTF depends on Gal3

We then measured LTF uptake under conditions in which the activity of endogenous galectins is inhibited. At high concentrations, lactose acts as a competitive inhibitor of galectin binding to carbohydrates on proteins and lipids. The incubation of LTF with small intestinal tissue in the presence of 200 mM lactose led to a strong reduction of the basolateral accumulation of LTF, while LTF uptake and transcytosis were as efficient as under control conditions when lactose was replaced by the disaccharide sucrose which does not act as a competitor (**Fig. 7a**, top 3 panels). The genetic deletion of Gal3 (Gal3-/-) also had a dramatic effect on basolateral accumulation of LTF, a phenotype that was efficiently rescued by the co-incubation of LTF-Cy3 (red) with exogenously added Gal3-488 (green) (**Fig. 7a**, bottom 2 panels)

The total levels of cell-associated LTF were similar in all conditions (**Fig. 7b**), most likely because LTF enters cells by several processes (see discussion), of which only the GL-Lect mechanism would couple to sorting towards the basolateral surface via transcytosis. We indeed found that more LTF accumulated in the nuclear region in lactose incubation and Gal3 knockout conditions (**Fig. 7c**), which likely originated from a redirection of the ligand into the nuclear targeting pathway[44].

In conclusion, it became apparent that endocytosis of Gal3 and LTF in enterocytes of the murine jejunum is GSL dependent, and that Gal3-dependent uptake of LTF is required for its transcytosis to the basolateral domain.

DISCUSSION

A likely explanation for the existence of different endocytic mechanisms is that they allow modulating the functions of given cargo molecules. It is therefore of critical importance to identify the physiological contexts in which they operate. In the current study, we provide convergent evidence for a critical contribution of the GL-Lect mechanism to transcytosis of LTF in murine enterocytes of the small intestine.

The mucus layer consists of crosslinked glycans that form a functional barrier implicated in inflammatory responses against pathogens. Endogenous Gal3 and other galectins are highly enriched in mucus[45], and in addition to contributing to its stability, they may also form a reservoir from which they can be recruited to build endocytic sites (**Fig. 8a**). Exogenous Gal3 and LTF, as used in our study, gain access to the apical surface of enterocytes only upon DTT-mediated permeabilization of the mucus layer (**Fig. 8a**). Using this experimental system, we show that GSL depletion reduces the total amount of internalized and transcytosed Gal3 and LTF, while the inhibition of Gal3 function with competing lactose or genetic deletion of the Gal3 gene specifically reduces the amount of transcytosed LTF, while favoring the accumulation of the protein in the nuclear area (**Fig. 8b**).

Galectins are key fabric of the GL-Lect mechanism[9]. Based on work with cells in culture, galectins have previously been implicated in apico-basal polarity, and in basolateral-to-apical transcytosis[46-49]. The Gal3-dependent transcytotic apical-to-basolateral trafficking process in the intact jejunum of mice that we described in this study has not been described before. In a previous study, the knockout of Gal3 has been shown in enterocytes of the murine small intestine to reduce membrane polarization[50], which is consistent with the findings of our current study.

The other key fabric of the GL-Lect mechanism are GSLs. These have also been implicated in apico-basal polarity in the living organism[41]. Of note, direct evidence has been provided for the transcytosic trafficking of GSL-binding pathogenic lectins, or of modified versions of GSLs themselves[51-53]. Via some yet unidentified quality, GSLs appear to have the propensity to favor transcytotic trafficking.

The discovery of GSL and Gal3-dependent transcytosis of a cellular cargo protein, LTF, as described here, argues in favor of a conceptual framework, the GL-Lect hypothesis, within which these previous findings can be analyzed from a fresh angle. This proposal may not be limited to the intestine. The GSL Gb3 has recently been shown to favor the reabsorption of

filtered proteins from urine at the level of proximal tubules[54], suggesting that GL-Lect endocytosis and transcytosis may operate on scavenger proteins such as megalin/cubilin.

When galectin function was blocked, LTF transcytosis was inhibited, but its global uptake levels into enterocytes were unaltered. Under these conditions, more LTF was found in the nuclear area, suggesting that the protein was re-routed intracellularly. Evidence for DNA binding and nuclear localization of LTF has indeed been provided[55, 56]. A likely interpretation of our findings is that GL-Lect endocytosis specifically couples to transcytotic trafficking, while an alternative form of endocytosis, possible the clathrin pathway[57], would be linked to targeting of the proteins into the nuclear area. In the absence of GSLs, Gal3 would still bind to LTF, which might prevent the latter from entering the alternative endocytic pathway. Collectively, our findings describe Gal3 as a new key player in basolateral sorting process.

The current study leads to the conclusion that GL-Lect endocytosis controls basolateral transcytotic processes in intestinal enterocytes. To what extent Gal3 function is seconded by other intestinal galectins, such as the abundant Gal4, and the exact scope of cargoes whose transcytosis might be controlled by the GL-Lect mechanism and the tissue contexts in which they operate even beyond the intestine are amongst the exciting questions that arise on the basis of the present work.

MATERIALS AND METHODS

Materials

Human Gal3-His, Cys-Gal3-His and Gal3-TEV-His plasmids in pHis-Parallel2 pGEX–6p–Gal3 (Avraham Raz, Detroit, USA)[7], antibodies against: Gal3 (Fu-Tong Gal Liu, UC Davis, USA), Zo-1 (Abcam, Ref. ab59720, discontinued; Thermo Fisher, Ref. 61-7300), villin (Fatima El Marjou, Institut Curie, France), UEA-1 (Vector Laboratories), 10 kDa and 40 kDa dextran (Chrondex), mouse LTF (Sino Biological), and the Gal3 specific inhibitor I3 (Hakon Leffler, Lund University, Sweden) were obtained from the indicated people or commercial sources.

Generation and genotyping of mouse lines

Wild-type, Gal3 knockout[58] and conditional *Ugcg* KO mice[20] were of C57BL/6 background. The animals were generated and genotyped as described previously[20, 58]. The animals were maintained in a specific pathogen-free animal house facility and handled strictly respecting the French regulation for animal care.

DNA extraction from tails

750 µl of the following solution were added to tails: 50 mM Tris-HCL, pH 8, 100 mM EDTA, 100 mM NaCl, 1% SDS, 20 µl proteinase K (10 µg/ml) (Sigma), followed by overnight incubation at 55°C. 250 µl of saturated NaCl (>5M) was added, followed by centrifugation for 20 min at 4°C at 13,000 rpm an Eppendorf centrifuge. 750 µl of supernatant was supplemented with 2 µl RNAse A (10 µg/ml) (Thermo Fisher), and RNA was digested for 20 min at 37°C. DNA was precipitated with 750 µl propanol-2, followed by centrifugation as above. After removal of the supernatant, 500 µl of ice-cold 80% ethanol was added and processed for centrifugation as above. The supernatant was removed, and Eppendorf tubes were inverted for 1 hour. 100 µl of distilled water was added, and DNA was resolved at 37°C for 2 hours.

DTT treatment of intestine

Mice were sacrificed by cervical dislocation, the jejunum was excised and washed with PBS until it became visually clean. The intestine was closed on one side with a clamp, injected with 10 mM DTT/PBS solution from the other side, and closed. The intestine segments were incubated for 15 min at 37°C, washed 3 times with DTT/PBS, and incubated again for 10 min with DTT/PBS. Intestine was washed 3 times with DTT/PBS, and 3 times with PBS.

Tissue fixation and generation of frozen blocks and sections

DTT treated jejunum was transferred for 2 hours at room temperature to freshly prepared 4% PFA in PBS (protected from light), washed 3 times 5 min with PBS, and then transferred to 30% sucrose (VWR chemicals, D(+)-Saccharose) in PBS solution at 4°C. After overnight incubation, tissue was transferred to 100% OCT solution in plastic molds (Sakura). Molds with tissue were located onto pieces of dry ice. When all of the OCT turned white, the tissue (still in the plastic mold) was placed in the –80°C freezer and stored until use. Frozen sections were prepared on a cryostat (Leica CM 1950). To mount tissue blocks on the specimen holder, some OCT was added on top of the metal holder inside the cryotome, and as it started to freeze, it was popped out of the frozen block containing the tissue and positioned flatly on the OCT. Sections of 25 μm were mounted on slides (Superfrost plus, Thermo Scientific).

Immunohistochemistry

Slides were thawed at room temperature for 5 min, rehydrated in PBS for 5 min, incubated for 10 min in 50 mM PBS/NH_4Cl, permeabilized for 15 min with 0.2% Triton X-100/PBS, incubated for 2 hours at room temperature in blocking buffer (2% PBS/BSA/0.2% Triton X-100), and overnight at 4°C with primary antibodies diluted in blocking buffer. After 3 washes in PBS for 5 min each, slides were incubated 60 min at room temperature with secondary antibodies diluted in 2% PBS/BSA. After 3 washes in PBS for 5 min each, sides were mounted with an anti-fade mounting media (Thermo Fisher Scientific, USA) containing DAPI (Thermo Fisher Scientific, USA) and visualized on a Nikon A1R confocal microscope with a 60x oil immersion objective. For quantification, confocal images were background subtracted, cellular regions were circled, and total fluorescence intensity was measured using the Image J program.

Gal3 conjugates

His-tagged Gal3 was purified as described before[7]. For Alexa-488 labeling, Gal3 (2 mg/ml) in PBS 10 mM lactose was incubated with amine-reactive (NHS-ester) Alexa488 (Invitrogen) in a molar ratio of 1:4, and the reaction was incubated for 1 hour at 21°C with agitation. The mixture was purified using PD-10 columns (GE Healthcare). Maleimide-activated horseradish peroxidase (HRP; Pierce) coupling to His-tagged Cys-Gal3 was performed for 12 hours at 4°C in PBS 10 mM lactose at a molar ratio of 1:2. To separate HRP, Cys-Gal3-His and HRP-Gal3-His, gel filtration chromatography was performed using a Superdex75 10 × 30 column. HRP-Gal3-His in 50% glycerol was snap-frozen and stored at -80°C for further usage.

Binding and internalization assays

DTT treated jejunum segments were either incubated for 30 min at 4°C in PBS, or directly processed as follows. The segments were closed at one end with a clamp, and Gal3-Alexa488 (20 µg/ml), LTF–Cy3 (20 µg/ml), or 40 kDa Dextran (31 µg/ml) in PBS were injected from the other end, which was then also closed with a clamp. Segments were incubated for the indicated periods of time at 4°C and/or 37°C in PBS (for pulse-chase experiments, segments were washed once with PBS between the 4°C and the 37°C incubation steps), longitudinally opened, and ligands that remained cell surface-exposed were removed by 3 washes of 10 min each at 4°C with ice-cold 200 mM lactose in PBS. For binding experiments, the lactose step was omitted. Segments were then washed, fixed, and processed for cryo-embedding, as described above.

Electron microscopy

DTT treated jejunum was incubated at 37°C for the indicated times with 10 mg/ml HRP in PBS, PBS alone, or 40 µg/ml HRP-Gal3 in PBS, or at 4°C for the cell surface binding. Cell surface-exposed markers were removed by 3 washes for 10 min each at 4°C with 200 mM lactose in PBS (step omitted for binding experiments). The intestine was opened in transverse orientation, cut in 3 mm x 2 mm pieces, incubated for 15 min at 4°C in freshly prepared 0.7 mg/ml 3,3'-diaminobenzidine (DAB) solution (Sigma), washed, incubated for 1 hour at 4°C with DAB + 30% H_2O_2, washed 3 times 5 min each with PBS, fixed for 2-3 days at 4°C with 2.5% glutaraldehyde (EMS) in 0,1 M Na-cacodylate (pH 7.2), washed 3 times for 5 min each at room temperature with 0.1 M Na-cacodylate, post-fixed for 1-2 hours at room temperature with OsO4 1% (EMS) in 0.1 M Na-cacodylate, washed 5 times for 5 min each with 0.1 M Na-cacodylate, followed by a final washing for 5 min with water. Tissue dehydration was performed at room temperature according to following incubation protocol: 50% ethanol 10 min, 70% ethanol 10 min, 90% ethanol 2 times 15 min each, 100% ethanol 3 times 20 min each, followed by infiltration of Epon resin LX112 at room temperature (LX112/EtOH 100% 1v/1v for 30 min, LX112/EtOH 100% 2v/1v for 45 min, LX112 for 1hour, LX112 overnight). The polymerization of tissue in LX112 was done in embedding mold (tissue bloc 2 mm) for 2-3 days at 60°C. Samples were sectioned in an ultramicrotome (Reichert Leica UCT), and sections of 65 nm thickness were deposited on formvar/carbon-coated grid (form/carbon square 100 mesh – Cu: FCF100-CU-SB EMS). Contrast was removed by incubation for 10 min with 4% uranyl acetate in water. Sections were imaged using a Tecnai Spirit electron microscope (FEI, Eindhoven, The Netherlands) equipped with a 4k CCD camera (EMSIS GmbH, Münster, Germany).

Mucus fixation with Carnoy's solution and whole-mount immunofluorescence staining

DTT treated jejunum was fixed overnight in freshly-prepared 60% ethanol, 30% chloroform, and 10% glacial acetic acid, cut with a scalpel in slices of ~1 mm, which were incubated for 1 hour at room temperature in 1% Triton X-100/PBS, for 1 hour at room temperature in 0.2% Triton X-100/PBS, 1% BSA, and 3% FCS, overnight at room temperature with primary antibodies in 0.2% Triton X-100/PBS, washed 3 times for 1 hour each with 0.2% Triton X-100/PBS, incubated overnight at room temperature with secondary antibodies and DAPI in 0.2% Triton X-100/PBS, washed 3 times for 1 hour each with 0.2% Triton X-100/PBS, mounted using an anti-fade mounting media (Thermo Fisher Scientific, USA), and stored at 4°C.

Pulldown experiments for Gal3 interacting partners

DTT treated jejunum was incubated for 30 min at 4°C in PBS alone, or PBS containing 20 µg/ml of Gal3-His. After rinsing twice with PBS, intestine was longitudinally opened and enterocytes of the jejunum were scraped with the glass slide (Thermo Scientific, USA) and lysed with 2% Triton X-100/0.5% NP40 in PBS in the presence of protease inhibitor cocktail. Cleared lysates (16,000xg, 30 min, 4°C) were incubated overnight at 4°C with cobalt Sepharose (Qiagen), washed with lysis buffer (without protease inhibitors), and sent to mass spectrometry for further analysis.

Gal3 interacting partners were eluted with two buffers (1. Loading buffer for SDS PAGE: 2% SDS 1X; 2. Hepes 50 mM, NaCl 50 mM, lactose 200 mM, pH 7.5 and LSB 1X) and separated by SDS-PAGE (30 min, 80V). After staining with colloidal blue, the complete band of each replicate (n = 3) was excised and processed. Excised gel slices were washed and proteins were reduced with 10 mM DTT prior to alkylation with 55 mM iodoacetamide. After washing and shrinking of the gel pieces with 100% acetonitrile, in-gel digestion was performed using trypsin/LysC (0.1µg) overnight in 25 mM ammonium bicarbonate at 30°C. Peptide were then extracted using 60/35/5 MeCN/H2O/HCOOH, vacuum concentrated to dryness. Sample were loaded onto homemade C18 StageTips for desalting. Peptides were eluted from beads by incubation with 40/60 MeCN/H2O + 0.1% formic acid. The peptides were dried in a Speedvac and reconstituted in 10 µL 2/98 MeCN/H2O + 0.3% trifluoroacetic acid (TFA) prior to liquid chromatography-tandem mass spectrometry (LC-MS/MS) analysis. Samples were chromatographically separated using an RSLCnano system (Ultimate 3000, Thermo Scientific) coupled online to a Q Exactive HF-X with a Nanospray Flex ion source (Thermo Scientific). Peptides were trapped onto a C18-reversed phase precolumn (75-µm inner diameter × 2 cm;

nanoViper Acclaim PepMapTM 100, Thermo Scientific), with buffer A (2/98 MeCN/H2O + 0.1% formic acid) at a flow rate of 2.5 µL/min over 4 min. Separation was performed on a 50 cm x 75-µm C18 column (nanoViper Acclaim PepMapTM RSLC, 2 µm, 100Å, Thermo Scientific) regulated to a temperature of 50°C with a linear gradient of 2% to 30% buffer B (100% MeCN and 0.1% formic acid) at a flow rate of 300 nL/min over 91 min. MS full scans were performed in the ultrahigh-field Orbitrap mass analyzer in ranges m/z 375–1500 with a resolution of 120,000 at m/z 200. The maximum injection time (MIT) was 50 ms, and the automatic gain control (AGC) was set to 3×10^6. The top 20 intense ions were subjected to Orbitrap for further fragmentation via high energy collision dissociation (HCD) activation and a resolution of 15,000 with the intensity threshold kept at 1.3×10^5. We selected ions with charge state from 2+ to 6+ for screening. Normalized collision energy (NCE) was set at 27. For each scan, the AGC was set at 1×10^5, the MIT was 60 ms, and the dynamic exclusion of 40s. For identification the data were searched against the UniProt *Mus musculus* canonical (house Mouse downloaded on 22/08/2017) database using Sequest^{HF} through proteome discoverer (version 2.0). Enzyme specificity was set to trypsin and a maximum of two missed cleavage sites were allowed. Oxidized methionine, N-terminal acetylation, and carbamidomethyl cysteine were set as variable modifications. Maximum allowed mass deviation was set to 10 ppm for monoisotopic precursor ions and 0.02 Da for MS/MS peaks. The resulting files were further processed using myProMS[59] v3.9. FDR calculation used Percolator and was set to 1% at the peptide level for the whole study. The label free quantification was performed by peptide Extracted Ion Chromatograms (XICs) computed with MassChroQ version 2 (Ref.[60]). For protein quantification, XICs from proteotypic peptides shared between compared conditions (TopN matching) with missed cleavages and carbamidomethyl modifications were used. Median and scale normalization was applied on the total signal to correct the XICs for each biological replicate. To estimate the significance of the change in protein abundance, a linear model (adjusted on peptides and biological replicates) was performed and p-values were adjusted with a Benjamini–Hochberg FDR procedure with a control threshold set to 0.05. To focus from this complex list on partners that were only present in Gal3 replicates, we selected in the qualitative comparison proteins with at least 1 peptide in each Gal3 replicate, 0 peptide in the PBS control, and only based on proteotypic peptides which allowed to capture only specific proteins.

Pulldown experiments to identify galectins in jejunum

Enterocytes were scraped off the lamina propria with a glass slide (Superfrost, Thermo Scientific). 1 ml of 2% Triton X-100/0.5% NP40 in PBS was added to the cells, which were passed 10 times through a 23G needle. Lysate was cleared at by 16,000xg centrifugation for 10 min at 4°C. Lactose agarose beads (L7634-5ml, Sigma) were prepared by 2 washes in lysis buffer. Lysates were incubated by end-over-end rotation for 1 hour at 4°C with beads. Beads were then washed in lysis buffer, and sent to mass spectrometry for further analysis.

Galectin beads sample was washed twice with 100 µl of 25 mM NH4HCO3 and on-beads digested with 0.2 µg of trypsine/LysC (Promega) for 1 hour in 50 µl of 25 mM NH4HCO3. Sample was desalted and analyzed by nanoLC-MS/MS using an UltiMate 3000 RSLCnano system (Thermo Scientific) coupled to an Orbitrap Fusion (Q-OT-qIT, Thermo Fisher Scientific) mass spectrometer[61].

***In vitro* interaction studies between Gal3 and LTF**

Purified mouse LTF-His and human Gal3-Cy3 without a His-tag (4 µg/ml each) in PBS supplemented with 0,1% Tween-20 (PBS-T) buffer were incubated under agitation for 15 min at 18°C in the presence or absence of the Gal3 inhibitor I3. Cobalt beads (#89965, Thermo Scientific) were added for 30 min incubation under rotation at 4°C, collected by centrifugation at 700xg, washed 3 times with PBS-T buffer, and eluted by incubation for 30 min at room temperature under agitation with 200 mM lactose, or by boiling in sample buffer for 10 min at 95°C. Eluted proteins were analyzed on stain-free SDS–PAGE gels (Bio-Rad).

Statistics and data repository

All the experiments were done with at least 3 biological replicates. All quantifications were performed with at least 34 cells per conditions. For each experiment we show representative data sets. Statistical analysis was performed either by unpaired Student's t-test, or with One-Way ANOVA (for multiple comparison).

All mass spectrometry proteomics data have been deposited to the ProteomeXchange Consortium via the PRIDE partner repository[62] with the dataset identifier PXD016499 (username reviewer18055@ebi.ac.uk, password: ARHPfQ1I).

ACKNOWLEDGEMENTS

We would like to thank the following people for help in experiments, providing materials, and/or expertise: Marina Glukhova, Anna Zagryazhskaya-Masson, Danijela Vignjevic, Hakon Leffler, Florent Dingli, Guillaume Arras, Caspar Caspersen, Fu-Tong Liu, Denis Krndija, Fatima El Marjou, *Institute Curie* and *Institut Jacques Monod* mice facility members. We acknowledge support by grants from the *Agence Nationale pour la Recherche* (ANR-14-CE14-0002-02, ANR-16-CE23-0005-02, ANR-19-CE13-0001-01), Human Frontier Science Program (RGP0029-2014), European Research Council (advanced grant 340485), the Swedish Research Council (K2015-99X-22877-01-6). The Johannes team is member of Labex CelTisPhyBio (11-LBX-0038) and Idex Paris Sciences et Lettres (ANR-10-IDEX-0001-02 PSL). We would also like to acknowledge the Cell and Tissue Imaging (PICT-IBiSA) and Nikon Imaging Centre, *Institut Curie*, member of the French National Research Infrastructure France-BioImaging (ANR10-INBS-04).

REFERENCES

1. Robinson, M.S. Forty Years of Clathrin-coated Vesicles. *Traffic* **16**, 1210-1238 (2015).
2. Kirchhausen, T., Owen, D. & Harrison, S.C. Molecular structure, function, and dynamics of clathrin-mediated membrane traffic. *Cold Spring Harb. Perspect. Biol.* **6**, a016725 (2014).
3. McMahon, H.T. & Boucrot, E. Molecular mechanism and physiological functions of clathrin-mediated endocytosis. *Nat. Rev. Mol. Cell. Biol.* **12**, 517-533 (2011).
4. Ferreira, A.P.A. & Boucrot, E. Mechanisms of Carrier Formation during Clathrin-Independent Endocytosis. *Trends Cell Biol.* **28**, 188-200 (2017).
5. Mayor, S., Parton, R.G. & Donaldson, J.G. Clathrin-independent pathways of endocytosis. *Cold Spring Harb. Perspect. Biol.* **6**, a016758 (2014).
6. Römer, W. *et al.* Shiga toxin induces tubular membrane invaginations for its uptake into cells. *Nature* **450**, 670-675 (2007).
7. Lakshminarayan, R. *et al.* Galectin-3 drives glycosphingolipid-dependent biogenesis of clathrin-independent carriers. *Nat. Cell Biol.* **16**, 595-606 (2014).
8. Mathew, M.P. & Donaldson, J.G. Distinct cargo-specific response landscapes underpin the complex and nuanced role of galectin-glycan interactions in clathrin-independent endocytosis. *J. Biol. Chem.* **293**, 7222-7237 (2018).
9. Johannes, L., Wunder, C. & Shafaq-Zadah, M. Glycolipids and lectins in endocytic uptake processes *J. Mol. Biol.* **428**, 4792-4818 (2016).
10. Johannes, L. Shiga toxin — A model for glycolipid-dependent and lectin-driven endocytosis. *Toxins* **9**, 340 (doi:310.3390/toxins9110340) (2017).
11. Mathew, M.P. & Donaldson, J.G. Glycosylation and glycan interactions can serve as extracellular machinery facilitating clathrin independent endocytosis. *Traffic* (2019).
12. Hemalatha, A. & Mayor, S. Recent advances in clathrin-independent endocytosis. *F1000Research* **8** (2019).
13. Banfer, S. *et al.* Molecular mechanism to recruit galectin-3 into multivesicular bodies for polarized exosomal secretion. *Proc. Natl. Acad. Sci. USA* **115**, E4396-e4405 (2018).
14. Nieminen, J., Kuno, A., Hirabayashi, J. & Sato, S. Visualization of galectin-3 oligomerization on the surface of neutrophils and endothelial cells using fluorescence resonance energy transfer. *J. Biol Chem.* **282**, 1374-1383 (2007).
15. Kirkham, M. *et al.* Ultrastructural identification of uncoated caveolin-independent early endocytic vehicles. *J. Cell Biol.* **168**, 465-476 (2005).
16. Howes, M.T. *et al.* Clathrin-independent carriers form a high capacity endocytic sorting system at the leading edge of migrating cells. *J. Cell Biol.* **190**, 675-691 (2010).
17. Ewers, H. *et al.* GM1 structure determines SV40-induced membrane invagination and infection. *Nat. Cell Biol.* **12**, 11-18 (2010).
18. Rydell, G.E., Svensson, L., Larson, G., Johannes, L. & Römer, W. Human GII.4 norovirus VLP induces membrane invaginations on giant unilamellar vesicles containing secretor gene dependent alpha-1,2-fucosylated glycosphingolipids. *Biochim. Biophys. Acta* **1828**, 1840-1845 (2013).
19. D'Angelo, G., Capasso, S., Sticco, L. & Russo, D. Glycosphingolipids: synthesis and functions. *Febs J.* **280**, 6338-6353 (2013).
20. Jennemann, R. *et al.* Glycosphingolipids are essential for intestinal endocytic function. *J. Biol. Chem.* **287**, 32598-32616 (2012).
21. Fish, E.M. & Burns, B. Physiology, Small Bowel, in *StatPearls* (StatPearls Publishing StatPearls Publishing LLC., Treasure Island (FL); 2019).

22. Reboul, E. & Borel, P. Proteins involved in uptake, intracellular transport and basolateral secretion of fat-soluble vitamins and carotenoids by mammalian enterocytes. *Prog. Lipid Res.* **50**, 388-402 (2011).
23. Fishman, J.B. & Fine, R.E. A trans Golgi-derived exocytic coated vesicle can contain both newly synthesized cholinesterase and internalized transferrin. *Cell* **48**, 157-164 (1987).
24. Lim, C.J., Norouziyan, F. & Shen, W.C. Accumulation of transferrin in Caco-2 cells: a possible mechanism of intestinal transferrin absorption. *J. Control Release* **122**, 393-398 (2007).
25. Shah, D. & Shen, W.C. Transcellular delivery of an insulin-transferrin conjugate in enterocyte-like Caco-2 cells. *J. Pharm. Sci.* **85**, 1306-1311 (1996).
26. Fung, K.Y.Y., Fairn, G.D. & Lee, W.L. Transcellular vesicular transport in epithelial and endothelial cells: Challenges and opportunities. *Traffic* **19**, 5-18 (2018).
27. Suzuki, Y.A., Shin, K. & Lonnerdal, B. Molecular cloning and functional expression of a human intestinal lactoferrin receptor. *Biochemistry* **40**, 15771-15779 (2001).
28. Lopez, V., Suzuki, Y.A. & Lonnerdal, B. Ontogenic changes in lactoferrin receptor and DMT1 in mouse small intestine: implications for iron absorption during early life. *Biochem. Cell Biol.* **84**, 337-344 (2006).
29. Hao, L., Shan, Q., Wei, J., Ma, F. & Sun, P. Lactoferrin: Major physiological functions and applications. *Curr. Protein Pept. Sci.* **20**, 139-144 (2019).
30. Wrackmeyer, U., Hansen, G.H., Seya, T. & Danielsen, E.M. Intelectin: a novel lipid raft-associated protein in the enterocyte brush border. *Biochemistry* **45**, 9188-9197 (2006).
31. Rawat, P., Kumar, S., Sheokand, N., Raje, C.I. & Raje, M. The multifunctional glycolytic protein glyceraldehyde-3-phosphate dehydrogenase (GAPDH) is a novel macrophage lactoferrin receptor. *Biochem. Cell Biol.* **90**, 329-338 (2012).
32. Tanaka, T. *et al.* The detection of bovine lactoferrin binding protein on Trypanosoma brucei. *J. Vet. Med. Sci.* **66**, 619-625 (2004).
33. Davidsson, L., Kastenmayer, P., Yuen, M., Lonnerdal, B. & Hurrell, R.F. Influence of lactoferrin on iron absorption from human milk in infants. *Pediatr. Res.* **35**, 117-124 (1994).
34. Ward, P.P., Mendoza-Meneses, M., Cunningham, G.A. & Conneely, O.M. Iron status in mice carrying a targeted disruption of lactoferrin. *Mol. Cell Biol.* **23**, 178-185 (2003).
35. Akiyama, Y. *et al.* Intracellular retention and subsequent release of bovine milk lactoferrin taken up by human enterocyte-like cell lines, Caco-2, C2BBe1 and HT-29. *Biosci. Biotechnol. Biochem.* **77**, 1023-1029 (2013).
36. Akiyama, Y. *et al.* A lactoferrin-receptor, intelectin 1, affects uptake, sub-cellular localization and release of immunochemically detectable lactoferrin by intestinal epithelial Caco-2 cells. *J. Biochem.* **154**, 437-448 (2013).
37. Nio-Kobayashi, J. Tissue- and cell-specific localization of galectins, beta-galactose-binding animal lectins, and their potential functions in health and disease. *Anat. Sci. Int.* (2016).
38. Poirier, F. & Robertson, E.J. Normal development of mice carrying a null mutation in the gene encoding the L14 S-type lectin. *Development* **119**, 1229-1236 (1993).
39. Park, A.M., Hagiwara, S., Hsu, D.K., Liu, F.T. & Yoshie, O. Galectin-3 plays an important role in innate immunity to gastric infection by Helicobacter pylori. *Infect. Immun.* **84**, 1184-1193 (2016).
40. Groschwitz, K.R. & Hogan, S.P. Intestinal barrier function: molecular regulation and disease pathogenesis. *J. Allergy Clin. Immunol.* **124**, 3-20; quiz 21-22 (2009).

41. Zhang, H. *et al.* Apicobasal domain identities of expanding tubular membranes depend on glycosphingolipid biosynthesis. *Nat. Cell Biol.* **13**, 1189-1201 (2011).
42. Pavelka, M. & Roth, J. Fluid-Phase Endocytosis and Phagocytosis. *Functional Ultrastructure*, 104-105 (2010).
43. Zetterberg, F.R. *et al.* Monosaccharide derivatives with low nM lectin affinity and high selectivity based on combined fluorine-amide, phenyl-arginine, sulfur-pi, and halogen bond interactions. *ChemMedChem* (2017).
44. Rubartelli, A. & Sitia, R. Entry of exogenous polypeptides into the nucleus of living cells: facts and speculations. *Trends Cell Biol.* **5**, 409-412 (1995).
45. Vasta, G.R. Roles of galectins in infection. *Nat. Rev. Microbiol.* **7**, 424-438 (2009).
46. Perez Bay, A.E., Schreiner, R., Benedicto, I. & Rodriguez-Boulan, E.J. Galectin-4-mediated transcytosis of transferrin receptor. *J. Cell Sci.* **127**, 4457-4469 (2014).
47. Delacour, D. *et al.* Galectin-4 and sulfatides in apical membrane trafficking in enterocyte-like cells. *J. Cell Biol.* **169**, 491-501 (2005).
48. Delacour, D. *et al.* Requirement for galectin-3 in apical protein sorting. *Curr. Biol.* **16**, 408-414 (2006).
49. Mishra, R., Grzybek, M., Niki, T., Hirashima, M. & Simons, K. Galectin-9 trafficking regulates apical-basal polarity in Madin-Darby canine kidney epithelial cells. *Proc. Natl. Acad. Sci. USA* **107**, 17633-17638 (2010).
50. Delacour, D. *et al.* Loss of galectin-3 impairs membrane polarisation of mouse enterocytes in vivo. *J. Cell Sci.* **121**, 458-465 (2008).
51. Garcia-Castillo, M.D., Chinnapen, D.J. & Lencer, W.I. Membrane Transport across Polarized Epithelia. *Cold Spring Harb. Perspect. Biol.* **9**, a027912 (2017).
52. Saslowsky, D.E. *et al.* Ganglioside GM1-mediated transcytosis of cholera toxin bypasses the retrograde pathway and depends on the structure of the ceramide domain. *J. Biol. Chem.* **288**, 25804-25809 (2013).
53. Muller, S.K. *et al.* Gb3-binding lectins as potential carriers for transcellular drug delivery. *Expert Opin. Drug Deliv.* **14**, 141-153 (2017).
54. Morace, I. *et al.* Renal globotriaosylceramide facilitates tubular albumin absorption and its inhibition protects against acute kidney injury. *Kidney Int.* **96**, 327-341 (2019).
55. Garre, C., Bianchi-Scarra, G., Sirito, M., Musso, M. & Ravazzolo, R. Lactoferrin binding sites and nuclear localization in K562(S) cells. *J. Cell Physiol.* **153**, 477-482 (1992).
56. Penco, S. *et al.* Identification of an import signal for, and the nuclear localization of, human lactoferrin. *Biotechnol. Appl. Biochem.* **34**, 151-159 (2001).
57. Jiang, R., Lopez, V., Kelleher, S.L. & Lonnerdal, B. Apo- and holo-lactoferrin are both internalized by lactoferrin receptor via clathrin-mediated endocytosis but differentially affect ERK-signaling and cell proliferation in Caco-2 cells. *J. Cell Physiol.* **226**, 3022-3031 (2011).
58. Colnot, C. *et al.* Maintenance of granulocyte numbers during acute peritonitis is defective in galectin-3-null mutant mice. *Immunology* **94**, 290-296 (1998).
59. Poullet, P., Carpentier, S. & Barillot, E. myProMS, a web server for management and validation of mass spectrometry-based proteomic data. *Proteomics* **7**, 2553-2556 (2007).
60. Valot, B., Langella, O., Nano, E. & Zivy, M. MassChroQ: a versatile tool for mass spectrometry quantification. *Proteomics* **11**, 3572-3577 (2011).
61. Zylicz, J.J. *et al.* The implication of early chromatin changes in X chromosome inactivation. *Cell* **176**, 182-197.e123 (2019).
62. Vizcaino, J.A. *et al.* 2016 update of the PRIDE database and its related tools. *Nucleic Acids Res.* **44**, 11033 (2016).

FIGURE LEGENDS

Figure 1: Galectin expression in murine jejunum

(**a**) For our studies, the jejunum part of the mouse intestine was used as a model system. Schematic overview of the functional structure and features of the intestinal epithelium and of enterocytes.

(**b**) Galectin expression profile in the jejunum: Mass spectrometry results of galectins that were immuno-purified from jejunum cell lysates of C57BL/6 mice, using lactose-coated beads.

(**c**) Localization of endogenous Gal3 (green): transverse sections of Gal3+/+ (BL6) mouse jejunum were analyzed by immunohistochemistry using an anti-Gal3 antibody. Gal3-deficient (Gal3-/-) mice were included as specificity controls. Insets represent magnification of a monolayer of cells. Nuclei were labeled with DAPI (blue). Scale bars: 10 μm.

(**d**) Gal3 localization within the mucosal barrier: Immunohistochemistry was performed using tissue sections from Carnoy's fixed jejunum tissue obtained from Gal3+/+ (BL6) or Gal3-/- mice. Labeling with antibodies directed against Gal3 (green) or the mucus marker UEA-1 (red). The absence of Gal3 signal in Gal3-/- conditions confirmed the specificity of the Gal3 signal. Note that DTT treatment didn't perturb Gal3 or UEA-1 localizations. Scale bars: 5 μm.

Figure 2: Interaction of exogenous Gal3 with murine jejunum

(**a**) Characterization of the integrity of the mouse jejunum under DTT treatment conditions. The tight junction marker ZO-1 (violet, left panels) and the microvilli marker villin (red, right panels) are localized normally in DTT conditions. Nuclei are labeled with DAPI. Electron dense tight junction structure have unperturbed morphology and localization in DTT conditions, as analyzed by electron microscopy (middle panels).

(**b**) No transcellular leakage under DTT treatment conditions. Neither 10 kDa dextran (violet, left panels) nor Gal3 (green, right panels) diffused into the tissue when incubated at 4°C with DTT-treated murine jejunum.

(**c**) DTT treatment is required for Gal3 to reach the brush border. DTT-permeabilized jejunum that was incubated with Gal3-HRP shows specific HRP-positive signal at the level of microvilli (dark dotted signal, right panel, arrowheads). This labeling is specific as it is not observed when incubations were done in the absence of Gal3-HRP (left panel).

(**d**) Without DTT treatment, Gal3-HRP signal is trapped within the mucus layer. Granular dark dotted structures are detected at the far tip part of the microvilli, further visible under higher

magnification (right panels, arrowheads). In contrast no signal is detected in the absence of Gal3-HRP (two left panels).
Scale bars: 10 μm for immunofluorescence, and 1 μm for electron microscopy images.

Figure 3: Internalization of exogenous Gal3 into enterocytes

(**a**) Pulse-chase experiment of Gal3 uptake in enterocytes. Gal3 (green) was bound at 4°C to enterocytes of DTT-treated jejunum. After washing, incubations were performed at 37°C for the indicated periods of time. Cell surface-exposed Gal3 was removed with lactose wash. Note that distinct intracellular structures are visible at all time points (arrowheads).
(**b**) Electron microscopy analysis of Gal3 uptake into enterocytes of the DTT-treated jejunum. After 30 min of incubation at 37°C with 40 ug/ml of HRP-coupled Gal3, electron-dense DAB precipitates (arrowheads) are found in vacuolar structures close to the basal membrane (top left panel), or in tubular crescent-shaped structures with typical CLIC morphologies (right panels). For comparison, an image of cells that were incubated in the absence of Gal3-HRP is shown in the bottom left panel.
Scale bars: 10 μm for immunofluorescence, and 1 μm for electron microscopy images.

Figure 4: Tissue integrity under GSL depletion conditions

(**a**) *Ugcg*flox/Cre^{+} or *Ugcg*flox/Cre^{-} mice were injected with 1 mg of tamoxifen for 3 consecutive days. At days 1, 2, or 3, the jejunum was excised and analyzed for GSL expression using thin layer chromatography. D1-3(-) samples contain a GSL-band migrating at the height of the GA1 standard, which is strongly reduced in the D1-3(+) samples. There is another band migrating a little bit below the NS-GalCer standard (NS: non-hydroxy-fatty acid; sphingosine). It is also gone by 90% in samples D2(+) and D3(+), but not in D1(+).
(**b**) Quantification of GSLs by LC-MS/MS.
(**c-e**) Conservation of tissue integrity under GSL depletion conditions. Immunohistochemistry on jejunum of *Ugcg*flox/Cre^{-} (+GLSs) or *Ugcg*flox/Cre^{+} (-GSLs) mice at the indicated days after tamoxifen injection. Immunolabeling for villin (c) or ZO-1 (e). Note that at days 1 and 2 after tamoxifen injection, staining patterns are not visibly altered under GSL depletion conditions. Data from (c) are quantified in (d). Student's unpaired t-test, **** $p<0,0001$, ns: non-significant.

Figure 5: Gal3 undergoes GSL-dependent endocytosis

(**a**) DTT-treated jejunum of tamoxifen-injected *Ugcg*flox/Cre^{+} (-GSLs) or *Ugcg*flox/Cre^{-} (+GLSs) mice was incubated at 4°C with 20 µg/ml of Gal3 (green). Nuclei in blue. Note that Gal3 binding to the apical surface was similar at days 1 and 2 after tamoxifen injection, while it dropped to background levels at day 3. Right: Quantification of apical signal of 11 tissue sections, each of which with 10 cells on average (means ± SEM, n=4 independent experiments).
(**b**) Experiment as in (a), except that incubation with Gal3 (green) was done for 30 min at 37°C. Cell surface-exposed Gal3 was removed with lactose wash. Note that Gal3 uptake was strongly inhibited in GSL-depleted enterocytes, starting with day 1. Right: Quantification on 114 cells per condition (means ± SEM, n=4 independent experiments).
(**c**) Experiment as in (b), except that incubation at 37°C was performed with at 31 µg/ml of 40 kDa dextran (green). Dextran uptake was similar at days 1 and 2 after tamoxifen injection, while it dropped to background levels at day 3. Right: Representative quantification on 106 cells per condition (means ± SEM, n=4 independent experiments).
Statistical analysis: Student's unpaired t-test, **** p<0,0001, ns: non-significant.
Scale bars = 10 µm.

Figure 6: LTF transcytosis is GSL dependent
(**a**) Identification of LTF as a Gal3 interacting protein in enterocytes of the jejunum of wild-type BL6 mice. Top: Quantitative analysis of proteins present in Gal3 (=B) samples compared to PBS control (=A) is shown as volcano plot. x axis = log2 (fold change Gal3/PBS), y axis = -log10 (p-value). The horizontal red line indicates p value = 0.05, vertical green lines indicates absolute fold change = 2. Data represent results of three independents immunoprecipitations. Proteins are shown with at least 1 peptide in each of the Gal3 replicates, and 0 peptide in the PBS control replicates in the qualitative comparison without Match-between-Runs-rescued peptides. Bottom: Pull-down experiment on cobalt-agarose beads of purified LTF-His and Gal3-Cy3. Note that Gal3 is co-purified with LTF in a Gal3 inhibitor (I3)-dependent manner, and specifically eluted with lactose.
(**b**) 20 µg/ml of Gal3-488 (green) and LTF-Cy3 (red) were co-incubated for 30 min at 37°C with DTT-permeabilized jejunum. Note the strong overlap between both markers. Right: Mander's coefficient analysis confirms colocalization between Gal3 and LTF, strongly suggesting that both proteins are co-internalized.
(**c**) At days 1, 2, or 3 after tamoxifen injection, DTT-permeabilized jejunum of *Ugcg*flox/Cre^{-} (+GSLs) or *Ugcg*flox/Cre^{+} (-GSLs) mice was incubated at 4°C with 20 µg/ml of LTF-Cy3 (red). Nuclei in blue. Note that LTF binding to the apical surface was similar in all conditions,

with the exception of day 3 after tamoxifen injection where it dropped to background levels. Right: Quantification of apical signal of 6 tissue sections, each of which with 10 cells on average (means ± SEM, n=4 independent experiments).

(**d**) Experiment as in (c), except that incubation was performed at 37°C. LTF endocytosis was strongly reduced already at day 1 after tamoxifen injection, and dropped to background levels at days 2 and 3. Right: Quantification of 102 cells per condition (means ± SEM, n=4 independent experiments).

Statistical analysis in (c) and (d): Student's unpaired t-test, **** p<0,0001, ns: non-significant.

Scale bars = 10 µm.

Figure 7: LTF transcytosis is Gal3 dependent

(**a**) In all panels that are shown in this figure, LTF-Cy3 (red) at 20 µg/ml was incubated for 30 min at 37°C with DTT-permeabilized jejunum. Nuclei in blue. The following experimental conditions are represented: Control conditions with wild-type BL6 mice; incubation in the presence of 200 mM sucrose, which did not affect LTF-Cy3 trafficking; incubation in the presence of 200 mM lactose as a competitor for galectin-binding to carbohydrates, which strongly reduced the basolateral accumulation of LTF-Cy3; incubation with jejunum from Gal3 KO mice, on which the basolateral accumulation of LTF-Cy3 was strongly reduced; co-incubation of LTF-Cy3 with 20 µg/ml of Gal3-488 (green) on the jejunum from Gal3 KO mice, which led to the rescue of LTF transcytosis to the basolateral surface.

(**b**) Quantification of experiments shown in (a) of total LTF-Cy3 labeling intensity per cell in the indicated conditions. Representative quantification of 108 cells per condition (means ± SEM, n=4 independent experiments).

(**c**) Quantification of experiments shown in (a) of the labeling intensity of LTF in the nuclear area. Quantification on 34 cells per condition (means ± SEM, n=2 independent experiments).

Statistical analysis in (b) and (c): (b) Student's unpaired t-test, **** p<0,0001, ns: non-significant; (c) One-Way ANOVA.

Scale bars = 10 µm.

Figure 8: The GL-Lect hypothesis in mouse intestinal epithelium

(**a**) Schematic representation of the GL-Lect hypothesis[9] transposed to the apical surface of enterocytes of the jejunum. In the absence of DTT-mediated permeabilization of the mucus, exogenous Gal3 and LTF do not gain access to the apical membrane surface and remains

trapped in the mucus (top panel). Upon DTT-mediated permeabilization of the mucus, monomeric Gal3 is recruited to apical membranes by binding to glycosylated cargo proteins on microvilli, such as LTF (middle panel). Membrane-bound Gal3 oligomerizes and gains the functional capacity to interact with GSLs to drive membrane bending (bottom panel). Gal3-mediated co-clustering of glycosylated cargo proteins and GSLs drives the formation of tubular endocytic pits from which CLICs are formed.

(**b**) Schematic representation of the outcomes of the current study. Left: Schematic representation of transcytosis in control conditions. Middle: Under GSL depletion conditions, GL-Lect endocytosis of LTF is inhibited, leading to reduced transcytosis. Right: Under Gal3 knockout conditions or in the presence of high lactose concentrations, GL-Lect endocytosis and transcytosis of LTF are inhibited, while LTF targeting to the nuclear region appears to be increased. See text for details.

Figure 1:

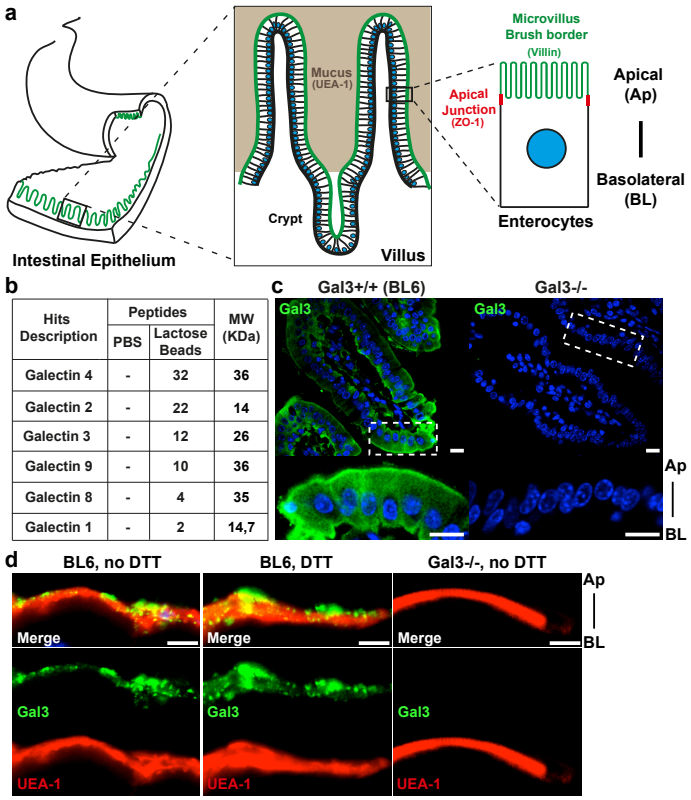

Hits Description	Peptides		MW (KDa)
	PBS	Lactose Beads	
Galectin 4	-	32	36
Galectin 2	-	22	14
Galectin 3	-	12	26
Galectin 9	-	10	36
Galectin 8	-	4	35
Galectin 1	-	2	14,7

Figure 2:

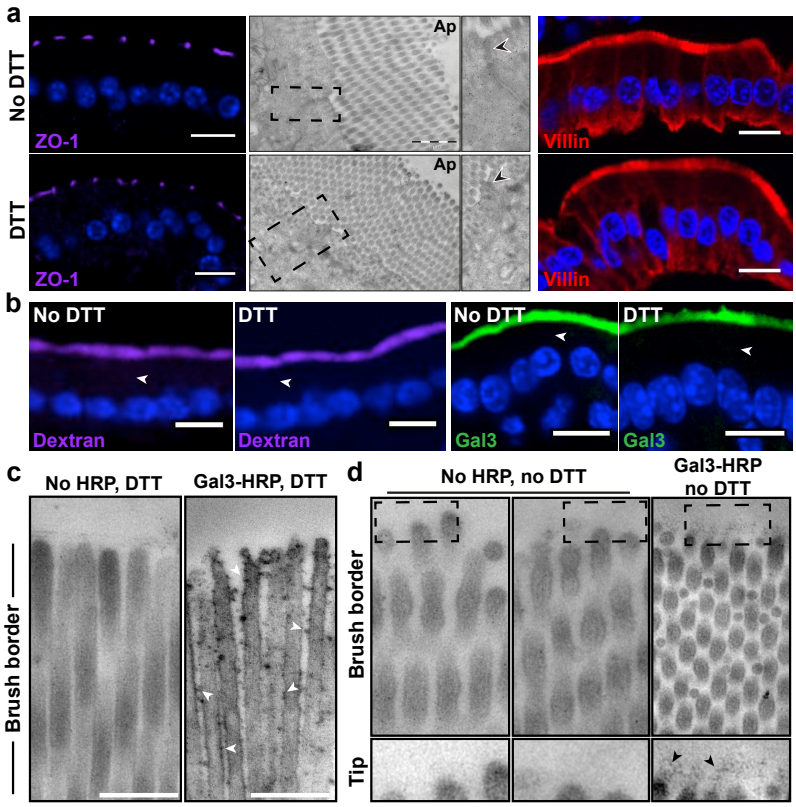
a
No DTT
DTT
ZO-1
Ap
Villin
b
No DTT
DTT
Dextran
Gal3
c
No HRP, DTT
Gal3-HRP, DTT
Brush border
d
No HRP, no DTT
Gal3-HRP
no DTT
Brush border
Tip

Figure 3:

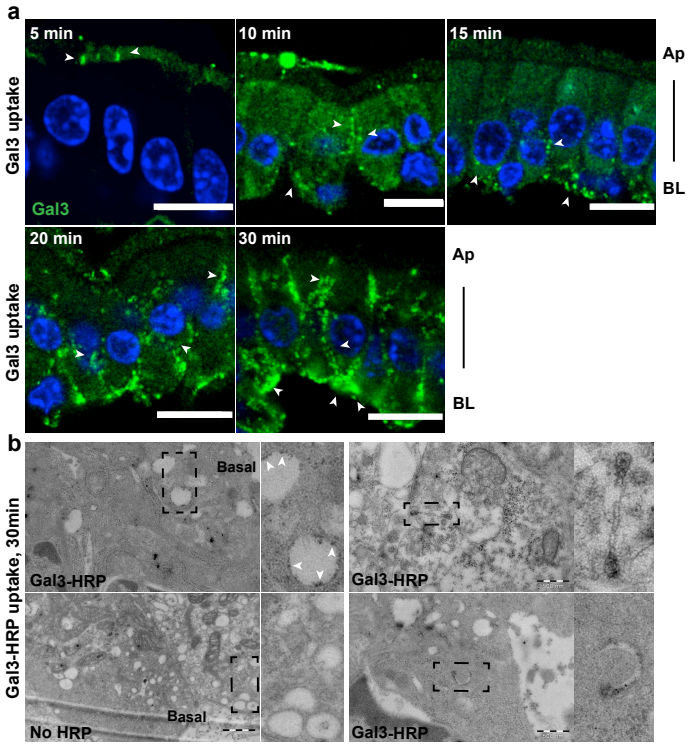
a
5 min
10 min
15 min
Ap
BL
Gal3 uptake
Gal3
20 min
30 min
Ap
BL
Gal3 uptake
b
Basal
Gal3-HRP
Gal3-HRP
Gal3-HRP uptake, 30min
Basal
No HRP
Gal3-HRP

Figure 4:

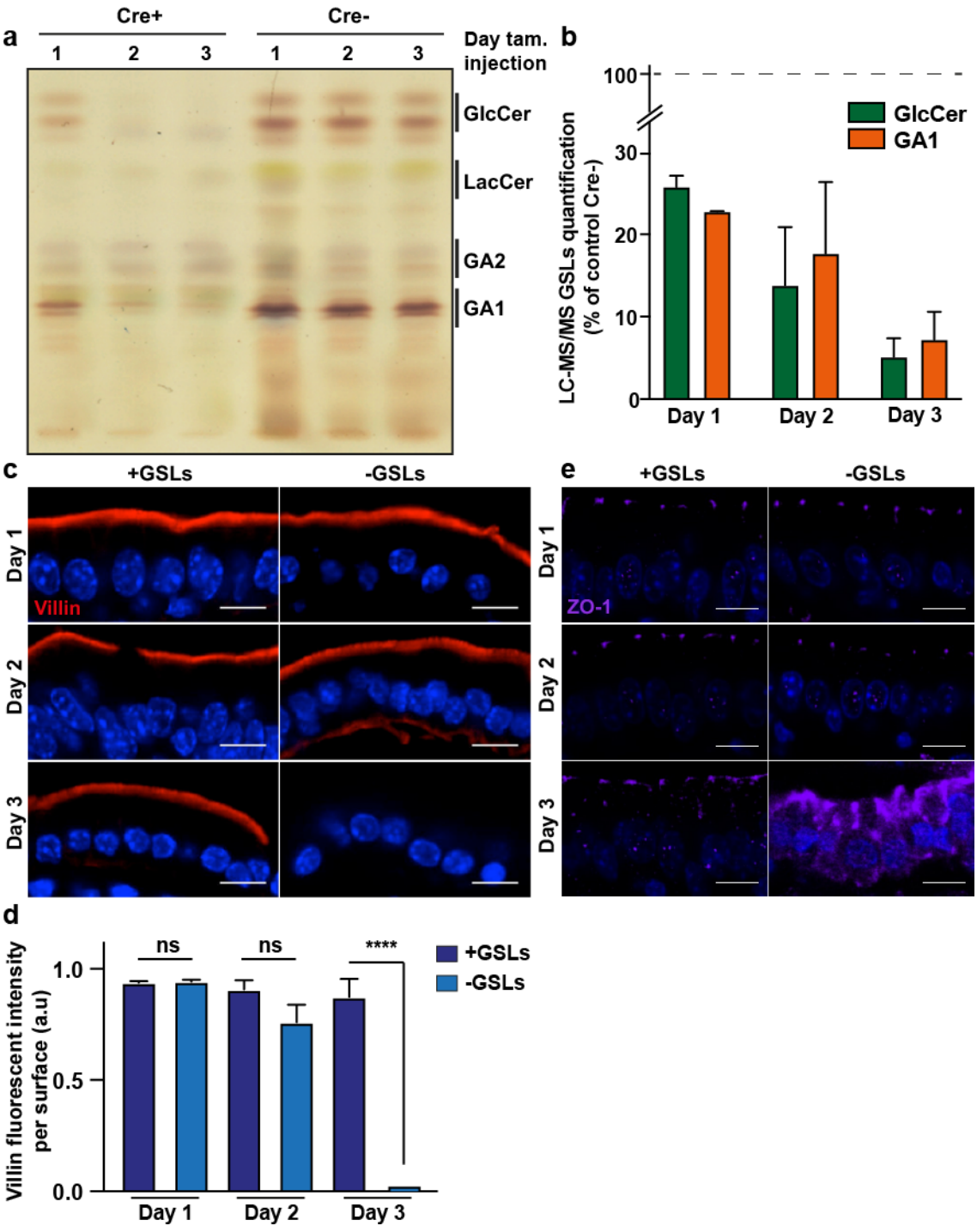
a
Cre+
Cre-
1
2
3
1
2
3
Day tam. injection
GlcCer
LacCer
GA2
GA1
b
LC-MS/MS GSLs quantification (% of control Cre-)
100
30
20
10
0
GlcCer
GA1
Day 1
Day 2
Day 3
c
+GSLs
-GSLs
Day 1
Day 2
Day 3
Villin
e
+GSLs
-GSLs
Day 1
Day 2
Day 3
ZO-1
d
Villin fluorescent intensity per surface (a.u)
1.0
0.5
0.0
ns
ns
****
+GSLs
-GSLs
Day 1
Day 2
Day 3

Figure 5:

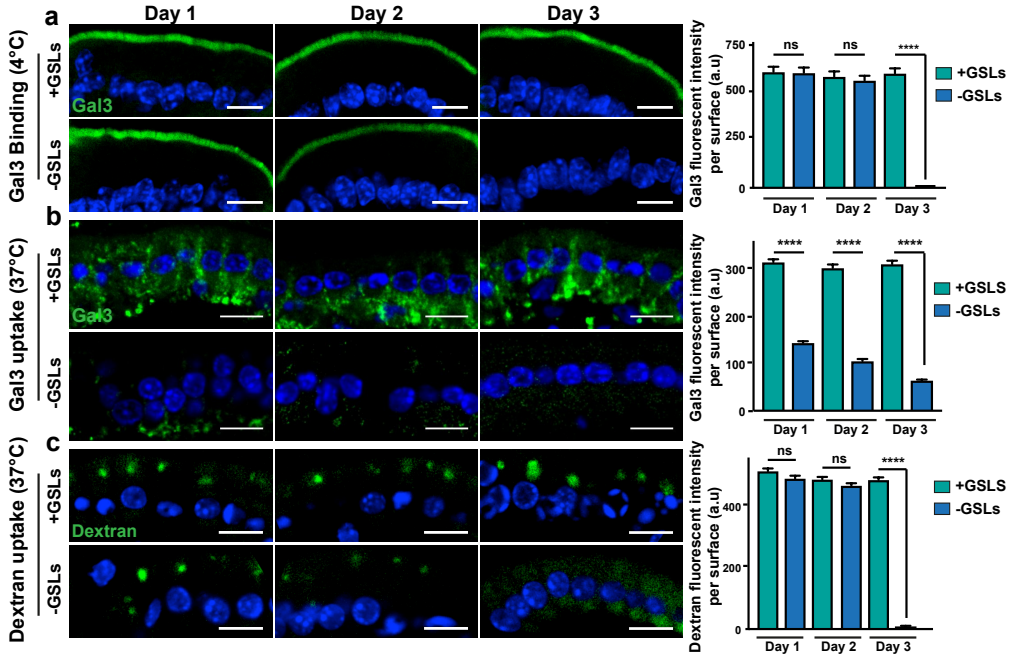
a
Day 1
Day 2
Day 3
Gal3 Binding (4°C)
+GSLs
-GSLs
Gal3
Gal3 fluorescent intensity per surface (a.u)
ns
ns
****
+GSLs
-GSLs
b
Gal3 uptake (37°C)
c
Dextran uptake (37°C)
Dextran
Dextran fluorescent intensity per surface (a.u)

Figure 6:

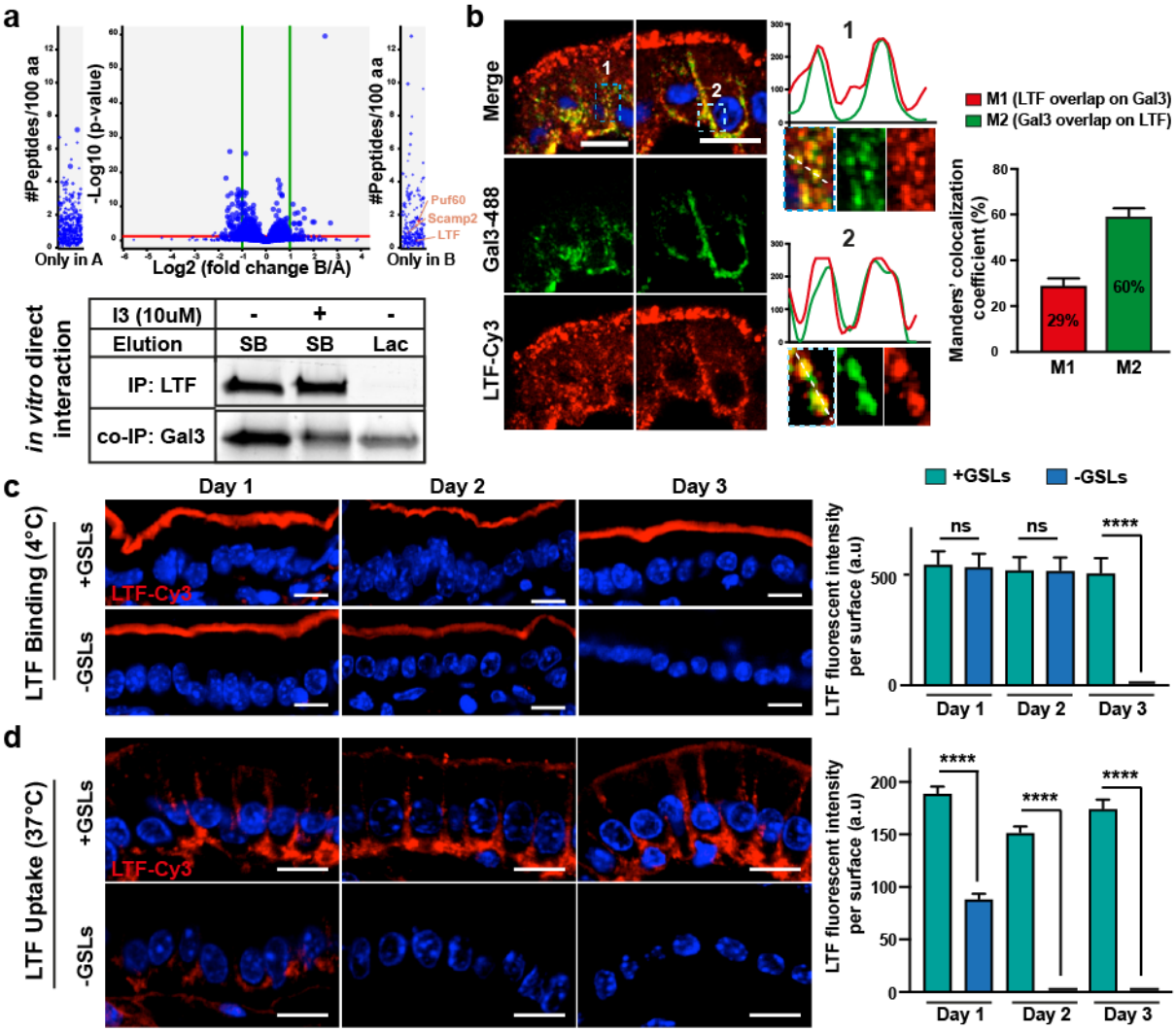
a
#Peptides/100 aa
-Log10 (p-value)
Log2 (fold change B/A)
Only in A
Only in B
Puf60
Scamp2
LTF
in vitro direct interaction
I3 (10uM) - + -
Elution SB SB Lac
IP: LTF
co-IP: Gal3
b
Merge
Gal3-488
LTF-Cy3
M1 (LTF overlap on Gal3)
M2 (Gal3 overlap on LTF)
Manders' colocalization coefficient (%)
29%
60%
M1
M2
c
Day 1
Day 2
Day 3
LTF Binding (4°C)
+GSLs
-GSLs
LTF-Cy3
+GSLs
-GSLs
ns
ns
****
LTF fluorescent intensity per surface (a.u)
d
LTF Uptake (37°C)
****
****
****

Figure 7:

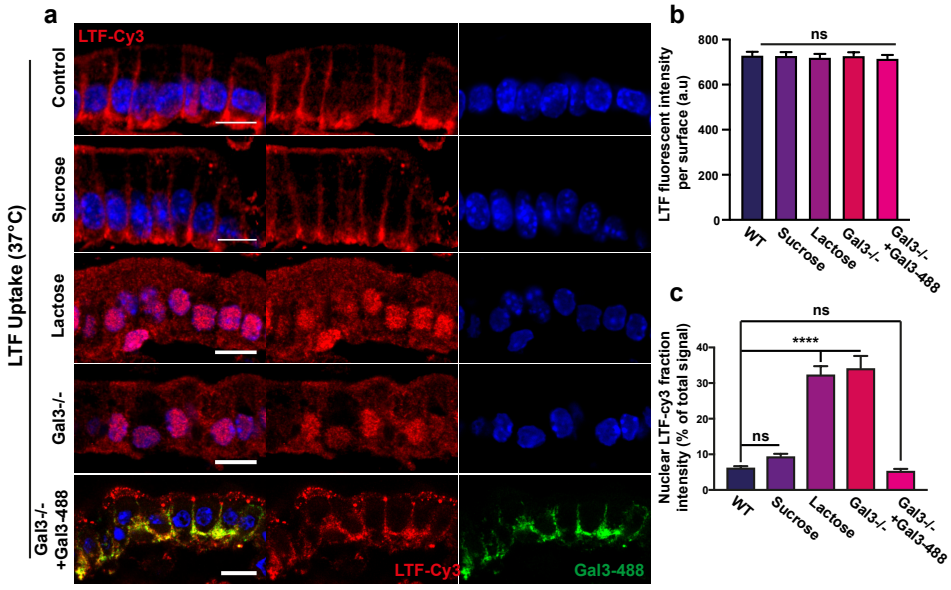
a
LTF-Cy3
Control
Sucrose
Lactose
Gal3-/-
Gal3-/-
+Gal3-488
LTF Uptake (37°C)
LTF-Cy3
Gal3-488
b
LTF fluorescent intensity
per surface (a.u)
800
600
400
200
0
ns
WT
Sucrose
Lactose
Gal3-/-
Gal3-/-
+Gal3-488
c
Nuclear LTF-cy3 fraction
intensity (% of total signal)
40
30
20
10
0
ns
****
ns
WT
Sucrose
Lactose
Gal3-/-
Gal3-/-
+Gal3-488

Figure 8:

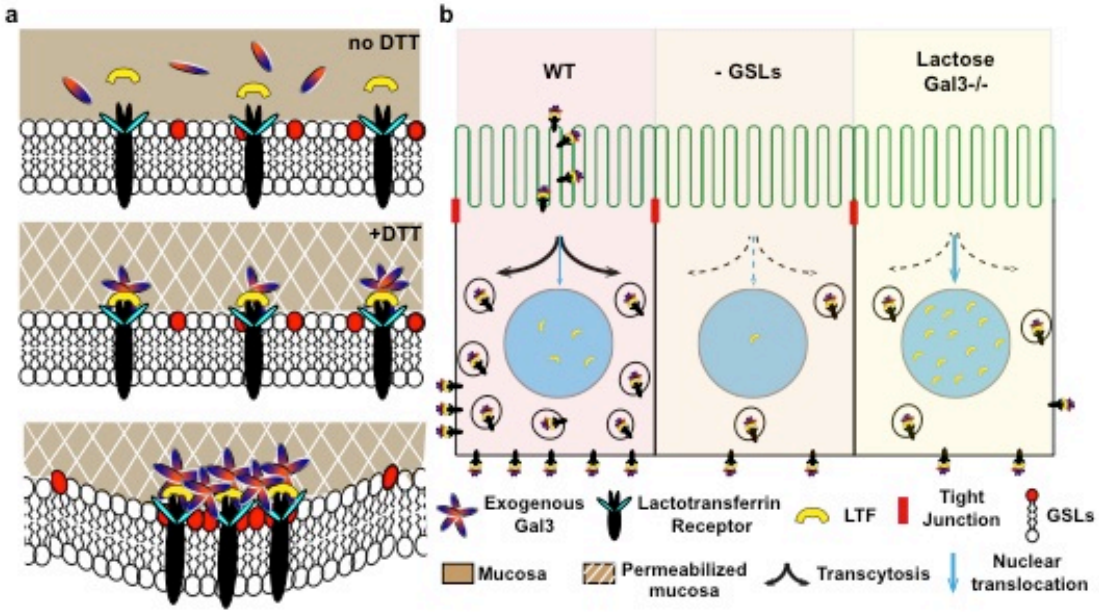
a
no DTT
+DTT
b
WT
- GSLs
Lactose
Gal3-/-
Exogenous
Gal3
Lactotransferrin
Receptor
LTF
Tight
Junction
GSLs
Mucosa
Permeabilized
mucosa
Transcytosis
Nuclear
translocation

Discussion

DISCUSSION

In this study, the internalization of the carbohydrate-binding protein Gal3 and its interacting partner LTF was demonstrated *in vivo*. Importantly, the depletion of GSLs inhibited this process of endocytosis, although Gal3 and LTF were still able to bind to mouse enterocytes. It is interesting to note here the intracellular distribution of the Gal3 and LTF was reminiscent of a transcytosis phenotype. Furthermore, the pattern of internalized LTF in Gal3 knockout mouse intestine was altered and led to predominantly nuclear localization. This suggested that specifically the transcytotic trafficking of LTF is dependent on Gal3.

In this section I will discuss the results obtained during my thesis from four perspectives: Gal3 and functional GSLs are required for LTF internalization; galectin redundancy; role of mucosa as reservoir for galectins; speculations on why BFA treatment of intestine and Rab6 depletion inhibited endocytosis.

6.1 Gal3 and GSLs are required for LTF internalization

We found that LTF is a cargo of Gal3 in the mouse intestine. LTF is a member of iron-binding glycoproteins present in milk, mucosal secretions, and the secondary granules of neutrophils, belonging to the transferrin family (Metz-Boutigue et al., 1984). LTF KO mice are viable and fertile, and developed normally, and displayed no overt abnormalities (Ward et al., 2003). A comparison of the iron status of suckling offspring from LTF KO intercrosses and from wild-type intercrosses showed that LTF is not essential for iron delivery during the postnatal period (Ward et al., 2003). Further studies of adult mice on a basal or a high-iron diet revealed no differences in transferrin saturation or tissue iron stores between WT and LTF KO mice on a special basal diet, although the serum iron levels were slightly raised in LTF KO mice on the basal diet (Ward et al., 2003). These results suggested that LTF does not play a major role in the regulation of iron homeostasis (Ward et al., 2003). The fact that LTF is not required for intestinal iron uptake and that Gal3 null mice are viable might be explained by the existence of redundancy (will be discussed in detail in the next section).

In comparison to stable Gal3 KO and LTF KO mice, conditional KO of GSLs from mouse intestine caused absorption failure in nutritional lipids from milk and impaired intestinal uptake of nutrients that leads to animal death (Jennemann et al., 2012). In these KO mice, where the Ugcg gene is genetically eliminated, there is no possibility to have compensation or rescue of GlcCer-based GSLs. We showed that GSLs in mouse intestine are required for Gal3 and LTF internalization. Previous work of the team showed that GSLs are required for Gal3

internalization *in vitro* (Lakshminarayan et al., 2014). Our results provide for the first time strong evidence for the relevance of GL-Lect endocytosis in a physiological context, i.e. endocytosis in intestinal enterocytes.

6.2 Galectin redundancy

In this study, we have demonstrated that LTF is a specific interacting partner of a Gal3 in the mouse intestine.

Galectin family members are soluble lectins that play important roles in different physiological and pathological processes (Cummings and Liu, 2009). Their redundant roles have been proposed (Johannes et al., 2018). The existence of redundancy of galectin functions is one of the major challenges in the glycobiology field. Functional redundancy may have significant biological implications, particularly for multicellular model organisms. Redundant functions between galectins are a major problem when studying galectin function, because these proteins have a capacity to converge under normal or pathological conditions, and compensate for one another (Cummings and Liu, 2009).

The cross-talk between intracellular and extracellular galectins remains not well understood as cells often express more than one galectin (Vladoiu et al., 2014). That's why a better understanding of the exact function of particular galectin and functional redundancy between galectins and their exclusive interacting partners, which is frequently observed in eukaryotes, is very critical. This redundancy often occurs in order to increase the maintenance of important gene function and to limit losses following mutations/deletions of specific genes (functional compensation).

According to our data in the jejunum of the intestine, Gal1, Gal2, Gal3, Gal4, Gal8 and Gal9 can be found. It is reasonable to postulate that these galectins will have overlapping interacting partners. For Gal3 and Gal4, the fact of having overlapping partners has already been documented (Lakshminarayan et al., 2014). Identifying the exclusive partner of each particular galectin is important for the identification of its specific physiological function. This was the case for Gal3 specific cargo in mouse intestine. We showed that LTF exhibits a similar pattern of internalization to Gal3 in the mouse intestine - i.e. transcytosis. The internalization of LTF was Gal3 dependent (in the absence of Gal3 LTF was found in the nuclear area) and sugar dependent, suggesting that this protein relies specifically on Gal3 for its transcytosis. Moreover, a transcytosis-like pattern of internalization in Gal3 KO mouse was rescued with the help of exogenously added Gal3.

These findings suggest that LTF is an interacting partner of Gal3, and that transcytosis of LTF specifically relies on Gal3.

6.3 Musoca as a physiological reservoir of Gal3

In this study, we have demonstrated in Gal3 immunofluorescence staining experiment that mucus is a reservoir of Gal3 and serves as a physiological barrier in the intestine that prevents exogenous Gal3 to reach the apical surface of enterocytes.

We showed that endogenous Gal3 is highly present in the mucus layer with the mucus potentially serving as a reservoir for galectins.

It was shown by Nio-Kobayashi that Gal2, Gal4/6 and Gal3 can be detected in the mucus of the small intestine (Nio-Kobayashi et al., 2009). Also, Fowler et al. (Fowler et al., 2006) reported that Gal3 was able to bind to *H. pylori*, which selectively colonizes the gastric mucosa, via the O-antigen side chains of LPS (Fowler et al., 2006). Furthermore, the authors demonstrated that Gal3 was rapidly up-regulated and secreted by a human gastric epithelial AGS cell line after interaction with *H. pylori* (Fowler et al., 2006). Park and colleagues showed that Gal3 provides an effective physical and biological barrier against gastric infection caused by *H. pylori* (Park et al., 2016). They confirmed that epithelial cells of the gastric mucosa selectively express Gal3 and abundantly secret the protein into the mucus (Park et al., 2016). In the presence of Gal3, *H. pylori* bacteria were trapped within the mucus layer where the bacteria were mostly aggregated (Park et al., 2016). In the absence of Gal3, however, *H. pylori* migrated further into the gastric glands. Given that gastric colonization of *H. pylori* requires adhesion to epithelial cells (Guruge et al., 1998), trapping and aggregation of bacterial cells within the surface mucus layer by Gal3 might be important host protective mechanisms against H. pylori infection and colonization. This will also promote the clearance of *H. pylori* bacterial cells from the gastric mucosa via the ciliary movement of microvilli (Park et al., 2016). Park also demonstrated that Gal3-deficient macrophages were inefficient in the killing of engulfed *H. pylori* (Park et al., 2016). They also further demonstrated that recombinant Gal3 can rapidly induce aggregation of *H. pylori*, due to the oligomerization of Gal3 upon binding to glycoconjugate ligands (Barondes et al., 1994), and also exerts a potent bactericidal effect on *H. pylori* (Park et al., 2016).

This information is in line with our data on the presence of Gal3 in mucus, and supports the idea that Gal3 could be recruited from this extracellular reservoir to drive endocytic uptake into enterocytes.

6.4 Effect of BFA treatment or Rab6 depletion on endocytosis

In our work, we showed that Gal3 is internalized in the intestine in a transcytosis-like phenotype. Transcytosis is a type of transcellular transport in which different macromolecules are transported across the interior of a cell. Macromolecules are captured in vesicles on one side of the cell, drawn across the cell, and ejected on the other side. The regulation of transcytosis is tissue specific. Brefeldin A (BFA) is well-known to cause the redistribution of Golgi markers into the endoplasmic reticulum and the morphological disappearance of the Golgi (Lippincott-Schwartz et al., 1989) and BFA has been shown to inhibit transcytosis in dog kidney cells (Taub and Shen, 1993). This data provided the first clues that the Golgi might be involved in transcytosis.

In an attempt to understand how transcytosis in the intestine is controlled we performed endocytosis of Gal3 in the absence of Rab6, and under BFA treatment conditions. We indeed hypothesized that Gal3-driven transcytosis might involve retrograde transport from the apical surface to the TGN, from where cargo proteins could then be secreted in a polarized manner to the basolateral surface. To our great surprise, it turned out that endocytic uptake was strongly inhibited under both conditions (Figures 15 and 16).

The absence of endocytosis in Rab6 KO animals might be explained due glycosylation deficiencies. Indeed, Kim et al. (2019) recently found that RAB-6.2, a highly conserved *C. elegans* orthologue of human Rab6, has the novel function in *C. elegans* cuticle development (Kim et al., 2019). They suggested that RAB-6.2 could mediate the trafficking of one or many secreted glycosylated cuticle proteins directly or indirectly by trafficking glycosylation enzymes to their correct intracellular localization (Kim et al., 2019).

Treatment of cells with BFA was shown to strongly perturb the endosomal network (Wang et al., 2001). It is reasonable to postulate that this effect of BFA can be seen in *in-vivo*.

Neither BFA treatment nor Rab6 depletion helped us to progress in our mechanistic understanding of the transcytosis process that in driven by Gal3. One possibility to overcome this issue would be to take advantage of the SNAP-tag system (will be discussed in detail in future perspectives).

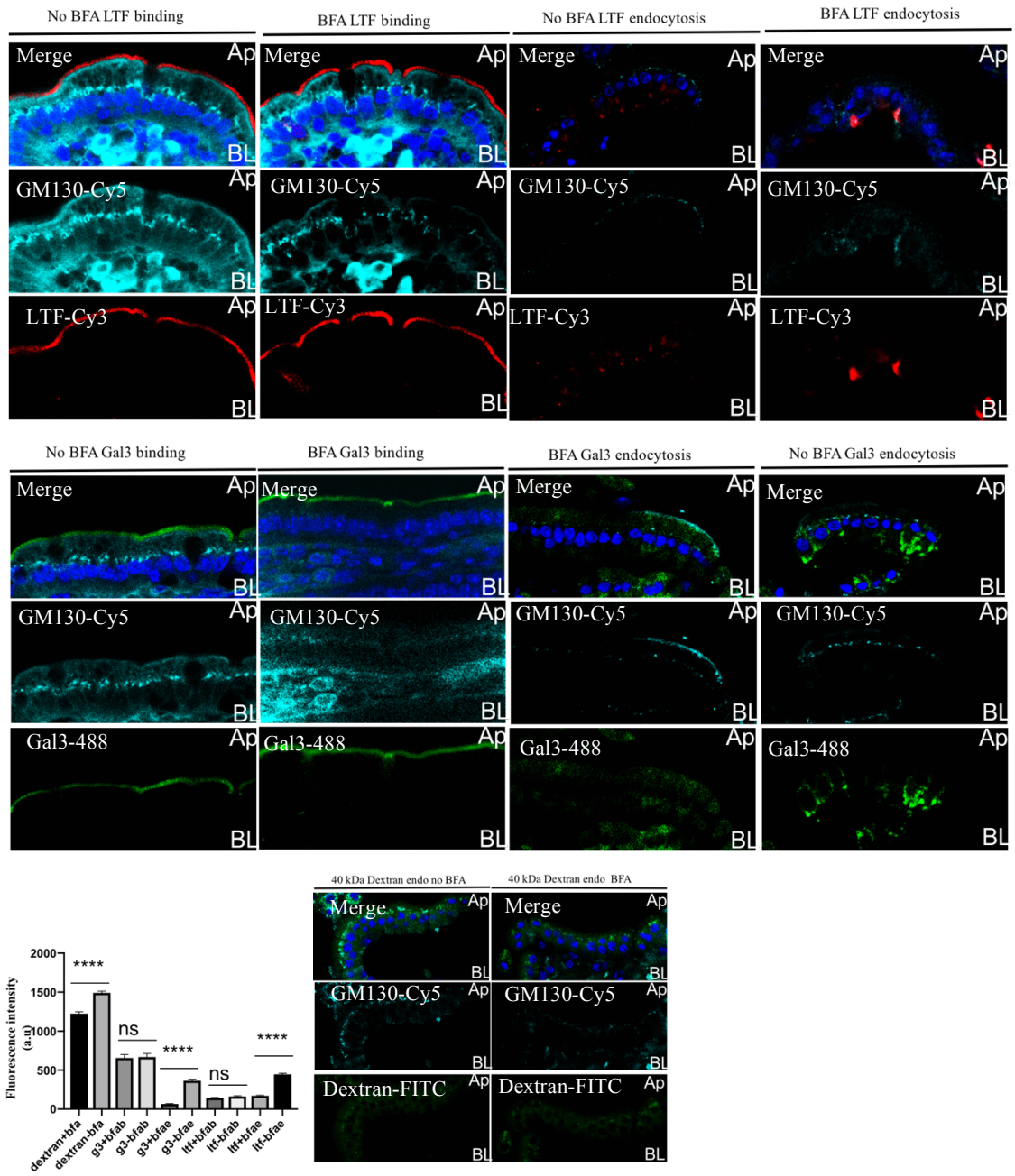

Figure 15: Binding and internalization of Gal3 and LTF with and without BFA treatment. Mice were sacrificed by cervical dislocation, the jejunum was excised and washed with PBS until it became visually clean. After DTT treatment, the intestine was incubated in fresh PBS solution supplemented with 15 µM BFA for 30 min and subsequently (in BFA treated conditions) or without BFA in no BFA conditions (upper and lower panel right) with Gal3-Alexa 488 (20 µg ml−1) (lower panel middle), LTF–Cy3 (20 µg ml−1)(upper panel, right), for 30 min in PBS (supplemented with BFA) at 37°C. Cell-surface-exposed markers were removed by 3 × 10 min washes with ice-cold 200 mM lactose at 4°C. Cells were then washed, fixed (2% PFA for 2

hours), and processed for cryo embedding. Note that endocytic uptake was strongly inhibited under BFA treated conditions (quantification lower panel,left).

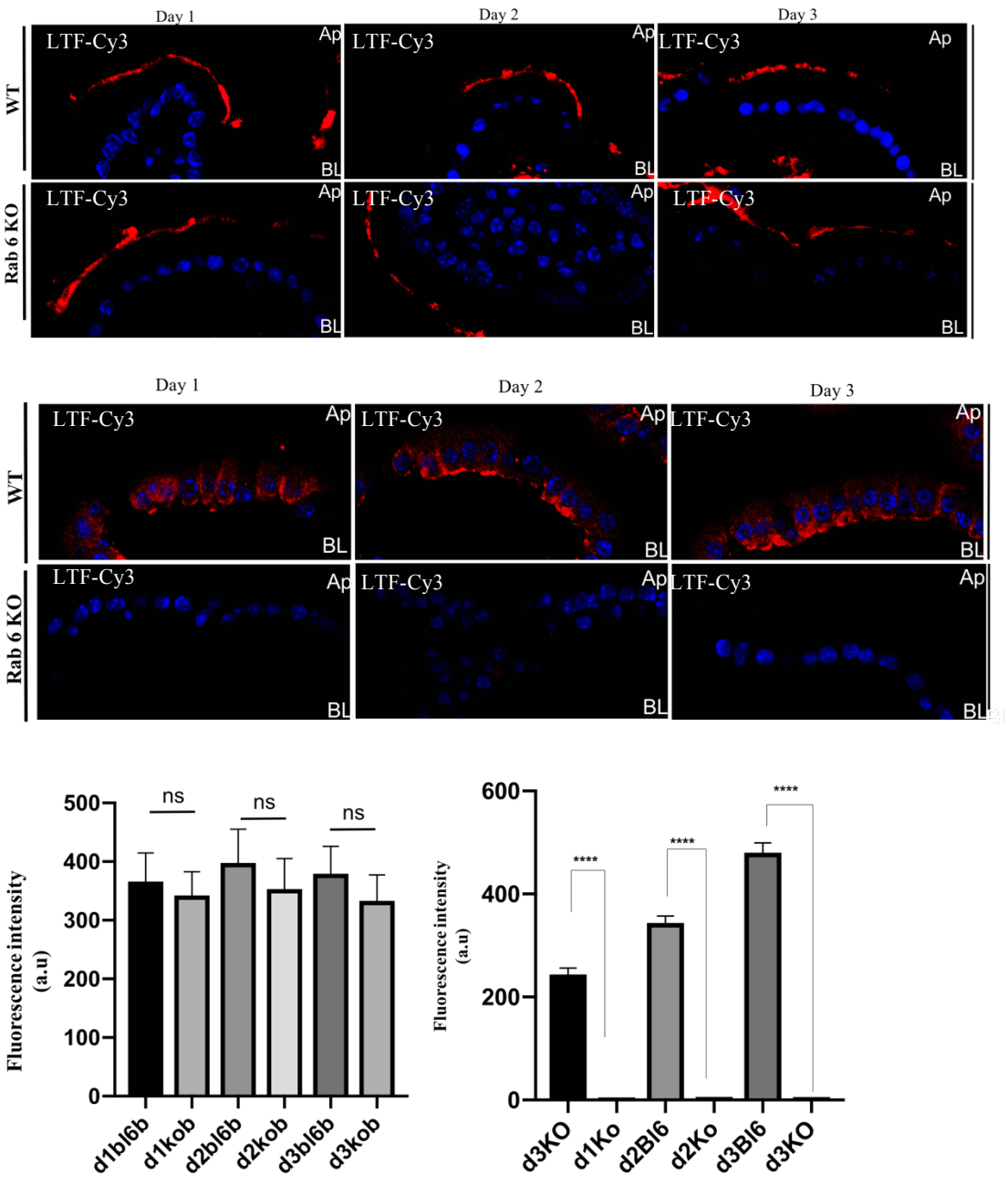

Figure 16: Binding and internalization of LTF with and without Rab6 during different days of tamoxifen treatment. Mice were sacrificed by cervical dislocation, the jejunum was excised and washed with PBS until it became visually clean. After DTT treatment, the intestine was incubated in fresh PBS solution for 30 min and subsequently with LTF–Cy3 (20 µg ml−1) for 30 min in PBS at 37°C (lower panel) or at 4°C (upper panel). Cells were then washed, fixed (2% PFA for 2 hours), and processed for cryo embedding. Results showing that endocytic uptake was strongly inhibited under Rab6 depletion conditions (quantification lower panel,left).

Future perspectives

In this study, we provided first evidence for a physiological function of the GL-Lect mechanism in transcytosis in murine enterocytes of the jejunum. This points to the possibility that the GL-Lect mechanism might play key roles in multiple physiological contexts, like immune responses and kidney function.

As there are 15 family members in the galactin family, it would be interesting to expand the study by testing other galectins in our experimental set up, to observe the inter-dependency and co-operation of galectins. As galectins can have common mechanisms of function, it will be interesting to test the role of other galectin family members in CLIC biogenesis and subsequent physiological activities.

The technique of performing Gal3 endocytic assays in mouse intestine was set up for the first time during my PhD work in my host laboratory. This technique can be extended to identify endocytic ligands for other galectins that are expressed in mouse intestine (Gal1, Gal2, Gal4, Gal8, Gal9), as also shown by our data.

It will be of interest to study the activity of Gal3 to drive the transcytotic trafficking of other associated cargoes from our data (MCT1, SCAMP1) in the intestine of wild-type mice, and under conditions of conditional GSL depletion (Ugcg mouse), as we have done here for LTF. These experiments would help to address one of the major challenges in the field of glycobiology: the redundancy of galectin function.

It will be useful to perform conditional knock-out of Gal3 in mouse intestine, or if possible of all galectins that are expressed in mouse intestine (Gal1, Gal3, Gal2, Gal4, Gal8, Gal9). As a first step in this direction, a collaboration with Dr. Alison Mackinnon has been started to bring her floxed Gal3 mice into the animal facility at *Institut Curie*.

In the attempt to show that Gal3 undergoes retrograde trafficking through the Golgi we performed internalization of this lectin in Rab6 KO mice, or under conditions of BFA treatment (addressed in discussion). The results that we have obtained were disappointing, as Gal3 and LTF uptake was found to be blocked under these conditions. To overcome that issue, we decided to take advantage of the SNAP-tag system to generate a mouse line that will express the SNAP-tag in the Golgi apparatus of enterocytes (in collaboration with Dr. Roberto Weigert). The principle of the SNAP-tag system is the following: A plasma membrane protein (in our case Gal3 and its interacting partners) is covalently tagged via its primary amino groups with a probe, termed benzylguanine (BG). If the protein is transported via the retrograde route to trans-

Golgi/TGN membranes, it will be covalently bound to a capture reagent, the SNAP-tag, that has been engineered to be located to this compartment. The SNAP-tag is indeed fused to the GFP-tagged Golgi membrane anchor from galactosyl transferase for proper positioning to trans-Golgi/TGN membranes (Shi et al., 2012). Cell-surface BG-tagged Gal3 (or its binding partners) that is transported to the trans-Golgi/TGN membrane is thereby covalently captured by the SNAP-tag fusion protein (Shi et al., 2012). If BG-tagged Gal3 undergoes transcytotic trafficking through the Golgi apparatus, we will be able to detect it in this SNAP-tag mouse, and it would lose its basolateral pattern of accumulation. This experiment would help us prove our idea that Gal3 drives transcytosis by linking GL-Lect endocytosis to retrograde trafficking to the Golgi and subsequent polarized secretion to the basolateral surface.

It is known that the mucin composition of mucus is unstable and can be modified with diet, problems with the immune system and gastrointestinal system diseases (Johansson et al., 2013). It will be interesting to analyze the galectin composition of mucus in different gastrointestinal diseases (like Crohn's disease, colitis, inflammatory bowel disease).

Sandberg and colleagues (Sandberg et al., 1994) concluded that the mucus lining the intestine constitutes a significant barrier to any attempts at material transfer via the lumenal route. Due to the mucus layer of the intestine, we faced problems to perform the internalization of exogenous Gal3. To favor the access of exogenous Gal3 to enterocytes, we had to perform DTT treatment. During Crohn's disease intestine is lacking a mucus layer (Johansson et al., 2013). It will be of interest to test the internalization of Gal3 in the absence of the mucus layer during Crohn's disease.

Overall, this my PhD project provided evidence that the GL-Lect mechanism is key to physiological processes, and is not simply a confined to tissue culture cells.

References

Alberts, B., Johnson, A., Lewis, J., Raff, M., Roberts, K., Walter, P. 2002. Molecular biology of the cell. *New York: Garland Science*.

Aigal, S., J. Claudinon, and W. Romer. 2015. Plasma membrane reorganization: A glycolipid gateway for microbes. *Biochim Biophys Acta*. 1853:858-871.

Akiyama, Y., K. Oshima, T. Kuhara, K. Shin, F. Abe, K. Iwatsuki, D. Nadano, and T. Matsuda. 2013. A lactoferrin-receptor, intelectin 1, affects uptake, sub-cellular localization and release of immunochemically detectable lactoferrin by intestinal epithelial Caco-2 cells. *J Biochem*. 154:437-448.

Allain, J.M., C. Storm, A. Roux, M. Ben Amar, and J.F. Joanny. 2004. Fission of a multiphase membrane tube. *Phys Rev Lett*. 93:158104.

Aspenstrom, P. 2014. BAR domain proteins regulate Rho GTPase signaling. *Small GTPases*. 5:7.

Banfer, S., D. Schneider, J. Dewes, M.T. Strauss, S.A. Freibert, T. Heimerl, U.G. Maier, H.P. Elsasser, R. Jungmann, and R. Jacob. 2018. Molecular mechanism to recruit galectin-3 into multivesicular bodies for polarized exosomal secretion. *Proc Natl Acad Sci U S A*. 115:E4396-E4405.

Barondes, S.H., D.N. Cooper, M.A. Gitt, and H. Leffler. 1994. Galectins. Structure and function of a large family of animal lectins. *J Biol Chem*. 269:20807-20810.

Bartoskova, A., L. Adlerova, H. Kudlackova, L. Leva, R. Vitasek, and M. Faldyna. 2009. Lactoferrin in canine sera: a pyometra study. *Reprod Domest Anim*. 44 Suppl 2:193-195.

Batt, R.M., and L. McLean. 1987. Comparison of the biochemical changes in the jejunal mucosa of dogs with aerobic and anaerobic bacterial overgrowth. *Gastroenterology*. 93:986-993.

Bellamy, W., M. Takase, H. Wakabayashi, K. Kawase, and M. Tomita. 1992. Antibacterial spectrum of lactoferricin B, a potent bactericidal peptide derived from the N-terminal region of bovine lactoferrin. *J Appl Bacteriol*. 73:472-479.

Blood, P.D., R.D. Swenson, and G.A. Voth. 2008. Factors influencing local membrane curvature induction by N-BAR domains as revealed by molecular dynamics simulations. *Biophys J*. 95:1866-1876.

Boucrot, E., A.P. Ferreira, L. Almeida-Souza, S. Debard, Y. Vallis, G. Howard, L. Bertot, N. Sauvonnet, and H.T. McMahon. 2015. Endophilin marks and controls a clathrin-independent endocytic pathway. *Nature*. 517:460-465.

Boucrot, E., and T. Kirchhausen. 2007. Endosomal recycling controls plasma membrane area during mitosis. *Proc Natl Acad Sci U S A*. 104:7939-7944.

Buddington, R.K., J. Elnif, C. Malo, and J.B. Donahoo. 2003. Activities of gastric, pancreatic, and intestinal brush-border membrane enzymes during postnatal development of dogs. *Am J Vet Res*. 64:627-634.

Caldieri, G., E. Barbieri, G. Nappo, A. Raimondi, M. Bonora, A. Conte, L.G. Verhoef, S. Confalonieri, M.G. Malabara, F. Bianchi, A. Cuomo, T. Bonaldi, E. Martini, D. Mazza, P. Pinton, C. Tacchetti, S. Polo, P.P. Di Fiore, and S. Sigismund. 2017. Reticulon3-dependent ER-PM contact sites control EGFR nonclathrin endocytosis. *Science*. 256:617-624.

Carman, P.J., and R. Dominguez. 2018. BAR domain proteins-a linkage between cellular membranes, signaling pathways, and the actin cytoskeleton. *Biophys Rev*. 10:1587-1604.

Cestra, G., L. Castagnoli, L. Dente, O. Minenkova, A. Petrelli, N. Migone, U. Hoffmuller, J. Schneider-Mergener, and G. Cesareni. 1999. The SH3 domains of endophilin and

amphiphysin bind to the proline-rich region of synaptojanin 1 at distinct sites that display an unconventional binding specificity. *J Biol Chem*. 274:32001-32007.

Chen, B., K. Brinkmann, Z. Chen, C.W. Pak, Y. Liao, S. Shi, L. Henry, N.V. Grishin, S. Bogdan, and M.K. Rosen. 2014. The WAVE regulatory complex links diverse receptors to the actin cytoskeleton. *Cell*. 156:195-207.

Christenson, R.H., S.H. Duh, A.H. Wu, A. Smith, G. Abel, C.R. deFilippi, S. Wang, A. Adourian, C. Adiletto, and P. Gardiner. 2010. Multi-center determination of galectin-3 assay performance characteristics: Anatomy of a novel assay for use in heart failure. *Clin Biochem*. 43:683-690.

Crawley, S.W., M.S. Mooseker, and M.J. Tyska. 2014. Shaping the intestinal brush border. *J Cell Biol*. 207:441-451.

Cummings, R.D., and F.T. Liu. 2009. Galectins. *In* Essentials of Glycobiology. nd, A. Varki, R.D. Cummings, J.D. Esko, H.H. Freeze, P. Stanley, C.R. Bertozzi, G.W. Hart, and M.E. Etzler, editors, Cold Spring Harbor (NY).

D'Angelo, G., S. Capasso, L. Sticco, and D. Russo. 2013. Glycosphingolipids: synthesis and functions. *FEBS J*. 280:6338-6353.

Dauca, M., F. Bouziges, S. Colin, M. Kedinger, M.K. Keller, J. Schilt, P. Simon-Assmann, and K. Haffen. 1990. Development of the vertebrate small intestine and mechanisms of cell differentiation. *Int J Dev Biol*. 34:205-218.

Daumke, O., A. Roux, and V. Haucke. 2014. BAR domain scaffolds in dynamin-mediated membrane fission. *Cell*. 156:882-892.

Davidsson, L., P. Kastenmayer, M. Yuen, B. Lonnerdal, and R.F. Hurrell. 1994. Influence of lactoferrin on iron absorption from human milk in infants. *Pediatr Res*. 35:117-124.

Dings, R.P.M., M.C. Miller, R.J. Griffin, and K.H. Mayo. 2018. Galectins as Molecular Targets for Therapeutic Intervention. *Int J Mol Sci*. 19.

Dmitrieff, S., A. Alsina, A. Mathur, and F.J. Nedelec. 2017. Balance of microtubule stiffness and cortical tension determines the size of blood cells with marginal band across species. *Proc Natl Acad Sci U S A*. 114:4418-4423.

Doherty, G.J., and H.T. McMahon. 2009. Mechanisms of endocytosis. *Annu Rev Biochem*. 78:857-902.

Donaldson, G.P., S.M. Lee, and S.K. Mazmanian. 2016. Gut biogeography of the bacterial microbiota. *Nat Rev Microbiol*. 14:20-32.

Donaldson, J.G., H. Radhakrishna, and P.J. Peters. 1995. The ARF GTPases: defining roles in membrane traffic and organelle structure. *Cold Spring Harb Symp Quant Biol*. 60:229-234.

Donovan, S.M. 2016. The Role of Lactoferrin in Gastrointestinal and Immune Development and Function: A Preclinical Perspective. *J Pediatr*. 173 Suppl:S16-28.

Drager, N.M., E. Nachman, M. Winterhoff, S. Bruhmann, P. Shah, T. Katsinelos, S. Boulant, A.A. Teleman, J. Faix, and T.R. Jahn. 2017. Bin1 directly remodels actin dynamics through its BAR domain. *EMBO Rep*. 18:2051-2066.

Duffy, K.R., and W.M. Pardridge. 1987. Blood-brain barrier transcytosis of insulin in developing rabbits. *Brain Res*. 420:32-38.

Ewers, H., W. Romer, A.E. Smith, K. Bacia, S. Dmitrieff, W. Chai, R. Mancini, J. Kartenbeck, V. Chambon, L. Berland, A. Oppenheim, G. Schwarzmann, T. Feizi, P. Schwille, P. Sens, A. Helenius, and L. Johannes. 2010. GM1 structure determines SV40-induced membrane invagination and infection. *Nat Cell Biol*. 12:11-18; sup pp 11-12.

Eyster, C.A., N.B. Cole, S. Petersen, K. Viswanathan, K. Fruh, and J.G. Donaldson. 2011. MARCH ubiquitin ligases alter the itinerary of clathrin-independent cargo from recycling to degradation. *Mol Biol Cell*. 22:3218-3230.

Eyster, C.A., J.D. Higginson, R. Huebner, N. Porat-Shliom, R. Weigert, W.W. Wu, R.F. Shen, and J.G. Donaldson. 2009. Discovery of new cargo proteins that enter cells through clathrin-independent endocytosis. *Traffic*. 10:590-599.

Farrugia, G. 2008. Interstitial cells of Cajal in health and disease. *Neurogastroenterol Motil*. 20 Suppl 1:54-63.

Ferguson, S.M., A. Raimondi, S. Paradise, H. Shen, K. Mesaki, A. Ferguson, O. Destaing, G. Ko, J. Takasaki, O. Cremona, O.T. E, and P. De Camilli. 2009. Coordinated actions of actin and BAR proteins upstream of dynamin at endocytic clathrin-coated pits. *Dev Cell*. 17:811-822.

Fishman, J.B., J.B. Rubin, J.V. Handrahan, J.R. Connor, and R.E. Fine. 1987. Receptor-mediated transcytosis of transferrin across the blood-brain barrier. *J Neurosci Res*. 18:299-304.

Fowler, M., R.J. Thomas, J. Atherton, I.S. Roberts, and N.J. High. 2006. Galectin-3 binds to Helicobacter pylori O-antigen: it is upregulated and rapidly secreted by gastric epithelial cells in response to H. pylori adhesion. *Cell Microbiol*. 8:44-54.

Fredman, P. 1998. The role of antiglycolipid antibodies in neurological disorders. *Ann N Y Acad Sci*. 845:341-352.

Frost, A., R. Perera, A. Roux, K. Spasov, O. Destaing, E.H. Egelman, P. De Camilli, and V.M. Unger. 2008. Structural basis of membrane invagination by F-BAR domains. *Cell*. 132:807-817.

Fung, K.Y.Y., G.D. Fairn, and W.L. Lee. 2018. Transcellular vesicular transport in epithelial and endothelial cells: Challenges and opportunities. *Traffic*. 19:5-18.

Gad, H., N. Ringstad, P. Low, O. Kjaerulff, J. Gustafsson, M. Wenk, G. Di Paolo, Y. Nemoto, J. Crun, M.H. Ellisman, P. De Camilli, O. Shupliakov, and L. Brodin. 2000. Fission and uncoating of synaptic clathrin-coated vesicles are perturbed by disruption of interactions with the SH3 domain of endophilin. *Neuron*. 27:301-312.

Gallop, J.L., C.C. Jao, H.M. Kent, P.J. Butler, P.R. Evans, R. Langen, and H.T. McMahon. 2006. Mechanism of endophilin N-BAR domain-mediated membrane curvature. *EMBO J*. 25:2898-2910.

Gao, X., D. Liu, Y. Fan, X. Li, H. Xue, Y. Ma, Y. Zhou, and G. Tai. 2012. The two endocytic pathways mediated by the carbohydrate recognition domain and regulated by the collagen-like domain of galectin-3 in vascular endothelial cells. *PLoS ONE*. 7:e52430.

Gowrishankar, K., S. Ghosh, S. Saha, R. C, S. Mayor, and M. Rao. 2012. Active remodeling of cortical actin regulates spatiotemporal organization of cell surface molecules. *Cell*. 149:1353-1367.

Grant, B.D., and J.G. Donaldson. 2009. Pathways and mechanisms of endocytic recycling. *Nat Rev Mol Cell Biol*. 10:597-608.

Grassart, A., V. Meas-Yedid, A. Dufour, J.C. Olivo-Marin, A. Dautry-Varsat, and N. Sauvonnet. 2010. Pak1 phosphorylation enhances cortactin-N-WASP interaction in clathrin-caveolin-independent endocytosis. *Traffic*. 11:1079-1091.

Groschwitz, K.R., and S.P. Hogan. 2009. Intestinal barrier function: molecular regulation and disease pathogenesis. *J Allergy Clin Immunol*. 124:3-20; quiz 21-22.

Gupta, G.D., G. Dey, M.G. Swetha, B. Ramalingam, K. Shameer, J.J. Thottacherry, J.M. Kalappurakkal, M.T. Howes, R. Chandran, A. Das, S. Menon, R.G. Parton, R. Sowdhamini, M. Thattai, and S. Mayor. 2014. Population distribution analyses reveal a hierarchy of molecular players underlying parallel endocytic pathways. *PLoS One*. 9:e100554.

Guruge, J.L., P.G. Falk, R.G. Lorenz, M. Dans, H.P. Wirth, M.J. Blaser, D.E. Berg, and J.I. Gordon. 1998. Epithelial attachment alters the outcome of Helicobacter pylori infection. *Proc Natl Acad Sci U S A*. 95:3925-3930.

Hakomori, S. 2003. Structure, organization, and function of glycosphingolipids in membrane. *Curr Opin Hematol*. 10:16-24.
Hall, A. 2012. Rho family GTPases. *Biochem Soc Trans*. 40:1378-1382.
Hanson, L.H., V. Sawicki, A. Lewis, J.H. Nuijens, M.C. Neville, and P. Zhang. 2001. Does human lactoferrin in the milk of transgenic mice deliver iron to suckling neonates? *Adv Exp Med Biol*. 501:233-239.
Hao, L., Q. Shan, J. Wei, F. Ma, and P. Sun. 2019. Lactoferrin: Major Physiological Functions and Applications. *Curr Protein Pept Sci*. 20:139-144.
Hendrixson, D.R., J. Qiu, S.C. Shewry, D.L. Fink, S. Petty, E.N. Baker, A.G. Plaut, and J.W. St Geme, 3rd. 2003. Human milk lactoferrin is a serine protease that cleaves Haemophilus surface proteins at arginine-rich sites. *Mol Microbiol*. 47:607-617.
Hirabayashi, J., T. Hashidate, Y. Arata, N. Nishi, T. Nakamura, M. Hirashima, T. Urashima, T. Oka, M. Futai, W.E. Muller, F. Yagi, and K. Kasai. 2002. Oligosaccharide specificity of galectins: a search by frontal affinity chromatography. *Biochim Biophys Acta*. 1572:232-254.
Hore, P., and M. Messer. 1968. Studies on disaccharidase activities of the small intestine of the domestic cat and other carnivorous mammals. *Comp Biochem Physiol*. 24:717-725.
Horgan, C.P., A. Oleksy, A.V. Zhdanov, P.Y. Lall, I.J. White, A.R. Khan, C.E. Futter, J.G. McCaffrey, and M.W. McCaffrey. 2007. Rab11-FIP3 is critical for the structural integrity of the endosomal recycling compartment. *Traffic*. 8:414-430.
Howes, M.T., M. Kirkham, J. Riches, K. Cortese, P.J. Walser, F. Simpson, M.M. Hill, A. Jones, R. Lundmark, M.R. Lindsay, D.J. Hernandez-Deviez, G. Hadzic, A. McCluskey, R. Bashir, L. Liu, P. Pilch, H. McMahon, P.J. Robinson, J.F. Hancock, S. Mayor, and R.G. Parton. 2010. Clathrin-independent carriers form a high capacity endocytic sorting system at the leading edge of migrating cells. *J Cell Biol*. 190:675-691.
Inoue, H., V.L. Ha, R. Prekeris, and P.A. Randazzo. 2008. Arf GTPase-activating protein ASAP1 interacts with Rab11 effector FIP3 and regulates pericentrosomal localization of transferrin receptor-positive recycling endosome. *Mol Biol Cell*. 19:4224-4237.
Iqbal, J., and M.M. Hussain. 2009. Intestinal lipid absorption. *Am J Physiol Endocrinol Metab*. 296:E1183-1194.
Iurisci, I., N. Tinari, C. Natoli, D. Angelucci, E. Cianchetti, and S. Iacobelli. 2000. Concentrations of galectin-3 in the sera of normal controls and cancer patients. *Clin Cancer Res*. 6:1389-1393.
Jennemann, R., S. Kaden, R. Sandhoff, V. Nordstrom, S. Wang, M. Volz, S. Robine, N. Amen, U. Rothermel, H. Wiegandt, and H.J. Grone. 2012. Glycosphingolipids are essential for intestinal endocytic function. *J Biol Chem*. 287:32598-32616.
Jeyakumar, M., T.D. Butters, R.A. Dwek, and F.M. Platt. 2002. Glycosphingolipid lysosomal storage diseases: therapy and pathogenesis. *Neuropathol Appl Neurobiol*. 28:343-357.
Jiang, R., and B. Lonnerdal. 2012. Apo- and holo-lactoferrin stimulate proliferation of mouse crypt cells but through different cellular signaling pathways. *Int J Biochem Cell Biol*. 44:91-100.
Jiang, R., V. Lopez, S.L. Kelleher, and B. Lonnerdal. 2011. Apo- and holo-lactoferrin are both internalized by lactoferrin receptor via clathrin-mediated endocytosis but differentially affect ERK-signaling and cell proliferation in Caco-2 cells. *J Cell Physiol*. 226:3022-3031.
Johannes, L., R. Jacob, and H. Leffler. 2018. Galectins at a glance. *J Cell Sci*. 131.
Johannes, L., and S. Mayor. 2010. Induced domain formation in endocytic invagination, lipid sorting, and scission. *Cell*. 142:507-510.
Johannes, L., R.G. Parton, P. Bassereau, and S. Mayor. 2015. Building endocytic pits without clathrin. *Nat Rev Mol Cell Biol*. 16:311-321.

Johannes, L., C. Wunder, and P. Bassereau. 2014. Bending "on the rocks"--a cocktail of biophysical modules to build endocytic pathways. *Cold Spring Harb Perspect Biol*. 6.

Johannes, L., C. Wunder, and M. Shafaq-Zadah. 2016. Glycolipids and Lectins in Endocytic Uptake Processes. *J Mol Biol*.

Jovanovic, O.A., F.D. Brown, and J.G. Donaldson. 2006. An effector domain mutant of Arf6 implicates phospholipase D in endosomal membrane recycling. *Mol Biol Cell*. 17:327-335.

Kalia, M., S. Kumari, R. Chadda, M.M. Hill, R.G. Parton, and S. Mayor. 2006. Arf6-independent GPI-anchored protein-enriched early endosomal compartments fuse with sorting endosomes via a Rab5/phosphatidylinositol-3'-kinase-dependent machinery. *Mol Biol Cell*. 17:3689-3704.

Kanyshkova, T.G., V.N. Buneva, and G.A. Nevinsky. 2001. Lactoferrin and its biological functions. *Biochemistry (Mosc)*. 66:1-7.

Kirkham, M., A. Fujita, R. Chadda, S.J. Nixon, T.V. Kurzchalia, D.K. Sharma, R.E. Pagano, J.F. Hancock, S. Mayor, and R.G. Parton. 2005. Ultrastructural identification of uncoated caveolin-independent early endocytic vehicles. *J Cell Biol*. 168:465-476.

Knedlik, T., B. Vorlova, V. Navratil, J. Tykvart, F. Sedlak, S. Vaculin, M. Franek, P. Sacha, and J. Konvalinka. 2017. Mouse glutamate carboxypeptidase II (GCPII) has a similar enzyme activity and inhibition profile but a different tissue distribution to human GCPII. *FEBS Open Bio*. 7:1362-1378.

Kononenko, N.L., D. Puchkov, G.A. Classen, A.M. Walter, A. Pechstein, L. Sawade, N. Kaempf, T. Trimbuch, D. Lorenz, C. Rosenmund, T. Maritzen, and V. Haucke. 2014. Clathrin/AP-2 mediate synaptic vesicle reformation from endosome-like vacuoles but are not essential for membrane retrieval at central synapses. *Neuron*. 82:981-988.

Kruhoffer, P., and J.A. Muntz. 1954. Carbohydrate metabolism of the isolated, perfused cat liver as studied by labelled glucose and fructose. *Acta Physiol Scand*. 30:258-274.

Kumari, S., and S. Mayor. 2008. ARF1 is directly involved in dynamin-independent endocytosis. *Nat Cell Biol*. 10:30-41.

Kumari, S., S. Mg, and S. Mayor. 2010. Endocytosis unplugged: multiple ways to enter the cell. *Cell Res*. 20:256-275.

Lakshminarayan, R., C. Wunder, U. Becken, M.T. Howes, C. Benzing, S. Arumugam, S. Sales, N. Ariotti, V. Chambon, C. Lamaze, D. Loew, A. Shevchenko, K. Gaus, R.G. Parton, and L. Johannes. 2014. Galectin-3 drives glycosphingolipid-dependent biogenesis of clathrin-independent carriers. *Nat Cell Biol*. 16:595-606.

Lamaze, C., A. Dujeancourt, T. Baba, C.G. Lo, A. Benmerah, and A. Dautry-Varsat. 2001. Interleukin 2 receptors and detergent-resistant membrane domains define a clathrin-independent endocytic pathway. *Mol Cell*. 7:661-671.

Lamaze, C., N. Tardif, M. Dewulf, S. Vassilopoulos, and C.M. Blouin. 2017. The caveolae dress code: structure and signaling. *Curr Opin Cell Biol*. 47:117-125.

Lammers, W.J., and B. Stephen. 2008. Origin and propagation of individual slow waves along the intact feline small intestine. *Exp Physiol*. 93:334-346.

Lee, S.H., F. Kerff, D. Chereau, F. Ferron, A. Klug, and R. Dominguez. 2007. Structural basis for the actin-binding function of missing-in-metastasis. *Structure*. 15:145-155.

Leffler, H., S. Carlsson, M. Hedlund, Y. Qian, and F. Poirier. 2002. Introduction to galectins. *Glycoconj J*. 19:433-440.

Levay, P.F., and M. Viljoen. 1995. Lactoferrin: a general review. *Haematologica*. 80:252-267.

Liao, Y., V. Lopez, T.B. Shafizadeh, C.H. Halsted, and B. Lonnerdal. 2007. Cloning of a pig homologue of the human lactoferrin receptor: expression and localization during intestinal maturation in piglets. *Comp Biochem Physiol A Mol Integr Physiol*. 148:584-590.

Lin, H.C., and J.H. Chen. 2003. Slowing of intestinal transit by fat depends on an ondansetron - sensitive, efferent serotonergic pathway. *Neurogastroenterol Motil*. 15:317-322.

Ling, H., A. Boodhoo, B. Hazes, M.D. Cummings, G.D. Armstrong, J.L. Brunton, and R.J. Read. 1998. Structure of the shiga-like toxin I B-pentamer complexed with an analogue of its receptor Gb3. *Biochemistry*. 37:1777-1788.

Lippincott-Schwartz, J., L.C. Yuan, J.S. Bonifacino, and R.D. Klausner. 1989. Rapid redistribution of Golgi proteins into the ER in cells treated with brefeldin A: evidence for membrane cycling from Golgi to ER. *Cell*. 56:801-813.

Liu, F.T., R.J. Patterson, and J.L. Wang. 2002. Intracellular functions of galectins. *Biochim Biophys Acta*. 1572:263-273.

Liu, J., M. Kaksonen, D.G. Drubin, and G. Oster. 2006. Endocytic vesicle scission by lipid phase boundary forces. *Proc Natl Acad Sci U S A*. 103:10277-10282.

Liu, J., Y. Sun, D.G. Drubin, and G.F. Oster. 2009. The mechanochemistry of endocytosis. *PLoS Biol*. 7:e1000204.

Llobet, A., J.L. Gallop, J.J.E. Burden, G. Camdere, P. Chandra, Y. Vallis, C.R. Hopkins, L. Lagnado, and H.T. McMahon. 2011. Endophilin drives the fast mode of vesicle retrieval in a ribbon synapse. *J Neurosci*. 31:8512-8519.

Lonnerdal, B., and A. Bryant. 2006. Absorption of iron from recombinant human lactoferrin in young US women. *Am J Clin Nutr*. 83:305-309.

Lopez, V., Y.A. Suzuki, and B. Lonnerdal. 2006. Ontogenic changes in lactoferrin receptor and DMT1 in mouse small intestine: implications for iron absorption during early life. *Biochem Cell Biol*. 84:337-344.

Lundmark, R., G.J. Doherty, M.T. Howes, K. Cortese, Y. Vallis, R.G. Parton, and H.T. McMahon. 2008. The GTPase-activating protein GRAF1 regulates the CLIC/GEEC endocytic pathway. *Curr Biol*. 18:1802-1808.

Magadan, J.G., M.A. Barbieri, R. Mesa, P.D. Stahl, and L.S. Mayorga. 2006. Rab22a regulates the sorting of transferrin to recycling endosomes. *Mol Cell Biol*. 26:2595-2614.

Maldonado-Baez, L., N.B. Cole, H. Kramer, and J.G. Donaldson. 2013. Microtubule-dependent endosomal sorting of clathrin-independent cargo by Hook1. *J Cell Biol*. 201:233-247.

Malo, C. 1988. Kinetic arguments for the existence of a single form of intestinal ornithine decarboxylase during the postnatal development of normal and sparse-fur mutant mice and after EGF treatment. *Experientia*. 44:251-252.

Mansbach, C.M., 2nd, and F. Gorelick. 2007. Development and physiological regulation of intestinal lipid absorption. II. Dietary lipid absorption, complex lipid synthesis, and the intracellular packaging and secretion of chylomicrons. *Am J Physiol Gastrointest Liver Physiol*. 293:G645-650.

Mayor, S., and R.E. Pagano. 2007. Pathways of clathrin-independent endocytosis. *Nat Rev Mol Cell Biol*. 8:603-612.

Mayor, S., R.G. Parton, and J.G. Donaldson. 2014. Clathrin-independent pathways of endocytosis. *Cold Spring Harb Perspect Biol*. 6.

Metz-Boutigue, M.H., J. Jolles, J. Mazurier, F. Schoentgen, D. Legrand, G. Spik, J. Montreuil, and P. Jolles. 1984. Human lactotransferrin: amino acid sequence and structural comparisons with other transferrins. *Eur J Biochem*. 145:659-676.

Mim, C., H. Cui, J.A. Gawronski-Salerno, A. Frost, E. Lyman, G.A. Voth, and V.M. Unger. 2012. Structural basis of membrane bending by the N-BAR protein endophilin. *Cell*. 149:137-145.

Mishra, R., M. Grzybek, T. Niki, M. Hirashima, and K. Simons. 2010. Galectin-9 trafficking regulates apical-basal polarity in Madin-Darby canine kidney epithelial cells. *Proc Natl Acad Sci U S A*. 107:17633-17638.

Montesano, R., J. Roth, A. Robert, and L. Orci. 1982. Non-coated membrane invaginations are involved in binding and internalization of cholera and tetanus toxins. *Nature*. 296:651-653.

Moravcevic, K., C.L. Oxley, and M.A. Lemmon. 2012. Conditional peripheral membrane proteins: facing up to limited specificity. *Structure*. 20:15-27.

Moya, M., A. Dautry-Varsat, B. Goud, D. Louvard, and P. Boquet. 1985. Inhibition of coated pit formation in Hep2 cells blocks the cytotoxicity of diphtheria toxin but not that of ricin toxin. *J Cell Biol*. 101:548-559.

Naslavsky, N., J. Rahajeng, M. Sharma, M. Jovic, and S. Caplan. 2006. Interactions between EHD proteins and Rab11-FIP2: a role for EHD3 in early endosomal transport. *Mol Biol Cell*. 17:163-177.

Naslavsky, N., R. Weigert, and J.G. Donaldson. 2003. Convergence of non-clathrin- and clathrin-derived endosomes involves Arf6 inactivation and changes in phosphoinositides. *Mol Biol Cell*. 14:417-431.

Naslavsky, N., R. Weigert, and J.G. Donaldson. 2004. Characterization of a nonclathrin endocytic pathway: membrane cargo and lipid requirements. *Mol Biol Cell*. 15:3542-3552.

Neu, U., K. Woellner, G. Gauglitz, and T. Stehle. 2008. Structural basis of GM1 ganglioside recognition by simian virus 40. *Proc Natl Acad Sci U S A*. 105:5219-5224.

Nieminen, J., A. Kuno, J. Hirabayashi, and S. Sato. 2007. Visualization of galectin-3 oligomerization on the surface of neutrophils and endothelial cells using fluorescence resonance energy transfer. *J Biol Chem*. 282:1374-1383.

Nio-Kobayashi, J. 2017. Tissue- and cell-specific localization of galectins, beta-galactose-binding animal lectins, and their potential functions in health and disease. *Anat Sci Int*. 92:25-36.

Nio-Kobayashi, J., H. Takahashi-Iwanaga, and T. Iwanaga. 2009. Immunohistochemical localization of six galectin subtypes in the mouse digestive tract. *J Histochem Cytochem*. 57:41-50.

Noon, K.F., M. Rogul, J.J. Brendle, and T.J. Keefe. 1977. Detection and definition of canine intestinal carbohydrases, using a standardized method. *Am J Vet Res*. 38:1063-1067.

Ochieng, J., D. Platt, L. Tait, V. Hogan, T. Raz, P. Carmi, and A. Raz. 1993. Structure-function relationship of a recombinant human galactoside-binding protein. *Biochemistry*. 32:4455-4460.

Ohshiro, H., M. Nonaka, and K. Ichikawa. 2008. Molecular identification and characterization of the dog motilin receptor. *Regul Pept*. 146:80-87.

Olsson, C., and S. Holmgren. 2001. The control of gut motility. *Comp Biochem Physiol A Mol Integr Physiol*. 128:481-503.

Park, A.M., S. Hagiwara, D.K. Hsu, F.T. Liu, and O. Yoshie. 2016. Galectin-3 Plays an Important Role in Innate Immunity to Gastric Infection by Helicobacter pylori. *Infect Immun*. 84:1184-1193.

Partridge, E.A., C. Le Roy, G.M. Di Guglielmo, J. Pawling, P. Cheung, M. Granovsky, I.R. Nabi, J.L. Wrana, and J.W. Dennis. 2004. Regulation of cytokine receptors by Golgi N-glycan processing and endocytosis. *Science*. 306:120-124.

Perez Bay, A.E., R. Schreiner, I. Benedicto, and E.J. Rodriguez-Boulan. 2014. Galectin-4-mediated transcytosis of transferrin receptor. *J Cell Sci*. 127:4457-4469.

Perez, J.H., W.J. Branch, L. Smith, B.M. Mullock, and J.P. Luzio. 1988. Investigation of endosomal compartments involved in endocytosis and transcytosis of polymeric immunoglobulin A by subcellular fractionation of perfused isolated rat liver. *Biochem J*. 251:763-770.

Peter, B.J., H.M. Kent, I.G. Mills, Y. Vallis, P.J. Butler, P.R. Evans, and H.T. McMahon. 2004. BAR domains as sensors of membrane curvature: the amphiphysin BAR structure. *Science*. 303:495-499.

Pezeshkian, W., L.J. Nabo, and J.H. Ipsen. 2017a. Cholera toxin B subunit induces local curvature on lipid bilayers. FEBS open bio. 7:1638-1645.

Pezeshkian, W., H. Gao, S. Arumugam, U. Becken, P. Bassereau, J.C. Florent, J.H. Ipsen, L. Johannes, and J. Shillcock. 2017b. Mechanism of Shiga toxin clustering on membranes. *ACS Nano*. 11:314-324.

Poirier, F., and E.J. Robertson. 1993. Normal development of mice carrying a null mutation in the gene encoding the L14 S-type lectin. *Development*. 119:1229-1236.

Powelka, A.M., J. Sun, J. Li, M. Gao, L.M. Shaw, A. Sonnenberg, and V.W. Hsu. 2004. Stimulation-dependent recycling of integrin beta1 regulated by ARF6 and Rab11. *Traffic*. 5:20-36.

Rabinovich, G.A., and V.L. Thijssen. 2014. Introduction to special issue: Galectins go with the flow. *Glycobiology*. 24:885.

Radhakrishna, H., and J.G. Donaldson. 1997. ADP-ribosylation factor 6 regulates a novel plasma membrane recycling pathway. *J Cell Biol*. 139:49-61.

Rak, K., D. Kornafel, D. Mazurek, and M. Bronkowska. 2018. Lactoferrin level in maternal serum is related to birth anthropometry - an evidence for an indirect biomarker of intrauterine homeostasis? *J Matern Fetal Neonatal Med*:1-8.

Rao, M., and S. Mayor. 2014. Active organization of membrane constituents in living cells. *Curr Opin Cell Biol*. 29:126-132.

Ravindran, M.S., L.B. Tanner, and M.R. Wenk. 2013. Sialic acid linkage in glycosphingolipids is a molecular correlate for trafficking and delivery of extracellular cargo. *Traffic*. 14:1182-1191.

Rehfeld, J.F. 1998. The new biology of gastrointestinal hormones. *Physiol Rev*. 78:1087-1108.

Renard, H.F., M. Simunovic, J. Lemiere, E. Boucrot, M.D. Garcia-Castillo, S. Arumugam, V. Chambon, C. Lamaze, C. Wunder, A.K. Kenworthy, A.A. Schmidt, H.T. McMahon, C. Sykes, P. Bassereau, and L. Johannes. 2015. Endophilin-A2 functions in membrane scission in clathrin-independent endocytosis. *Nature*. 517:493-496.

Ridley, A.J. 2015. Rho GTPase signalling in cell migration. *Curr Opin Cell Biol*. 36:103-112.

Romer, W., L. Berland, V. Chambon, K. Gaus, B. Windschiegl, D. Tenza, M.R. Aly, V. Fraisier, J.C. Florent, D. Perrais, C. Lamaze, G. Raposo, C. Steinem, P. Sens, P. Bassereau, and L. Johannes. 2007. Shiga toxin induces tubular membrane invaginations for its uptake into cells. *Nature*. 450:670-675.

Romer, W., L.L. Pontani, B. Sorre, C. Rentero, L. Berland, V. Chambon, C. Lamaze, P. Bassereau, C. Sykes, K. Gaus, and L. Johannes. 2010. Actin dynamics drive membrane reorganization and scission in clathrin-independent endocytosis. *Cell*. 140:540-553.

Rosa, L., A. Cutone, M.S. Lepanto, R. Paesano, and P. Valenti. 2017. Lactoferrin: A Natural Glycoprotein Involved in Iron and Inflammatory Homeostasis. *Int J Mol Sci*. 18.

Rubartelli, A., and R. Sitia. 1995. Entry of exogenous polypeptides into the nucleus of living cells: facts and speculations. *Trends Cell Biol*. 5:409-412.

Rydell, G.E., L. Svensson, G. Larson, L. Johannes, and W. Romer. 2013. Human GII.4 norovirus VLP induces membrane invaginations on giant unilamellar vesicles containing secretor gene dependent alpha1,2-fucosylated glycosphingolipids. *Biochim Biophys Acta*. 1828:1840-1845.

Sabharanjak, S., P. Sharma, R.G. Parton, and S. Mayor. 2002. GPI-anchored proteins are delivered to recycling endosomes via a distinct cdc42-regulated, clathrin-independent pinocytic pathway. *Dev Cell*. 2:411-423.

Sarna, S.K. 2008. Are interstitial cells of Cajal plurifunction cells in the gut? *Am J Physiol Gastrointest Liver Physiol*. 294:G372-390.

Saslowsky, D.E., Y.M. te Welscher, D.J. Chinnapen, J.S. Wagner, J. Wan, E. Kern, and W.I. Lencer. 2013. Ganglioside GM1-mediated transcytosis of cholera toxin bypasses the retrograde pathway and depends on the structure of the ceramide domain. *J Biol Chem*. 288:25804-25809.

Schnaar, R.L., and T. Kinoshita. 2015. Glycosphingolipids. *In* Essentials of Glycobiology. rd, A. Varki, R.D. Cummings, J.D. Esko, P. Stanley, G.W. Hart, M. Aebi, A.G. Darvill, T. Kinoshita, N.H. Packer, J.H. Prestegard, R.L. Schnaar, and P.H. Seeberger, editors, Cold Spring Harbor (NY). 125-135.

Schonteich, E., G.M. Wilson, J. Burden, C.R. Hopkins, K. Anderson, J.R. Goldenring, and R. Prekeris. 2008. The Rip11/Rab11-FIP5 and kinesin II complex regulates endocytic protein recycling. *J Cell Sci*. 121:3824-3833.

Schubert, T., and W. Romer. 2015. How synthetic membrane systems contribute to the understanding of lipid-driven endocytosis. *Biochim Biophys Acta*. 1853:2992-3005.

Sciacchitano, S., L. Lavra, A. Morgante, A. Ulivieri, F. Magi, G.P. De Francesco, C. Bellotti, L.B. Salehi, and A. Ricci. 2018. Galectin-3: One Molecule for an Alphabet of Diseases, from A to Z. *Int J Mol Sci*. 19.

Shalom-Feuerstein, R., S.J. Plowman, B. Rotblat, N. Ariotti, T. Tian, J.F. Hancock, and Y. Kloog. 2008. K-ras nanoclustering is subverted by overexpression of the scaffold protein galectin-3. *Cancer Res*. 68:6608-6616.

Sharma, M., N. Naslavsky, and S. Caplan. 2008. A role for EHD4 in the regulation of early endosomal transport. *Traffic*. 9:995-1018.

Shi, A., S. Pant, Z. Balklava, C.C. Chen, V. Figueroa, and B.D. Grant. 2007. A novel requirement for C. elegans Alix/ALX-1 in RME-1-mediated membrane transport. *Curr Biol*. 17:1913-1924.

Shi, G., M. Azoulay, F. Dingli, C. Lamaze, D. Loew, J.C. Florent, and L. Johannes. 2012. SNAP-tag based proteomics approach for the study of the retrograde route. *Traffic*. 13:914-925.

Shimada, A., H. Niwa, K. Tsujita, S. Suetsugu, K. Nitta, K. Hanawa-Suetsugu, R. Akasaka, Y. Nishino, M. Toyama, L. Chen, Z.J. Liu, B.C. Wang, M. Yamamoto, T. Terada, A. Miyazawa, A. Tanaka, S. Sugano, M. Shirouzu, K. Nagayama, T. Takenawa, and S. Yokoyama. 2007. Curved EFC/F-BAR-domain dimers are joined end to end into a filament for membrane invagination in endocytosis. *Cell*. 129:761-772.

Sigismund, S., E. Argenzio, D. Tosoni, E. Cavallaro, S. Polo, and P.P. Di Fiore. 2008. Clathrin-mediated internalization is essential for sustained EGFR signaling but dispensable for degradation. *Dev Cell*. 15:209-219.

Simunovic, M., J.B. Manneville, H.F. Renard, E. Evergren, K. Raghunathan, D. Bhatia, A.K. Kenworthy, G.A. Voth, J. Prost, H.T. McMahon, L. Johannes, P. Bassereau, and A. Callan-Jones. 2017. Friction Mediates Scission of Tubular Membranes Scaffolded by BAR Proteins. *Cell*. 170:172-184 e111.

Smith, S.M., M. Baker, M. Halebian, and C.J. Smith. 2017. Weak Molecular Interactions in Clathrin-Mediated Endocytosis. *Front Mol Biosci*. 4:72.

Solovyeva, V., L. Johannes, and A.C. Simonsen. 2015. Shiga toxin induces membrane reorganization and formation of long range lipid order. *Soft Matter*. 11:186-192.

Sorre, B., A. Callan-Jones, J. Manzi, B. Goud, J. Prost, P. Bassereau, and A. Roux. 2012. Nature of curvature coupling of amphiphysin with membranes depends on its bound density. *Proc Natl Acad Sci U S A*. 109:173-178.

Suzuki, Y.A., K. Shin, and B. Lonnerdal. 2001. Molecular cloning and functional expression of a human intestinal lactoferrin receptor. *Biochemistry*. 40:15771-15779.

Taub, M.E., and W.C. Shen. 1993. Regulation of pathways within cultured epithelial cells for the transcytosis of a basal membrane-bound peroxidase-polylysine conjugate. *J Cell Sci*. 106 (Pt 4):1313-1321.

Thottacherry, J.J., M. Sathe, C. Prabhakara, and S. Mayor. 2019. Spoiled for Choice: Diverse Endocytic Pathways Function at the Cell Surface. *Annu Rev Cell Dev Biol*.

Torgersen, M.L., G. Skretting, B. van Deurs, and K. Sandvig. 2001. Internalization of cholera toxin by different endocytic mechanisms. *J Cell Sci*. 114:3737-3747.

Treuting, P.M., C.B. Clifford, R.S. Sellers, and C.F. Brayton. 2012. Of mice and microflora: considerations for genetically engineered mice. *Vet Pathol*. 49:44-63.

Tuma, P., and A.L. Hubbard. 2003. Transcytosis: crossing cellular barriers. *Physiol Rev*. 83:871-932.

Vladoiu, M.C., M. Labrie, and Y. St-Pierre. 2014. Intracellular galectins in cancer cells: potential new targets for therapy (Review). *Int J Oncol*. 44:1001-1014.

Wang, X.Y., J.Y. Yin, M.M. Zhao, S.Y. Liu, S.P. Nie, and M.Y. Xie. 2018. Gastroprotective activity of polysaccharide from Hericium erinaceus against ethanol-induced gastric mucosal lesion and pylorus ligation-induced gastric ulcer, and its antioxidant activities. *Carbohydr Polym*. 186:100-109.

Ward, P.P., M. Mendoza-Meneses, G.A. Cunningham, and O.M. Conneely. 2003. Iron status in mice carrying a targeted disruption of lactoferrin. *Mol Cell Biol*. 23:178-185.

Watanabe, S., T. Trimbuch, M. Camacho-Perez, B.R. Rost, B. Brokowski, B. Sohl-Kielczynski, A. Felies, M.W. Davis, C. Rosenmund, and E.M. Jorgensen. 2014. Clathrin regenerates synaptic vesicles from endosomes. *Nature*. 515:228-233.

Weigert, R., A.C. Yeung, J. Li, and J.G. Donaldson. 2004. Rab22a regulates the recycling of membrane proteins internalized independently of clathrin. *Mol Biol Cell*. 15:3758-3770.

Wen, J., E. Luque-de Leon, L.J. Kost, M.G. Sarr, and S.F. Phillips. 1998. Duodenal motility in fasting dogs: humoral and neural pathways mediating the colonic brake. *Am J Physiol*. 274:G192-195.

Young, W., C.D. Moon, D.G. Thomas, N.J. Cave, and E.N. Bermingham. 2016. Pre- and post-weaning diet alters the faecal metagenome in the cat with differences in vitamin and carbohydrate metabolism gene abundances. *Sci Rep*. 6:34668.

Zentek, J., E.J. Hall, A. German, K. Haverson, M. Bailey, V. Rolfe, R. Butterwick, and M.J. Day. 2002. Morphology and immunopathology of the small and large intestine in dogs with nonspecific dietary sensitivity. *J Nutr*. 132:1652S-1654S.

Zhang, R.G., D.L. Scott, M.L. Westbrook, S. Nance, B.D. Spangler, G.G. Shipley, and E.M. Westbrook. 1995. The three-dimensional crystal structure of cholera toxin. *J Mol Biol*. 251:563-573.

Zhang, X., and F.L. Kiechle. 2004. Review: Glycosphingolipids in health and disease. *Ann Clin Lab Sci*. 34:3-13.

Zhao, H., A. Michelot, E.V. Koskela, V. Tkach, D. Stamou, D.G. Drubin, and P. Lappalainen. 2013. Membrane-sculpting BAR domains generate stable lipid microdomains. *Cell Rep*. 4:1213-1223.

Titre : L'endocytose GL-Lect dans des systèmes *in vivo*

Mots clés : Glycosphingolipide, galectine, lactotransferrine, entérocytes, modèle souris d'intestin, endocytose

Résumé : Une multitude de voies endocytiques existent à la surface de la membrane plasmique, ce qui conduit à l'internalisation de la majeure partie des membranes ainsi que des protéines associées, des molécules de signalisation, des facteurs de croissance et autres cargos (Smith et al. 2017). Pendant des décennies, la voie majeure dite clathrine-dépendante a été la plus étudiée, Cette voie d'endocytose se caractérise par la polymérisation de molécules de clathrine et de protéines adaptatrices au niveau de récepteurs liés à leurs ligands, entrainant la courbure de la membrane, avant sa scission et son endocytose (Smith et al. 2017). Récemment, plusieurs mécanismes alternatifs ont été découverts facilitant l'absorption endocytique des protéines cargo et des récepteurs membranaires, même en l'absence de la voie clathrine-dépendante (Mayor et al. 2014). Un modèle d'endocytose qui ne requiert pas de clathrine mais à la place des galectines et des glycolipides a été proposé par mon laboratoire hôte (Lakshminarayan et al. 2014). Les galectines sont des lectines qui se lient aux bêta-galactosides et qui, à ce jour, regroupent 15 membres (galectine-1 à galectine-15) chez les mammifères et sont retrouvées dans de nombreux types de cellules et tissus (Leffler et al., 2004). Les galectines sont probablement sécrétées extra-cellulairement par une voie encore mal caractérisée et non-classique (Hughes, 1999). Les glycosphingolipides (GSL) sont des constituants membranaires ubiquitaires, divisés en fractions neutres ou acides. Le terme GSL s'applique aux composés contenant au moins un monosaccharide et une céramide. Il est à noter que l'enzyme UDP-glucose céramide glucosyltransférase (Ugcg) catalyse l'étape initiale de la biosynthèse de GSLs à base de glycosylcéramides.

Notre modèle de travail actuel, impliquant les glycolipides et les lectines, a été qualifié d'hypothèse GL-Lect (Johannes et al. 2016), et préliminairement soutenu par des données expérimentales comme décrit par Lakshminarayan et al. en 2014. Il peut être décrit comme suit :

i) la galectine-3 (Gal3) se lie sous forme monomérique aux glycoprotéines

ii) Gal3 commence alors à oligomériser

iii) Gal3 oligomérisée a la capacité de se lier aux GSLs, ce qui conduit vraisemblablement à la formation de clusters de GSLs

iv) Ces clusters Gal3-GSL induisent une invagination de la membrane plasmique, une endocytose des protéines cargo liées à Gal3 et la formation subséquente de CLIC (clathrin-independent carriers), endosomes pré-précoces.

Selon ce modèle, l'oligomère Gal3 est capable de se lier aux GSLs et d'induire une déformation de la membrane de la même manière qu'une autre lectine, la sous-unité B de la toxine de Shiga (STxB). Par conséquent, les deux processus pourraient être résumés sous la même hypothèse GL-Lect, où GL représente les glycolipides (Gb3 pour STxB et des gangliosides pour Gal3) et Lect corresponds aux lectines (STxB, Gal3 et éventuellement d'autres). Comprendre dans quels contextes physiologiques les processus d'internalisation indépendantes de la clathrine, mais dépendantes de la Gal3, sont opérés non est un défi majeur pour l'hypothèse GL-Lect.

Dans mon travail de thèse, j'ai obtenu des indications directes sur une implication du mécanisme GL-Lect dans l'endocytose et la transcytose au niveau de l'intestine grêle de la souris. Ce mécanisme implique la Gal3 et agit dans les entérocytes intestinaux dans un processus de transcytose qui s'avère d'être dépend des GSLs. En effet, nous avons découvert que la lactotransferrine (LTF), une protéine que nous avons identifié par pull-down et spectrométrie de masse comme étant un partenaire d'interaction de la Gal3, dépendait fortement de la cette dernière pour son endocytose efficace, et des GSLs pour son mode de distribution analogue à la transcytose. Sur la base de ces découvertes dans l'épithélium intestinal de souris, nous avons établi un système modèle *in vivo* fonctionnel dans lequel le mécanisme endocytique récemment proposé, appelé dans notre laboratoire GL-Lect, semble se produire physiologiquement.

Title : GL-Lect endocytosis in *in-vivo* model systems

Keywords : Glycosphingolipid, galectin, lactotransferrin, enterocytes, mouse intestinal model, endocytosis

Abstract : A host of endocytic pathways exist at the surface of eukaryotic cells, which lead to the internalization of the bulk of membranes along with membrane proteins, signaling receptors, growth factors, and other cargoes (Smith et al. 2017). For decades, the clathrin-mediated pathway has been the best characterized endocytic process where clathrin polymerizes along with the associated adaptor proteins to include ligand-bound receptors, leading to membrane bending, membrane scission, and endocytosis (Smith et al. 2017). Recently, multiple alternative mechanisms have been uncovered which facilitate the endocytic uptake of cargo molecules and membrane receptors even in the absence of clathrin machinery (Mayor et al.2014). A model of endocytosis that doesn't require clathrin but rather sugar-binding galectins and glycolipids has been proposed by my host laboratory (Lakshminarayan et al. 2014). Galectins constitute a family of beta-galactoside–binding lectins, which to date consists of 15 members in mammals. Galectins are broadly distributed in a variety of cells and tissues (Leffler et al. 2004). They are translocated from the cytosol to the extracellular space by a process of non-classical secretion (Hughes 1999). Glycosphingolipids (GSLs) are ubiquitous membrane constituents that are subdivided in neutral or acidic fractions. The term GSLs

applies to compounds that contain at least one monosaccharide and a ceramide. Of note, the enzyme UDP-glucose ceramide glucosyltransferase (Ugcg) catalyzes the initial step for the biosynthesis of glycosylceramide-based GSLs.

Our current working model, which involves glycolipids and lectins, was termed the GL-Lect hypothesis (Johannes et al. 2016). It is backed up by experimental data as described in Ref. (Lakshminarayan et al. 2014) and can be described as follows:

i) Monomeric Gal3 binds to glycoproteins

ii) Gal3 then starts to oligomerize

iii) Oligomerized Gal3 has the capacity to bind to GSLs, and this may induce their clustering

iv) Gal3-GSL cluster are inducing the invagination of the plasma membrane to generate tubular endocytic pits from which clathrin-independent carriers (CLICs, which are pre-early endosomes) are generated.

Oligomeric Gal3 is indeed able to bind to GSLs and to induce membrane deformation (Lakshminarayan et al. 2014) in a similar way the pathogenic lectin Shiga toxin-B subunit (STxB) does. Therefore, both processes could be summarized under the same hypothesis, the GL-Lect hypothesis, where GL stands for the glycolipid (Gb3 for STxB and gangliosides for Gal3) and Lect summarizes the lectins (STxB, Gal3 and possibly others as well).

Understanding in which physiological situations this clathrin-independent but Gal3-dependent internalization mechanism operates is one of the main challenge for the GL-Lect hypothesis.

We characterized for the first time that in the gut the GL-Lect mechanism facilitates endocytic uptake of cargo. This mechanism is driven by Gal3 and operates in intestinal enterocytes for a transcytosis-like process, and is GSL dependent. Indeed, we have found that lactotransferrin (LTF), a Gal3-binding protein that we have identified by pull-down and mass spectrometry, strongly required Gal3 and GSLs for its efficient endocytosis and its transcytosis-like distribution pattern, respectively. Based on these findings in the mouse intestinal epithelium, we established a functional *in vivo* model system where the newly proposed endocytic mechanism termed in our lab as GL-Lect, was physiologically relevant.